UNIVERSITY OF SOUTHAMPTON

APPROACHES TO LIGHT-RESPONSIVE, METAL-ION SENSORS
FOR BIOLOGICAL SYSTEMS

SAM WILLIAM ROBERT BARDWELL

SUBMITTED FOR THE DEGREE OF MASTER OF PHILOSOPHY

CHEMISTRY

AUGUST 2000

UNIVERSITY OF SOUTHAMPTON

ABSTRACT

FACULTY OF SCIENCE

CHEMISTRY

Master of Philosophy

APPROACHES TO LIGHT-RESPONSIVE, METAL-ION SENSORS FOR BIOLOGICAL SYSTEMS

by Sam William Robert Bardwell

The loss of articular cartilage, whether through degenerative disease, wear and tear, or accidental trauma, is a debilitating and painful condition. The work reported in this thesis describes two separate approaches towards addressing this situation. The primary focus of this work involved an attempt to help the study of cartilage damage. Two novel fluorescent probes have been prepared based on crown ether core units to which are attached photoactive side arms. The cation-binding properties of these ionophores were investigated by spectroscopic methods, extraction binding studies and fluorescence measurements. Comparison of these results with those for model compounds has provided some insight into those structural modifications which lead to enhanced selectivity in favour of Na^+ over K^+ but reduced overall binding efficiency, both factors which are critical for sodium-ion sensing within the cartilage matrix. In a brief parallel study a range of PVA-based hydrogels incorporating a hydroxyapatite gradient were synthesised for evaluation as potential replacement for cartilage tissue.

CONTENTS

SECTION 2 HYDROGELS

SECTION 3 APPENDICES & REFERENCES

LIST OF SCHEMES

LIST OF FIGURES

LIST OF TABLES

For all my family

ACKNOWLEDGEMENTS

Firstly, I would like to thank Martin, who not only gave me the opportunity to pursue this work but the support, faith and help in order to complete it. Additional thanks must go to Robert Wilkins for the funding and support of this project and to Joe Browning for his help, advice and hospitality.

It would be criminal if I did not give a mention to all the members of the Grossel group I have worked with, project students and postgrads alike, past and present. All of who have helped to make the lab a place where I thoroughly enjoyed working. Thank you. Special thanks goes to Fred for all the glassware and endless talks about fitness, John for mullet conversations and dancing displays, Paul for drinking partnerships and an equally unhealthy interest in overly long write-ups and Dan for managing to make it look like even I got in early.

Thanks to Joan Street, John Langley and Julie Herniman for their help with all my NMR and mass spectroscopy needs. Thanks to Professor Tom Brown and his group for letting me monopolise their fluorimeter. Thanks also to Rob Wood who worked hard and managed to produce results in spite of my supervision.

Many thanks to John, Paul and Peter for allowing me to stay in their spare room at the "end" of my study. To Faye, Fay and Nigel for their generosity and hospitality in letting me be a housemate for "two or three weeks". And to Claire for letting me use her entire house in a mutually beneficial arrangement, which was far more to my benefit than hers.

An extremely grateful mention must go to the fine collection of cooks at nine Crofton Close. Who, in an unequivocal show of altruism and benignity, threw open their doors, welcomed me unquestionably and furnished we with an innumerable number of piping hot meals, choice desserts and evenings of entertaining company.

Finally, but most importantly, I'd like to thank my Mum. Without her endless support, both emotionally and financially, this work would never have been started, let alone finished.

NOTES AND ABBREVIATIONS

Abs	absorbance
Ac	acetyl
ADP	adenosine diphosphate
Ar	aromatic
ATP	adenosine triphosphate
Cat	catalytic
DMF	dimethylformamide
DMSO	dimethylsulfoxide
d.p.	decimal place
ECM	extracellular matrix
Et	ethyl
ISE	ion selective electrode
K_a	association or stability constant
K_d	dissociation or instability constant
K_{di}	distribution constant
Me	methyl
mM	milli-molar
PET	photo-induced electron transfer
PnAO	propylene amine oxime
ppm	parts per million
PVA	polyvinyl alcohol
Sat	saturated
SBFI	sodium-binding benzofuran isophthalate
SBFI-AM	sodium-binding benzofuran isophthalate acetoxymethyl ester
TLC	thin layer chromatography
TMS	trimethylsilane
Ts	tosylate
UV	ultraviolet visible
Vol	volume

SECTION 1 SENSORS

"In two words: im-possible."

Samuel Goldwyn

1 INTRODUCTION

1.1 Crowns as Ionic Sensors in Biological Cells

1.1.1 Cartilage Cells

The role of articular cartilage is to bear load, absorb shock and minimise wear between articulating joint surfaces. Chondrocytes, the cells of articular cartilage do not directly contribute to these physical properties; only the extracellular matrix (ECM) plays a direct structural role.[1] However, as the only cell type normally resident within articular cartilage, chondrocytes are solely responsible for the synthesis and maintenance of a viable ECM that is suitably adapted to cope with the physical pressures of its environment.[1]

There has been much research investigating the mechanisms involved in the regulation of cartilage matrix biosynthesis by chondrocytes. It is expected that a fuller understanding of the synthesis of cartilage in healthy tissue will reveal details about the cellular mechanisms that underlie debilitating degenerative cartilage pathologies such as osteoarthritis.[2]

1.1.2 The Biological Role of Sodium

The extracellular environment of cartilage is unusual when compared with other tissues. There exists a high density of fixed negative charges within the ECM (predominantly from proteoglycans) which attracts high concentrations of diffusible cations (Na^+, H^+, K^+, Ca^{2+}) relative to the levels found in serum or synovial fluid. Consequently, the extracellular concentration of Na^+ in cartilage is high (250-350 mM).[3,4] Furthermore, loading of articular cartilage - essential for its normal synthesis *in vivo* - expresses fluid from the tissue, which further concentrates the fixed negative charges and increases the mobile extracellular cation concentrations and extracellular osmolality.[1]

The intracellular concentration of Na^+ in chondrocytes is about 40mM, which is still relatively high in comparison with that found in other cells.[4] The difference between the intracellular and extracellular concentrations of Na^+ results in a steep, inwardly directed gradient for Na^+ used by chondrocytes to transport a variety of ions and essential metabolites into the cell.[5,6] However, for healthy cell metabolism, the $Na^+:K^+$ ratio must be maintained at a low level, and Na^+ ions accumulated in the cytosol are actively extruded by the operation of the Na^+, K^+-ATPase in the cell membrane.[7] This primary active transporter utilises the energy derived from the hydrolysis of ATP to pump Na^+ ions out of the cytosol against the natural electrochemical gradient.

1.1.3 Cartilage Studies

The rate of matrix synthesis in chondrocytes is strongly affected by changes in extracellular concentrations of Na^+. A number of investigators have attempted to determine the effects of changes in extracellular Na^+ levels on intracellular Na^+ activities using fluorescent dyes. These dyes are superior to other methods for studying intracellular ion activities since they allow continual, non-invasive recording of an individual ionic species with high spatial and temporal resolution. Many commercially produced dyes exist to measure key cell parameters such as pH_i, $[Ca^{2+}]_i$, $[K^+]_i$ and $[Na^+]_i$. In each case, the central property of these indicators is a change in fluorescence behaviour upon the binding of a specific ion. Such dyes are synthesised as membrane-permeant ester derivatives, which can be easily loaded into cells, but on hydrolysis of the ester function become trapped within the cytosol.

Our aim is to use Na^+-sensitive fluorescent dyes to characterise the role of Na^+ ions in modulating matrix turnover. It follows that in order to be a useful fluorescent probe, a putative Na^+ dye must: (i) exhibit a high degree of selectivity towards Na^+; (ii) be available as an ester derivative; (iii) be non toxic to living cells; (iv) display marked changes in its fluorescence when the ion of interest is bound; and (v) not saturate in the concentration range of metal ion required to be monitored. To some extent, commercially available Na^+ dyes can be considered as over-engineered; they have a high Na^+ affinity and consequently suffer from varying degrees of K^+ ion sensitivity. They are designed to have a high sodium ion-affinity in order to reflect accurately changes in $[Na^+]_i$ in the range experienced by most mammalian cells. For example, the K_d for SBFI[8,9] (1), a sodium-specific indicator, is 18mM for Na^+.

1
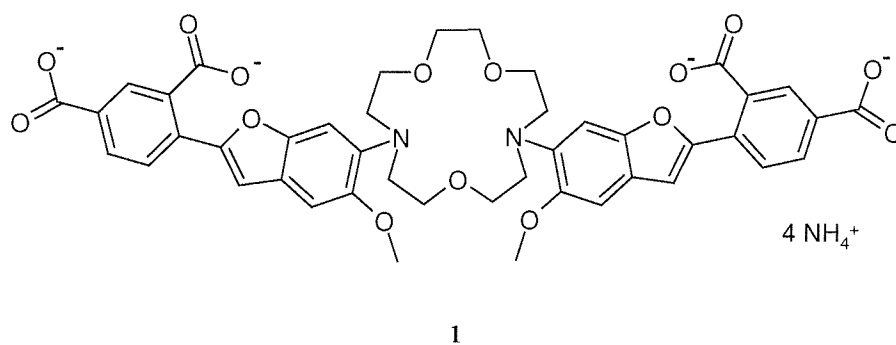
However, it has been shown that Na^+ concentrations significantly higher than this are found in articular chondrocytes so that the dye becomes saturated and its sensitivity towards changes in Na^+ concentration is markedly reduced. It has therefore been difficult to monitor dynamic changes in Na^+ concentration in chondrocytes using commercially available dyes. Aside from using radioisotopic flux techniques, there are no satisfactory means to carry out these studies. It is therefore proposed, to synthesise a range of novel macrocyclic ligands, based on a mixed oxy- and aza-crown ether skeleton. The resulting crowns should have a reduced affinity for Na^+ ions, while minimising the contaminating effects of K^+ ions and without increasing the affinity for other metal ions. This will render such indicators suitable for use at the higher Na^+ concentrations found in chondrocytes whilst retaining a high degree of Na^+ specificity, and thus allowing the physiological importance of Na^+ in articular cartilage to be investigated more fully.

1.2 Supramolecular Chemistry

1.2.1 Definition and Significance

The field of Supramolecular Chemistry has dramatically expanded since the original discovery of large macrocycles such as crown ethers and cryptands. Its development has revolutionised approaches to topologically complex molecules.[10] The scope of this new field has been well defined by Jean-Marie Lehn, who has stated that "Supramolecular Chemistry is the chemistry of the intermolecular bond, concerning the structure and functions of the entities formed by the association of two or more chemical species".[11] Such intermolecular bonds may result from ion pairing, hydrophobic or hydrophilic effects, hydrogen bonding, π-stacking or donor-acceptor interactions,[12] and because of these interactions, Supramolecular Chemistry has become a field now studied by many disciplines. It is no longer restricted to inorganic, organic and physical chemistry but today encompasses aspects of biochemistry, engineering and physics.

Perhaps the best way to define Supramolecular Chemistry is through its relationship with traditional molecular chemistry *via* a diagram [Figure 1[13]].

Molecular Chemistry

| Starting Materials |
| Covalent Bonds   **Synthesis** |

Receptor + Substrate

Supramolecular Chemistry

Intermolecular Bonds   **Complex Formation**

Supermolecule

Recognition   *Transformation*   *Translocation*   **Functions**

Molecular Devices
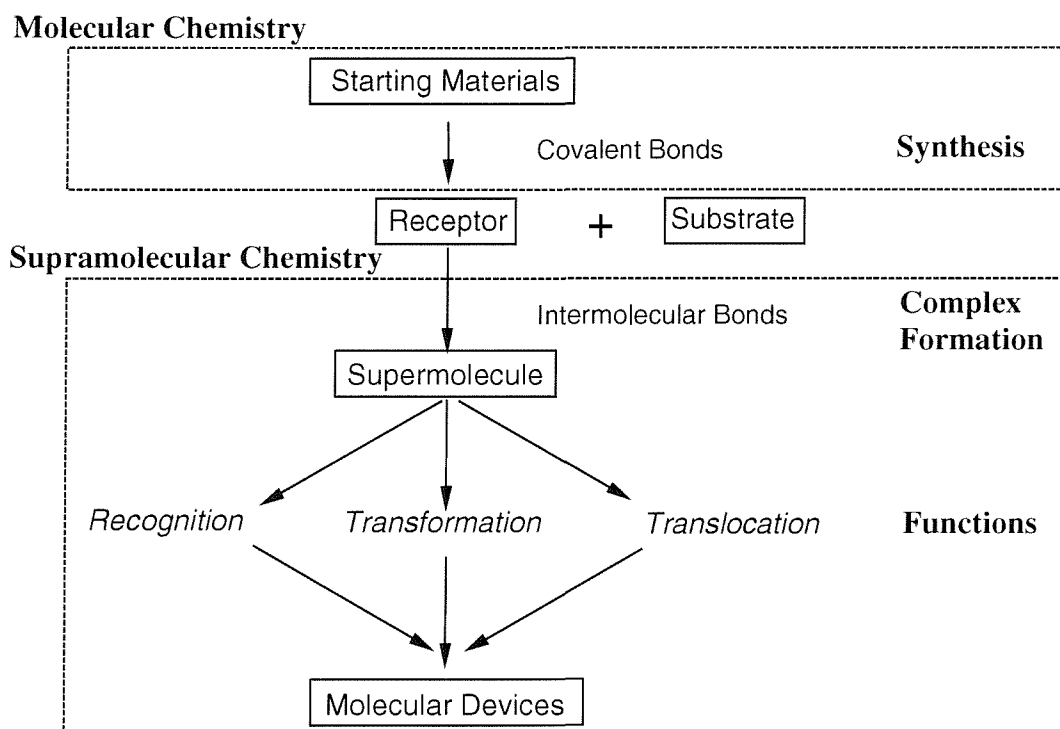
Figure 1: The relationship between molecular and supramolecular chemistry

In the first stage, molecules are synthesised from starting materials through the formation of covalent bonds. In an analogous process, the second stage shows the formation of supermolecules from substrates and receptors using intermolecular bonds. The diagram also shows several functions of a 'supermolecule' and the possibilities of combining these functions to create molecular devices.

Supramolecular Chemistry provides a route for the design of totally synthetic materials having varied applications ranging from switches, magnets, sensors and superconductors through to pharmaceutical delivery systems.[14,15] Indeed the area of molecular electronics has been particularly active recently, molecular components for sensors being of great interest. An essential step in the development of such species has been the design of large molecules capable of selectively binding ions or neutral compounds.

1.2.2 Molecular Recognition

Molecular recognition involves the selection and binding of a substrate by a specific receptor. Such a process requires a pattern of complementary intermolecular interactions, so that the binding of a particular substrate by a given receptor will be identical from one molecular pairing to the next. Recognition is best brought about through a large contact area with the substrate in question. This is achieved by designing the receptor with as many sites for recognition as possible and with a geometry that allows for orientation of those sites to complementary sites on the substrate.

Any supermolecule formed by substrate-receptor binding has high thermodynamic and kinetic stability and selectivity, reflecting the optimal information content of a receptor for a given substrate.[16] Molecular recognition can be defined as information storage and read out at a supramolecular level.

1.2.3 Self-Assembly

Once molecular recognition has been achieved, the goal is for spontaneous 'self-assembly' of two or more molecules to form large-scale aggregates. There are many definitions of self-assembled structures,[17] however the complexes formed can be said to include the following characteristics:[18]

i)   Non-covalent interactions hold together the different units.

ii)   The most stable aggregate is formed through co-operative binding of subunits.

iii)   The properties of the aggregates are different from those of the individual units.

iv)   The aggregates have a definite size and composition; forming finite lattices.

These characteristics are not all-encompassing but do include most of the features of a self-assembled system. The simplest case of a self-assembly would be a self-complimentary molecule which dimerises, e.g. benzoic acid.
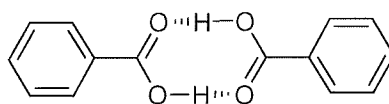
Figure 2: Hydrogen-bonded dimerization of benzoic acid

Developing this concept through the creation of more recognition sites leads to an increase in the size of aggregates formed from ribbons through to sheets and infinite lattices [e.g. Figure 3, below].
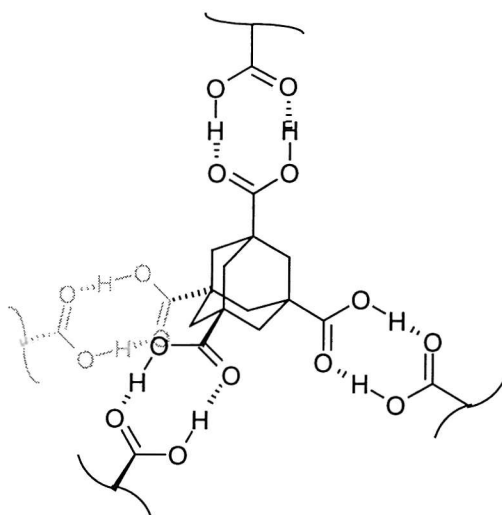
Figure 3: 3D Lattice of adamantane 1,4,5,8-tetracarboxyclic acid

Such recognition is not limited to hydrogen bonding; electrostatic interactions between heteroatoms and metal cations have wide-ranging uses in the formation of supramolecular assemblies. The favoured co-ordination geometry of different cations (e.g. tetrahedral, square planar, octahedral) allows the design of a host to force assembly into very specific architectures.
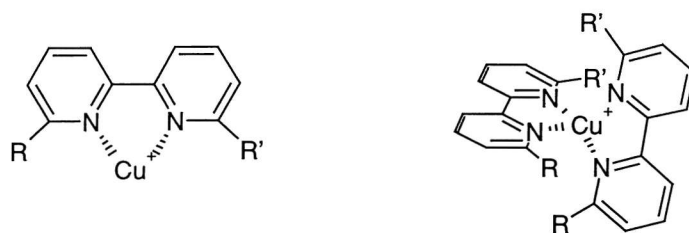
Figure 4: The bipy unit and its tetrahedral co-ordination with copper(I)

The bipy (bipyridyl) unit has two nitrogen centres available for co-ordination and when it is combined with, for example, a Cu^+ salt, a tetrahedral complex is formed. By using sterically constrained bipy dimers, trimers, tetramers etc, self-assembling helicates can be formed in which the polymeric units wind around a 'string' of cations.
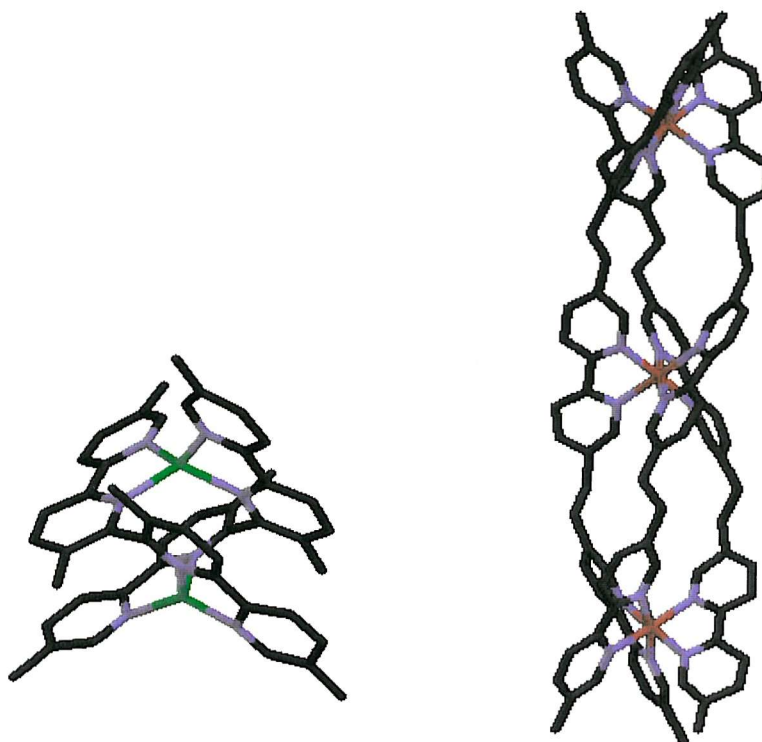
Figure 5a   Figure 5b

Figure 5: Self-assembling-double and triple helicates (hydrogens omitted)

Figure 5a,[19] shows how two bipy dimers will self assemble into a double-stranded helicate, the stoichiometry of 2 dimers:2 cations being forced by the steric demands of the ligand and a tetrahedral requirement of the cation (Cu^I). By changing the position and length of the methylene linkers between bipy units, trimers can be obtained involving octahedral co-ordination about Ni^{II} thereby forming a triple-stranded helicate [Figure 5b].

1.2.4 Crown Ethers

If a number of potential metal-ion co-ordination centres are incorporated into a macrocyclic ring, crown ethers and their analogues result. Crown ethers were discovered serendipitously in 1967,[20] by the late Charles J. Pedersen during an attempt to prepare non-cyclic phenolic ligands (e.g. **2**) capable of binding divalent metal cations. The reaction had been successful (indeed Pedersen went on to patent his work in this area) but because of the presence of some unprotected starting material a further reaction had occurred producing a crystalline by-product.

Pedersen followed his inquisitive nature and investigated further this small amount of crystalline material, the consequence of which was the opening up of a whole new area of chemistry initially through the preparation of a myriad of related compounds. Pedersen had prepared dibenzo-18-crown-6 (**3**); it was this fortunate breakthrough and his subsequent work in the field, which earned him a Nobel Prize in 1987.[21] His interest in the compound was originally stirred when attempting to elucidate its structure; he found that the compound's solubility in organic solvents, such as methanol, was improved by the presence of sodium salts. Pederson explained this observation through the binding of a metal ion in the centre of the cavity, held in place by strong electrostatic forces created between the oxygen lone pairs and the cationic charge [Figure 6]. This was the first example of a synthetic compound capable of forming stable complexes with a metal ion such as Na^+ or K^+.

Electrostatic Forces
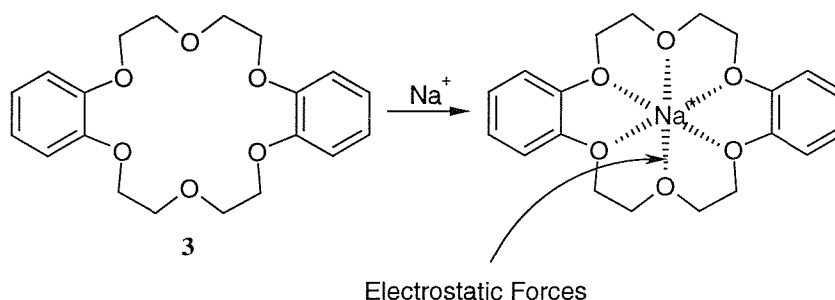
Figure 6: Dibenzo-18-crown-6 complexed with sodium

Pedersen concluded that if such a large ring could form unintentionally, a concerted effort could produce a higher yield. He attempted the reaction of catechol (**4**) and bis(2-chloroethyl) ether (**5**) with sodium hydroxide in *n*-butanol [Scheme 1, below].
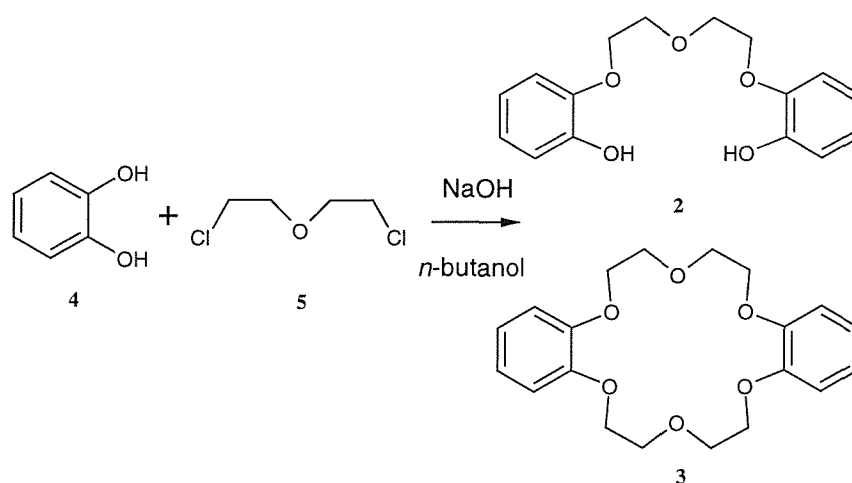
Scheme 1: Pedersen's first synthesis of dibenzo-18-crown-6 (**3**)

The macrocycle was isolated in a 45% yield[22] which is very impressive for condensation of four separate molecules, and reflects what is now known as 'the template effect' (see 1.3.2.2). After this discovery, the number of crown ethers known grew rapidly. Pedersen himself went on to create a range of crown ethers incorporating a variety of different heteroatoms such as nitrogen and sulfur. Chemists soon realised the almost endless structural possibilities and the importance of compounds that could selectively bind different metal ions because of the nature and size of their internal cavities.

The large and symmetrical nature of these new macrocycles led to the development of a simplified naming system, which avoided the need for the clumsy and overly long systematic names. This system uses ring size and number of heteroatoms as its basis. Perhaps the simplest and best-known example would be 18-crown-6 (**6**), where the first number is the total ring size and the second is the number of donor atoms in the ring, which are oxygen unless otherwise stated.

6
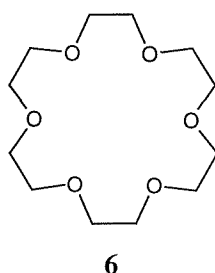
1.2.5 Cyclic Polyamines

As would be expected the structure of a cyclic polyamine is similar to that of a polyether macrocycle but with amine functionalities replacing the ether linkages. However there are large differences in the properties of these two systems; cyclic polyamines show a very high preference for the complexation of transition metals while crown ethers favour alkali and alkaline earth metals. Such behaviour can be attributed primarily to the principle of hard and soft acids and bases (HSAB theory). This states that the strongest complexes are formed when soft acids (transition metals) are paired with soft bases like nitrogen or sulfur atoms or when hard acids (alkali and alkaline earth metals) are paired with hard bases such oxygen.

To date only a relatively small number of complexes of aza-crowns with metal ions have been studied in detail, and most of these involve first row transition metal ions in their standard oxidation states. The most widely reported examples are complexes of cyclam (**7**, tetra-aza-14-crown-4).

7
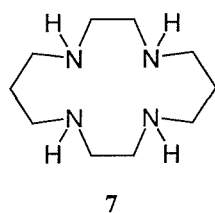
Cyclam is the classic example of a cyclic polyamine as it adopts a tetradentate conformation, by far the most common. Examples of higher order, polydentate macrocycles in the polyamine series are rare.[23] The four nitrogens co-ordinate in a single plane around the metal ion [Figure 7b, below], freeing the axial sites above and below for interaction with counter ions.
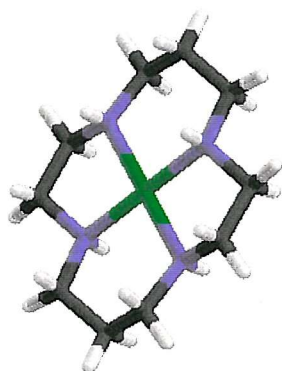
Figure 7a   Figure 7b

(hydrogens omitted)

Figure 7: Top and side view of cyclam copper(I) complex[24]

In such cases, complexation is generally very strong (so much so that it is often impossible to remove the cation to liberate the free macrocycle). This has led to an overall lack of association constant data being published for such systems. Such complexes often have bonds of covalent strength between the cation and the nitrogen atoms,[25b] formed during their synthesis because of the template effect (see 1.3.2.2).

It is possible for macrocyclic binding behaviour to be displayed by non-macrocyclic analogues. For example the PnAO's and their derivatives are tetra-amine ligands that are capable of binding transition metals such as Tc^{99m} and with deprotonation of one of the oxime functionalities allowing for the formation of an intermolecular hydrogen bond,[26] lead to a pseudo-macrocycle [Scheme 2]. In the case below the complex is that of the radiopharmaceutical imaging agent, Ceretec™.[27]
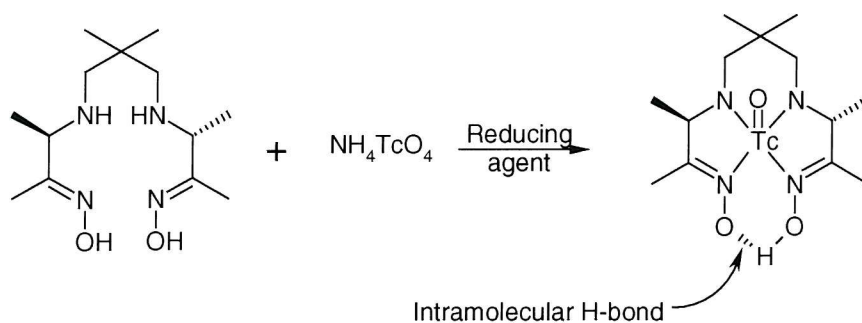
Scheme 2: Ceretec™ – Tc complex, displaying pseudo macrocyclic behaviour

1.2.6 Cryptands

In 1969, Lehn extended the concept of crown ethers through the preparation of their three-dimensional analogues, the "cryptands".[28,29] By exploiting the branching nature of nitrogen heteroatoms in the ring, he was able to create a 3D analogue of a crown ether. Here the guest would be encapsulated within the flexible 3D cavity of the host, the latter being typically lined with oxygen and nitrogen binding sites. The greater rigidity of cryptands leads to enhanced stability of their complexes and greater binding selectivity when compared with similar crown ethers; in effect they act as the first solvation shell for a cation. The increased rigidity also means that an ion that is too small or too large will only bind weakly or even not at all.
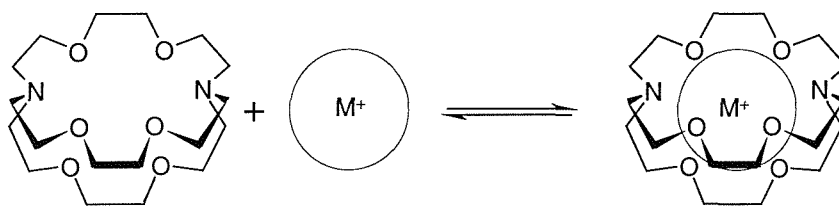
Figure 8: Formation of a cryptate from a cation and parent cryptand

The enhanced strength and selectivity of binding combined with the complete encapsulation of any complexed ion is termed the "cryptate" effect and is analogous to the macrocyclic effect (see 1.3.1.3). Lehn termed his cryptand complexes as "cryptates" [Figure 8] which in turn led to crowns being referred to as "coronands" when in their free ligand state and "coronates" when complexed.

1.3 Crown Ethers

1.3.1 Crown Ether Complexation

The knowledge that crown ethers selectively complex alkali metal and alkaline earth cations has led to widespread efforts to vary all possible structural components in order to study the relationship between structure and cation selectivity as well as to discover new ligand systems.

1.3.1.1 Host-Guest Chemistry

Cram first coined the phrase 'host-guest chemistry' in 1974[30] with reference to the new field of complexation by crowns and cryptands. Hosts possess binding sites that tend to converge upon the guest. Guests are molecules or atoms, which can be ionic or neutral in nature, that present binding sites complementary to those present in the host. The binding sites can interact with guests through various intermolecular interactions. These intermolecular bonds may result from electrostatic, π-π, cation-π, or van der Waals' interactions and hydrogen bonding.[31]

	Typical Strength (kJ mol^{-1})
Hydrogen Bonding	10-190
Electrostatic Interactions	1-250
π-π Interactions	5
Cation-π Interactions	25-160
Van der Waals' Interactions	2

Table 1: Magnitudes of intermolecular forces

These interactions are clearly weaker [see Table 1,[32,33] above] than that of a typical covalent bond at around 350 kJ mol^{-1}. Their weak nature allows for quick and easy assembly and aggregation. However, the accumulation of many weak interactions leads to more stable assemblies.

1.3.1.2 Association Constants

Association or stability constants are the equilibrium constants relating to the following equation:

$$m\text{H} \; + \; n\text{G} \; \underset{K_d}{\overset{K_a}{\rightleftharpoons}} \; \text{H}_m\text{G}_n$$
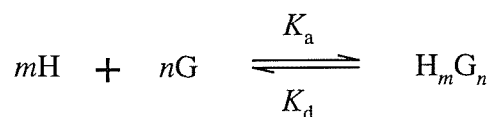
Equation 1

where   H is host

G is guest

m and n are the stoichiometry of each.

where K_a is defined by:

$$K_a = \frac{[H_m G_n]}{[Host]^m [Guest]^n} \qquad \text{Equation 2}$$

As shown by Equation 2 the units of K_a are M^{-1} and the larger the value the stronger the association between host and guest. However, these values are large and cumbersome figures, so they are typically quoted as log K_a values which are unit-less but much more comprehensible values, allowing for easier comparison.

1.3.1.3 Macrocyclic Effect

Cation complexation by crowns is attractive because of the increased binding strength that they show when compared with their open-chain analogues.[34] This phenomenon is referred to as 'the macrocyclic effect', a phrase introduced by Cabbiness and Margerum,[35] though it is applicable to macrocyclic compounds in general. The macrocyclic effect, although well recognised and documented, has yet to have its thermodynamic origins established, unlike the chelate effect, which concerns the increased binding strength of multidentate ligands over their unidentate analogues and is known to be entropic in origin. It is clearly seen that the association of a bidentate ligand and a cation is a two-particle process while a cation binding to two unidentate ligands is a three-particle process [Figure 9, above]; the latter is therefore entropically less favourable.
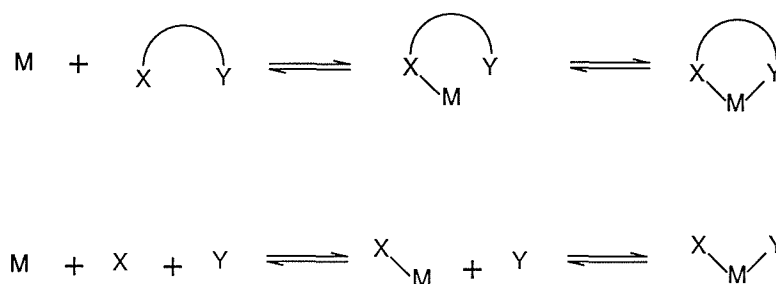
Figure 9: Equations depicting the two particle vs. three particle association of bidentate and unidentate ligands

However, complexation by a macrocycle or an acyclic analogue is always a two-particle process. The nature of crown ethers and the cations with which they are forming complexes, influences whether enthalpy or entropy dominates. Interaction of crown ethers with alkali metal and alkaline earth cations tends to be enthalpically controlled, whereas for aza-crown systems complexed with transition metals the thermodynamic origin is less well defined.

The essential factor in the macrocyclic effect is the preorganisation of the ligand. The difference between the cavity size of the host and the size of the guest does not vary considerably from crown to open chain but the difference in association constants can be substantial [Table 2].

	Cation	Solvent	Log K_a
18-Crown-6	K^+	MeOH	6.08
Pentaglyme	K^+	MeOH	2.30

Table 2: Example of the macrocyclic effect

The reason for the large effect of preorganisation can be explained through the relative amounts of conformational adjustment needed for complexation to occur. While a macrocycle needs little reorganisation (assuming the cavity and cation are suitably paired) an open chain ligand needs to undergo a significant change in its conformation, which is both enthalpically and entropically expensive. In effect, the entropic penalty is 'prepaid' during the synthesis of the crown. However, as Figure 10 shows, while a crown ether has a much reduced entropic barrier to complexation, the crumpled conformation it adopts in the solid state, where the methylene groups are disposed *anti* to one another, requires reorganisation to a *gauche* geometry upon complexation. The entropic penalty for this reduces binding efficiency. The rigid 3D nature of cryptands means this effect is reduced giving a high level of preorganisation and consequently cryptates have very high complex stability.
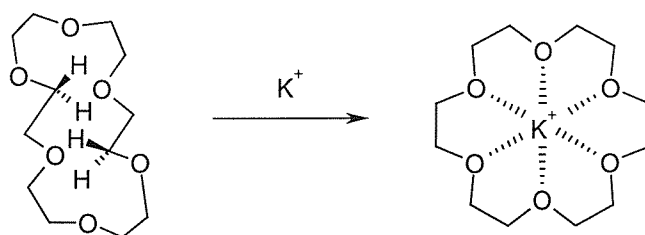
Figure 10: Reorganisation of 18-crown-6 upon complexation of potassium

This however is the case for the solid state and in solution, the crown will try to change its conformation to suit the solvent, turning the hydrophilic oxygen heteroatoms outward in a polar solvent and vice versa for a non-polar solvent. It is therefore possible to aid complexation by choosing a favourable solvent.

Three additional factors that also contribute are: (i) the reduced energy strain (favourable $\rightarrow G$) achieved by ion complexation arising from the increased solubility leading to reduced dipole-dipole repulsion in the cavity; (ii) the symmetry of the molecule, which contributes to greater donor atom basicity creating a stronger ligand field than its open chain counterparts[36] (again leading to favourable $\rightarrow G$); and (iii) compatibility of the donor atoms, 'soft' donor atoms such as sulfur preferring soft cations while 'hard' donors such as oxygen favour hard cations. Poor matching of donor and cation will lead to low complex stability. These factors all suggest that enthalpic changes dominate over entropic changes in the macrocyclic effect.

1.3.1.4 Size Selectivity

In addition to the increased binding strength attributed to the macrocyclic effect, a macrocycle will also show considerable size selectivity between different guest ions. This effect is most noticeable for crown ethers combined with non-transition metal cations. Clearly, when a metal-ion radius matches that of the internal cavity of a host ligand, optimal ion-donor atom distances can be achieved and the resulting complex will be more stable than a poorly matching host-guest pair [Table 1]. In some cases a poor match of cavity size and cation can lead to enhanced binding strength through complexation stoichiometries other than 1:1.

	Radius (pm)	Solvent	Log K_a of 15C5 (r = 86-92pm)	Log K_a of 18C6 (r = 134-143pm)	Log K_a of 21C7 (r ~ 170pm)
Na^+	95	MeOH	3.48	4.38	1.73
Cs^+	169	MeOH	2.18	4.79	5.01

Where r = cavity radius

Table 3: Size selectivity of three crowns with sodium and caesium ions

However, although size matching is definitely the predominant effect, some combinations of macrocycle and metal ion do not give the expected results for binding strength, which suggests that in such cases other factors are important. These include conformational changes of the macrocycle and differences in solvation patterns from cation to cation. A macrocyclic ligand may adopt a completely different conformation when complexed compared with that of its free state, with the result that calculations of selectivity based on free ligand cavity size could easily lead to inaccurate predictions. In addition, a flexible ligand may be able to adopt several different conformations as well as change its cavity size in order to accommodate different cations. For this reason, flexible ligands often show a reasonable level of selectivity for a range of cations. Conversely, rigid ligands exhibit much greater size selectivity and this is shown for cryptands with increased size selectivity and epitomised in spherands, ligands which are so rigid that they are totally pre-organised and undergo no conformational change upon binding.[37]

1.3.1.5 Solvent Effects

Solvation of the crown and cation play an important role in determining the selectivity of binding. Assuming the crown is neutral, donor groups inside the cavity will be poorly solvated and the ΔH and ΔS effects upon complexation will be small. The desolvation of a metal ion upon complexation is a far more significant factor, so much so that a different solvent or even different solvation pattern can have a considerable effect on the size selectivity of the macrocycle, towards a cation. Figure 11[38] shows the drastic change in selectivity that 15-crown-5 displays towards different alkali metals upon changing the solvent from methanol to acetonitrile. This can be rationalised by the solvent's interaction with the cation, compared to methanol, acetonitrile stabilises large cations but destabilises small cations, therefore preferably binding the latter. In addition the solvation energies for Rb^+ and Cs^+ are lower than that of Li^+-K^+, resulting in an enhanced affinity.
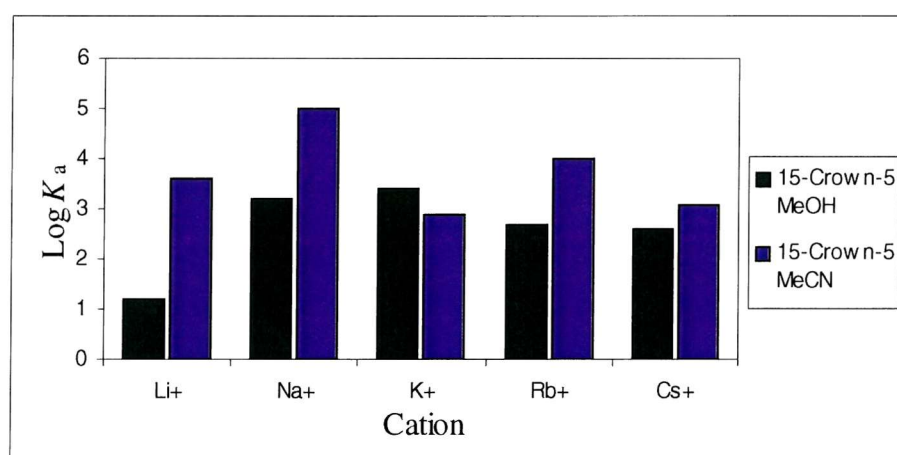
Figure 11: Change in complexation selectivity with solvent for 15-crown-5

1.3.1.6 Known Selectivity

The ions of interest in the present work are sodium and potassium and current sensors for these are based on a 15-crown-5 template. A study of the relevant review[25] data shows how binding constants for sodium and potassium ions are very similar for a series of 15-crown-5 systems-based systems [see Figure 12, below]. It is clear that the introduction of nitrogen in place of a ring oxygen, drastically reduces the binding strength but a benzene molecule incorporated into the crown has little effect and the binding with potassium is actually increased. However, there is little or no data for dibenzo-15-crown-5 or any combination of aza and benzo crowns. Hopefully, there is scope for the manipulation of these structural properties to modify selectivity.
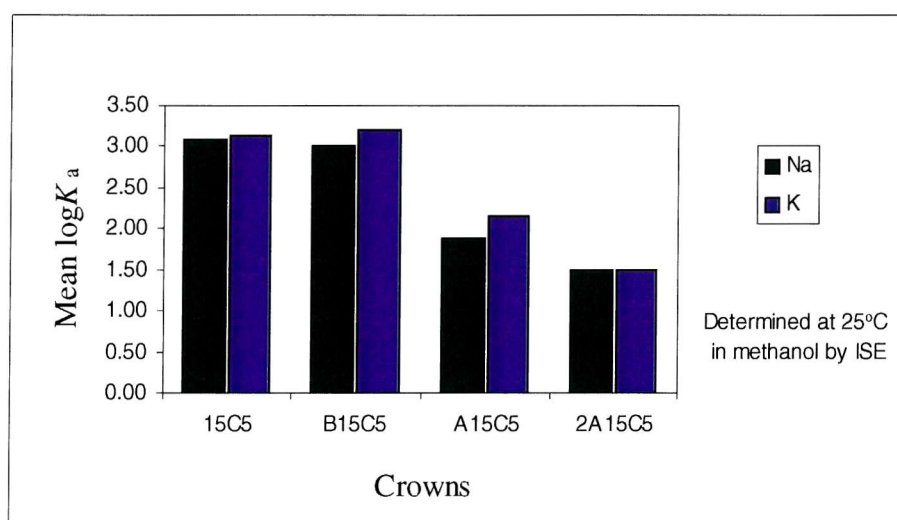
Figure 12: Log K_a values for Na^+ and K^+ ions plotted against a range of crowns[25]

1.3.2 Crown Ether Synthesis

Today, a desired property rather than a specific structure of the target determines the design of a particular crown ether. There are three main factors to consider when designing a synthetic target; (i) the ring size; (ii) the inclusion of any heteroatoms other than oxygen; and (iii) whether any ancillary units are required (sidearms, aromatics etc.). Once these have been addressed there are two basic synthetic approaches to choose from; nucleophilic substitution using an incipient macro-ring donor atom as the nucleophile;[39] or a one-to-one reaction of diamine and diacid chloride. The latter relies on high dilution techniques whilst the former exploits 'the template effect'. Both methods push the reaction in favour of the first order cyclisation pathway relative to second order polymerisation processes.

1.3.2.1 High Dilution Methods

The principle of high dilution is simple in that the cyclisation process is favoured through distribution of individual molecules throughout a large bulk of the solvent, thereby reducing the chance of an intermolecular reaction and increasing the chances of intramolecular processes. This method therefore promotes the first order (cyclisation) process as its rate is increased relative to that of polymerisation.

For cyclisation:

$$Rate_{cyc} \propto [Substrate]$$

Whereas for polymerisation:

$$Rate_{pol} \propto [Substrate]^2$$

The most straightforward way to create these conditions would seem to be through use of a small quantity of reactants dissolved in a vast volume of solvent. However, because of the large volumes of solvent required compared with the small mass of product produced, this is highly impractical. A more judicious method is to have a small amount of solvent and to add the reagents slowly *via* a syringe. As long as the rate of reaction is faster than the rate of addition, the overall reaction concentration is kept to a minimum and a pseudo-high dilution state is therefore achieved.

1.3.2.2 The Template Effect

In Pedersen's original synthesis [Scheme 1, above] the concentration was too high to be considered high dilution, so what caused cyclisation? Again the reaction was forced towards the first order process but in this case the intermediate polyether chain organised itself around a cation thereby forcing the end groups into close proximity and promoting an intramolecular reaction pathway [Scheme 3].
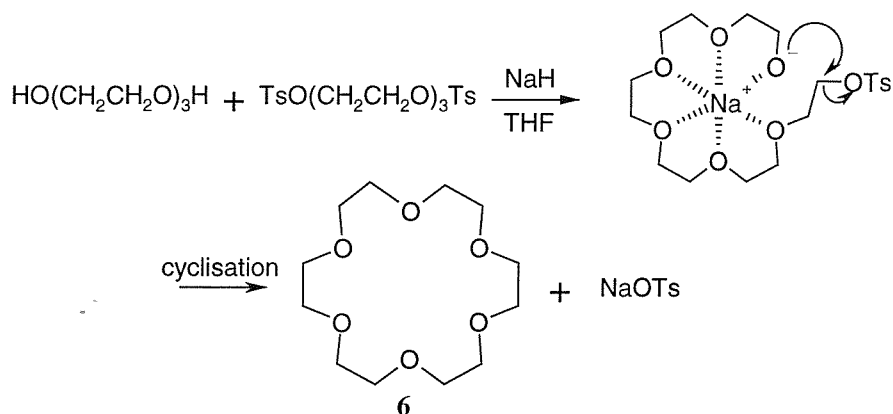
Scheme 3: Synthesis of 18-crown-6 (6) with 'the template effect'

Pedersen was far from the first to notice this phenomenon, or even to name it. Several years earlier Daryl Busch had shown that formation of cyclam (7) could be templated by transition metals.

1.4 Chromophores and Fluorophores

Once a crown ether has been designed and synthesised, its purpose will often involve binding cations. In order to determine their ability to do so, binding studies must be undertaken. These studies aim to quantify the stabilities of the complexes formed, using thermodynamic or kinetic techniques. Such measurements give values for K_a, ΔH and ΔS for the interaction of a crown ether (or any macrocycle) with a cation (or other guest molecule). The results are not definitive, as they depend not only on the technique used but also on the solvent involved. However they do give values which allow for comparison and therefore determination of the relative binding effectiveness of different host-guest combinations. Extensive work in this area has led to the publication of several review articles, the most well known perhaps being those by Izatt and co-workers.[25]

There are a variety of spectroscopic methods which can be used to determine association constants such as NMR, IR, UV or fluorescence. UV and fluorescence studies are made possible by the presence of a suitable chromophore attached to the crown that can be monitored and quantified as a measure of binding strength or selectivity. Ultimately, fluorescence is a more desirable property, as fluorescence can be switched on by co-ordination to a metal ion (see 1.4.2.2), whereas the UV absorbance may alter only very slightly upon binding. The fluorescence response is also likely to be of a larger magnitude, thus making measurement much easier.

1.4.1 Chromophores

Crown ether chemistry has been used for the determination of alkali metal-ion concentrations through creation of chromoionophores[40c] (i.e. compounds in which a metal-ion binding host has a chromophore incorporated within its structure) which undergo a colour change on complex formation.

1.4.1.1 Ultraviolet Visible Theory

UV absorbance is caused by transitions between electronic energy levels. The wavelength of absorption is a measure of the separation of these levels. The excitation of electrons from p-, d- or ᴨ- orbitals and especially ᴨ-conjugated systems gives rise to absorbencies above 200nm. The chromophore describes the system containing the electrons undergoing excitation. The probability of exciting an electron from one orbital to another upon irradiation is dependent on the length of that kind of chromophore and in general, the longer the chromophore, the stronger the absorption. In addition the longer the conjugation, the longer the wavelength of the absorption maximum.[41]

1.4.1.2 Background

Vögtle has published much work in this field.[40] He has shown how simple, UV

responsive units can be attached through either a ring nitrogen or an aromatic

substitutent. He has synthesised a range of neutral chromoionophores that give a UV

response. They can be divided into two types depending on the change in that

response as a result of metal-ion complexation, either hypsochromic band shifts (to

longer wavelengths) or bathochromic band shifts (to shorter wavelengths) being

observed. Structurally the two types are very similar, the basic difference being the

orientation of the chromophore.
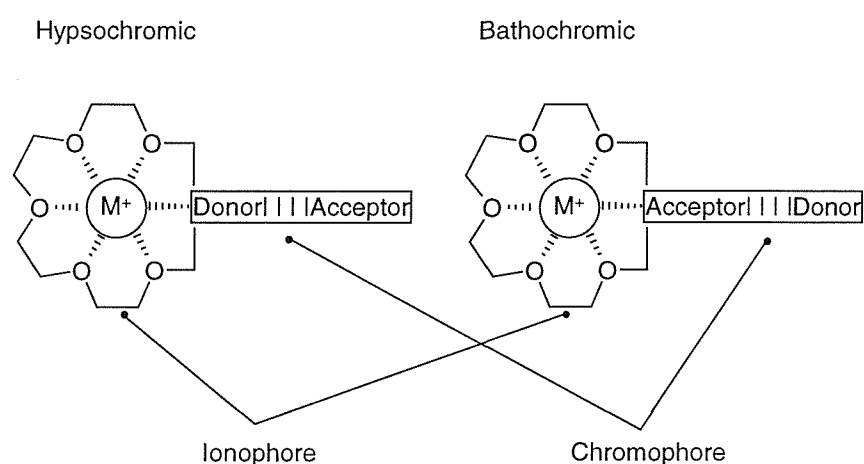
Figure 13: Structures of hypsochromic and bathochromic chromoionophores

The principle behind this design strategy is relatively simple. A hypsochromic sensor

has the electronic donor end of the chromophore positioned to allow maximum

interaction between the metal ion and the chromophore. Upon photoexcitation, there is

a net change in the electronic distribution across the chromophore from the donor to

the acceptor end. The effect of metal ion complexation is to destabilise the excited

state while stabilising the ground state of the chromophore comparison with the

electronic states of the uncomplexed sensor. The resulting structural change [Figure

14, above] therefore gives rise to a hypsochromic shift of the absorption maxima.
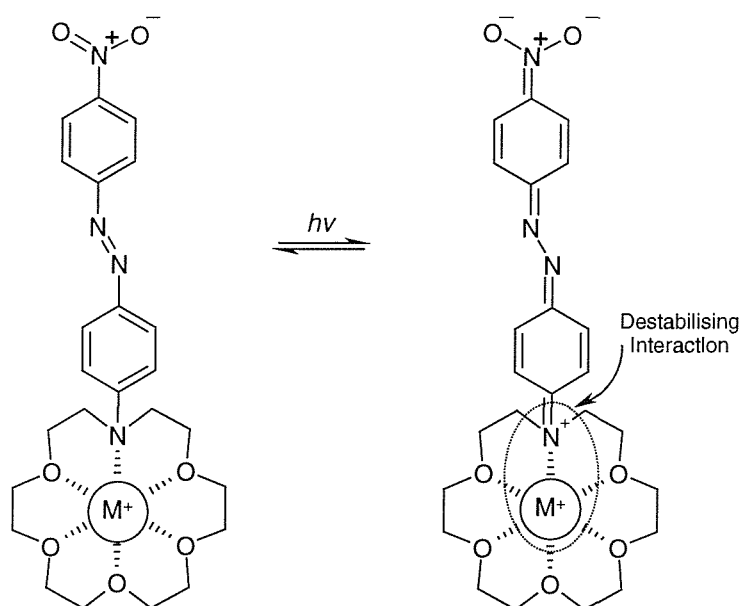
Figure 14: Structural change in a chromoionophore upon photoexcitation

The converse is obviously the case for bathochromic shifting sensors that rely on the electronic acceptor-end interacting with the metal-ion to stabilise the excited state and destabilise the ground state.

One objective of the present study was to investigate whether the combination of a simple crown ether with a colour responsive moiety such as an azo-dye can provide a useful quantitative metal-ion sensor.
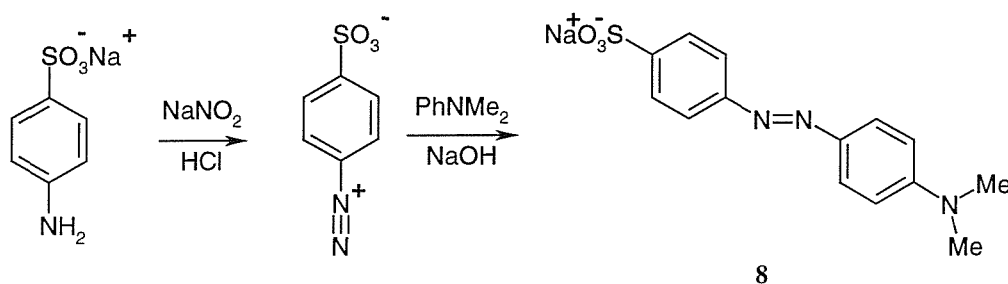
Scheme 4: Synthesis of Methyl Orange (**8**), an early azo-dye

Methyl Orange, an early and simple azo-dye offers a useful starting point for selecting a chromophore which could be incorporated into a crown-based sensor. The synthesis is simple[42] and azo-dyes have the advantage of possible incorporation through either a ring nitrogen or through a benzene ring.
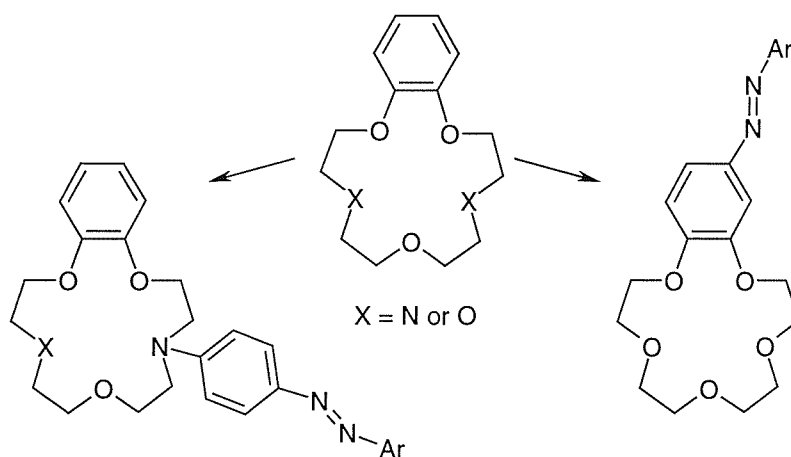
Figure 15: Two possible points for attachment for an azo-dye to benzo-crown ethers

1.4.2 Fluorophores

An analogous approach to the problem involves incorporation of a fluorescent component into the crown ether skeleton, giving rise to a fluoroionophore.

1.4.2.1 Fluorescence Theory

Fluorescence is a type of luminescence caused by the absorption of a photon and subsequent loss of energy through a fast radiative process [Figure 16]. A singlet excited state is created upon photon absorption which can return to the ground state via a radiative (fluorescence) or non-radiative process (internal conversion) or can be transformed into a lower energy triplet state (intersystem crossing). The radiative decay of the triplet state is called phosphorescence. Fluorescence is the dominant process for low molecular weight compounds in solution, as phosphorescence is collision quenched at room temperature.
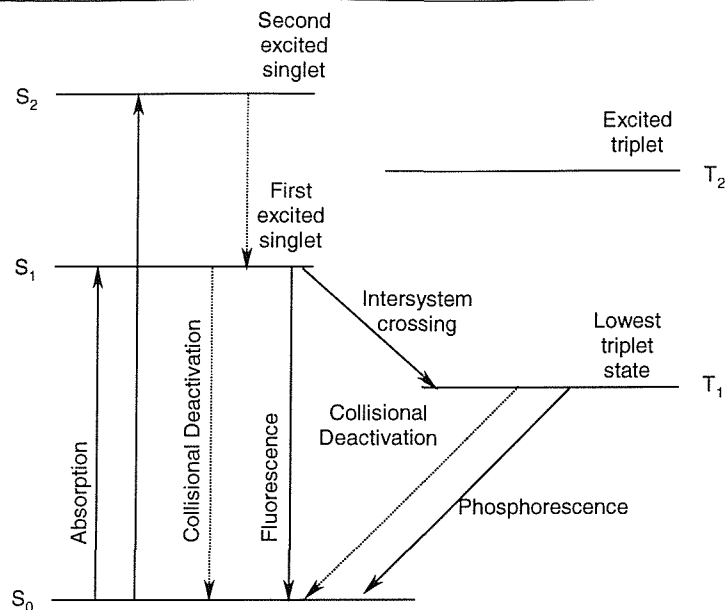
Figure 16: Schematic energy-level diagram of a polyatomic molecule

Exactly what properties ensure fluorescence is unclear, although both the presence of conjugated double bonds and molecular rigidity are thought to be important factors. For example both fluorescein (**9**) and the analogous phenolphthalein (**10**) strongly absorb light but only the former is fluorescent.[38]
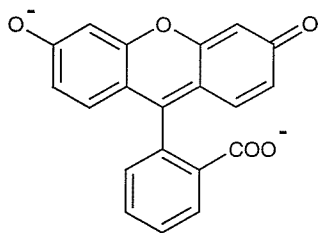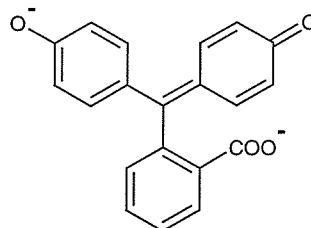
9   **10**

1.4.2.2 Background

A significant volume of literature has been published in this area, with especially relevant work being performed by de Silva and co-workers.[43] His studies have progressed from the simple fluorescence of anthracene derivatives, *via* anthracene functionalised crowns, to the design of photoionic devices using ion receptors and fluorophores. His work relating to crowns and their use as sensors is of obvious value to the present study. The first reported crown moieties used were *N*-(9-anthrylmethyl)monoaza-18-crown-6 (**11a**; $n = 1$) and its 15-crown-5 analogue (**11b**; $n = 0$). The behaviour of these was compared with that of *N*-(9-anthrylmethyl)diethanolamine (**12**), and all three were found to be weakly fluorescent.

11   **11a**; $n = 1$ **12**
             11b; $n = 0$
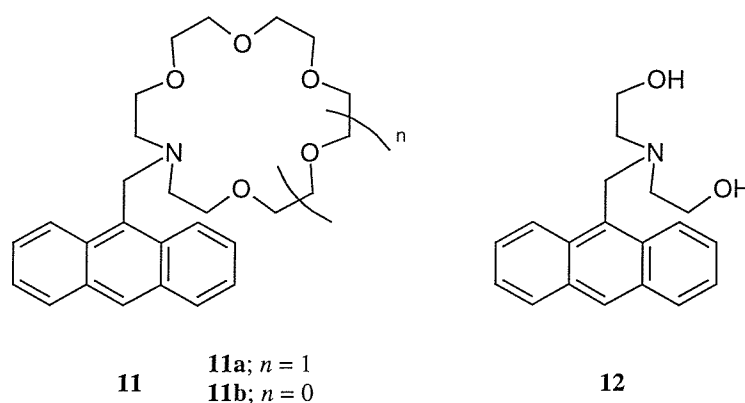
It was discovered, however, that the addition of sodium or potassium ions resulted in increases in fluorescence quantum yield of up to 47 times for crowns **11a** and **11b** but gave no corresponding increase in the case of the open chain analogue **12**. This phenomenon was named photo-induced electron transfer (PET). It was explained by the presence of a free nitrogen lone pair, which can quench the fluorescence of the anthracene in the parent ligand, a process which is not possible when it is involved in complexation of an alkali metal, i.e. fluorescence is 'switched on' during binding [see Figure 17, above]. It is worth noting that during complexation, absorption and emission spectral parameters remained unaffected.

PET quenches fluorescence   PET not possible
(free lone pair)   (Lone pair involved in complexation)
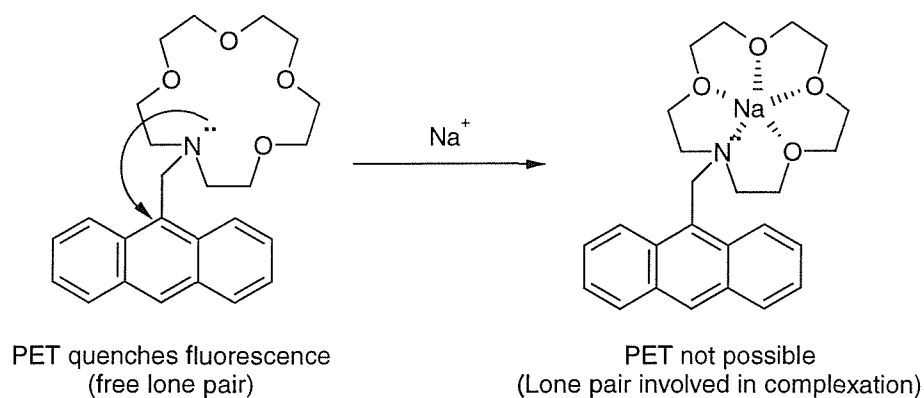
Figure 17: Diagrammatic representation of PET quenched fluorescence

In later work, he showed how a similar anthracene unit could be attached to the benzene ring of a benzo-crown. These designs (**13b, 13c**) again showed greatly increased fluorescence upon complexation with alkali metals but there was no change in other spectral properties. Such structures also overcame the problem present in previous sensors where the presence of a basic nitrogen could lead to an undesirable increase in fluorescence as a result of protonation.
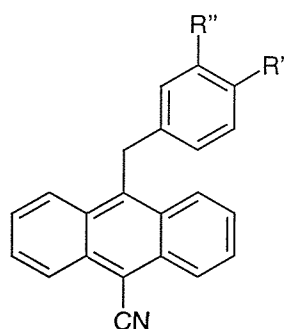
13a; R' = R" = OMe
13b; R' = R" = $(OCH_2CH_2)_4O$
13c; R' = R" = $(OCH_2CH_2)_5O$

13

In extended work, beyond the scope of this study, de Silva went on to create a molecular "AND gate" (**14**) by combining the two principles above. Here the anthracene is bound to nitrogen, which in turn is attached to the benzene of benzo-15-crown-5. This species gives different fluorescent responses to hydrogen ions, sodium ions or both giving the input (chemical binding) and output (fluorescence intensity) characteristic of an "AND gate".
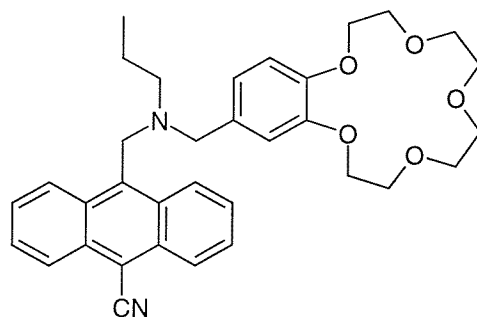
14

The above work shows the potential for attachment of a fluorescent unit to any synthesised crowns. Whilst de Silva's work exclusively uses anthracene as its fluorophore there is also the possibility of using naphthalene as an equally efficient indicator. Any crown synthesised for the present study would ideally incorporate both aromatic and nitrogen sites as possible fluorophore attachment points.

1.5 Incorporation of an Ester Functionality

1.5.1 Background

The presence of an ester group is vital to the function of any sensor produced in this study as it allows the probe to be used for both extra and intracellular studies. Current probes come in esterified and non-esterified (i.e. free acid) forms. The ester groups allow the probe to permeate the cell's lipid membrane, after which they are hydrolysed by cystolic esterases native to the cell's interior. This renders them impermeable and any subsequent measurements are purely intracellular. Using the previous example of SBFI, typically suitable esters are the acetoxymethyl (CH_2OCOCH_3) group.
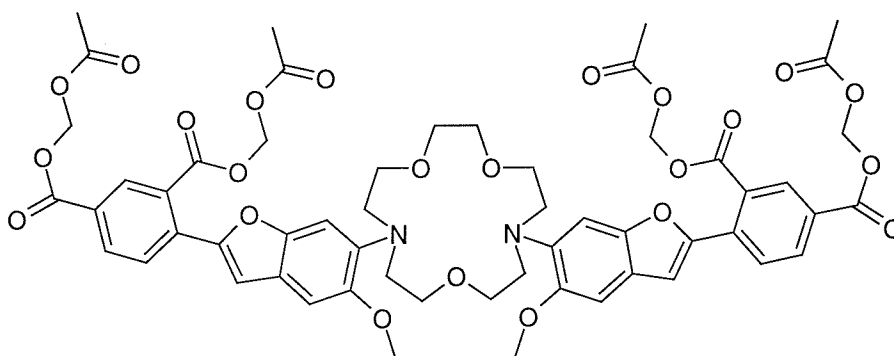
15

1.5.2 Ester Location and Incorporation

The ester functionality in SBFI-AM (**15**) is an integral part of the fluorescent sidearm. If this characteristic is replicated, any synthetic route to a probe will have to attach the ester group to the fluorescent sidearm before or after it is itself bound to the crown. This however is not the only possible option for attachment. If one of the two secondary amine sites were to be selectively protected then one site could be functionalised with a fluorescent side arm and the other site, after de-protection, could be functionalised with an ester. In addition, if the crown contains aromatic bridges between the heteroatoms instead of ethylene bridges, it is conceivable that an ester could be attached to an aromatic unit.

1.6 Aims of the Research

- To synthesise a crown based on the diaza-15-crown-5 skeleton (**16**) that has selectivity a for sodium ion in the presence of other cations.

16
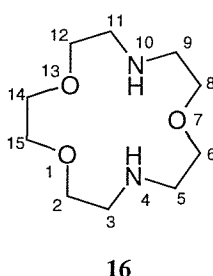
- To incorporate a species that will give a definitive optical response to binding.

- To incorporate an ester functionality to allow for transport into and, after hydrolysis, solubility within biological cells

2 RESULTS AND DISCUSSION

2.1 Route to 14,15-Benzo-4,5-diaza-15-crown-5

The first synthetic target was the benzodiaza-15-crown-5 (**17**), a crown ether incorporating a single benzene unit attached at the 14 and 15 positions of the macrocyclic ring. A retrosynthetic analysis suggests an obvious route to the desired target.[44]
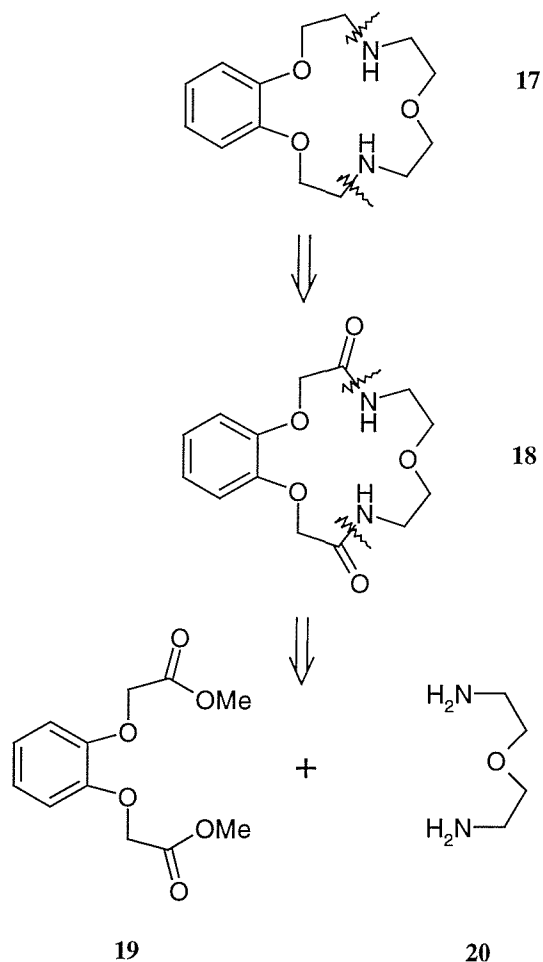
Scheme 5: Retrosynthetic analysis of benzodiaza-15-crown-5 (**17**)

The formation and reduction of two amide bonds shown here provides an efficient synthesis for the macrocyclic ring as well as incorporating the desired nitrogen atoms.

2.1.1 Synthesis of Dimethyl Ester
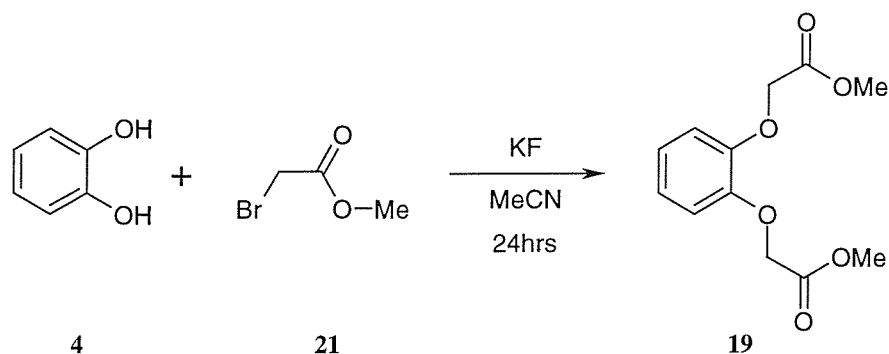
Scheme 6: Synthesis of dimethyl ester **19**

This process is readily carried out following Amabilino's procedure for the preparation of the analogous diethyl ester.[45] This reaction appears to be quite straightforward yet has several complicating factors. Firstly, the standard method requires use of a seven-fold excess of potassium fluoride to ensure complete sequential deprotonation of the catechol. The presence of this excess of solid material requires continual mechanical stirring yet the reaction also needs a nitrogen atmosphere and reflux conditions for 24 hours. For these reasons, the set up of the apparatus is critical. Unfortunately, the first time this was attempted the reaction boiled dry as a result of an unidentified leak and although work-up was attempted, no product was isolated from the reaction. However, when the procedure was repeated, the product was successfully isolated in 62% yield.

2.1.2 Synthesis of Diamine 20

The basic unit employed as a starting material was diethylene glycol, the alcohol functionalities of which must first be turned into good leaving groups in order to allow conversion into the diamine using the Gabriel Synthesis.[46]

2.1.2.1 Modification of Alcohol Functionality in Diethylene Glycol

Initial studies have suggested that halides are the most effective leaving group.[46] However, previous work in this area has come across difficulty in the first step of the Gabriel Synthesis,[47] namely very low yields that prevented further progress. It was therefore decided initially to convert the alcohol into a ditosylate as this should provide a convenient synthetic route *via* a potentially crystalline intermediate.

The diethylene glycol was treated with a two and a half molar excess of tosyl-chloride in DCM and pyridine was used to ensure full substitution, successfully producing the di-tosylate (**22**) in high yield (86%).

2.1.2.2 Gabriel Synthesis Step One

This step involves the simple nucleophilic substitution of the tosylate leaving group by a phthalimide anion.
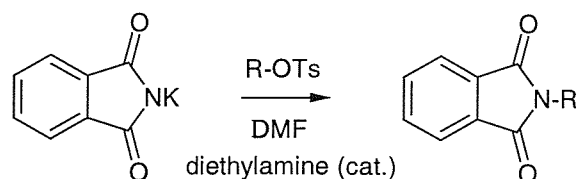
Scheme 7: Step one of the Gabriel synthesis

The mechanism is most likely an S_N2 process as the molecule is a primary tosylate and the presence of DMF solvent will increase the nucleophilicity of the anion.[48]

A moderate yield was achieved in this step (50%) but this was most likely a reflection of difficulties arising in the removal of the DMF.

2.1.2.3 Gabriel Synthesis Step Two

The second step involves the removal of the phthalimide functionality which can be achieved by either hydrolysis or hydrazinolysis.[46] The latter was chosen and a mechanism for this process is outlined below.

However, isolation of the desired amine product from this reaction proved to be difficult. This is most likely a reflection of the high water solubility of the product, a problem which would also arise in the alternative option, base catalysed imide hydrolysis. Possibilities for the modification of the experimental procedure were investigated and an alternative approach was discovered which overcame these difficulties
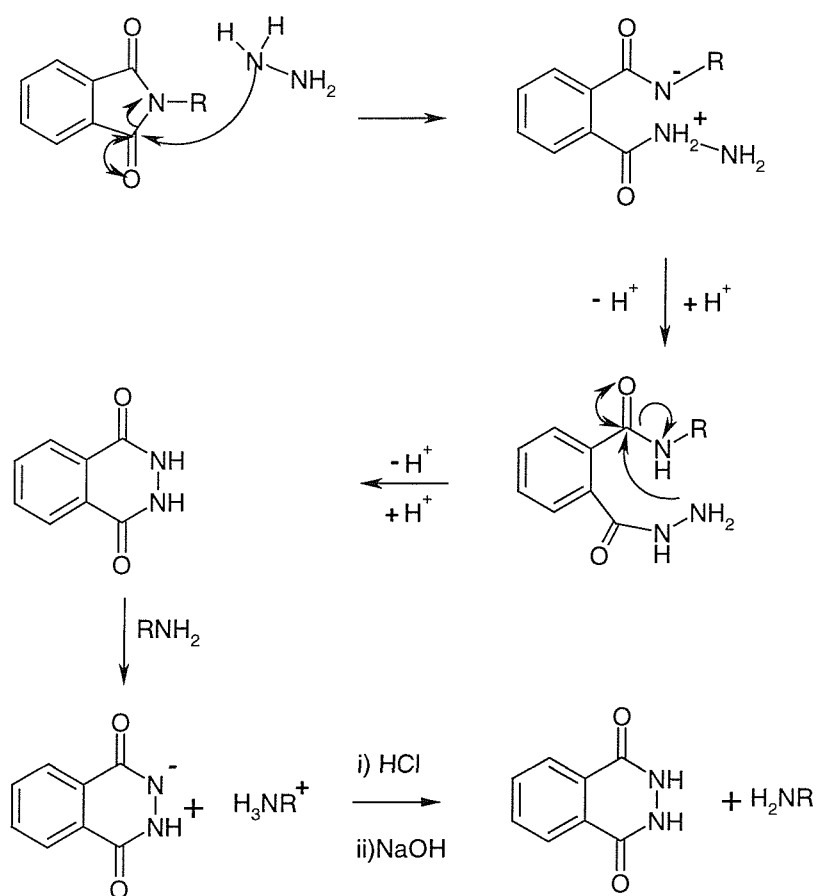
Scheme 8: Mechanism of the second step of the Gabriel synthesis - hydrazinolysis

2.1.2.4 Alternative to Gabriel Step Two

The synthesis of the diamine **20** was achieved by reacting the diphthalimide **23** species with a eutectic mixture of KOH and NaOH. The diamine was isolated in a relatively disappointing 33% yield, again probably a reflection of the high water solubility of the product making isolation difficult.

2.1.3 Cyclisation of Dimethyl Ester 19 and Diamine 20
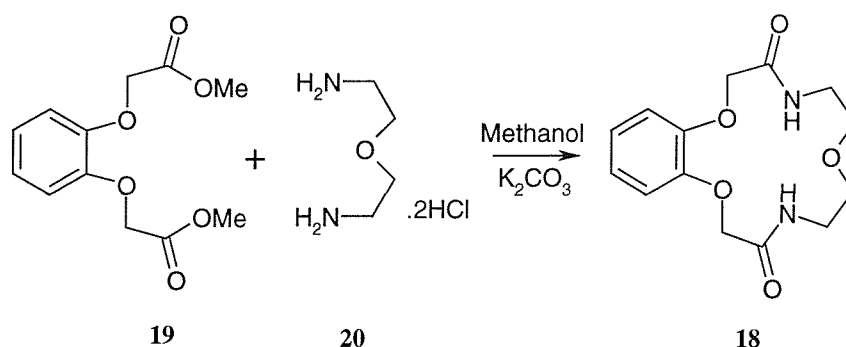
Scheme 9: Cyclisation of dimethyl ester **19** and diamine **20**

The reaction was successfully carried out using either the diamine as its hydrochloride salt in the presence of an equivalent of base, or with the free amine itself, the yields being good (76% and 71%) in both cases. Surprisingly, this process does not seem to require high dilution or templating in order to produce a moderate yield,[44] unlike reaction of diamine with diacid chloride mentioned in section 1.3.2.1. Undoubtedly the potassium carbonate would act as a possible source of a templating cation but the reaction is almost identically efficient with or without the base.

2.1.4 Reduction of Benzodiamide-15-crown-5 to its Diamine (17)

Two possible routes were considered for this reduction: either LiAlH$_4$ or borane in THF solution. It was decided that borane would give a cleaner and more efficient route to the desired product. The product was isolated in a reasonable yield (63%), thought this is a little lower than that previously reported,[44] but some problems with solvent loss overnight could have contributed to this. Scheme 10, below, summarises the synthetic route to **16**, with an overall yield of 5% over five steps.
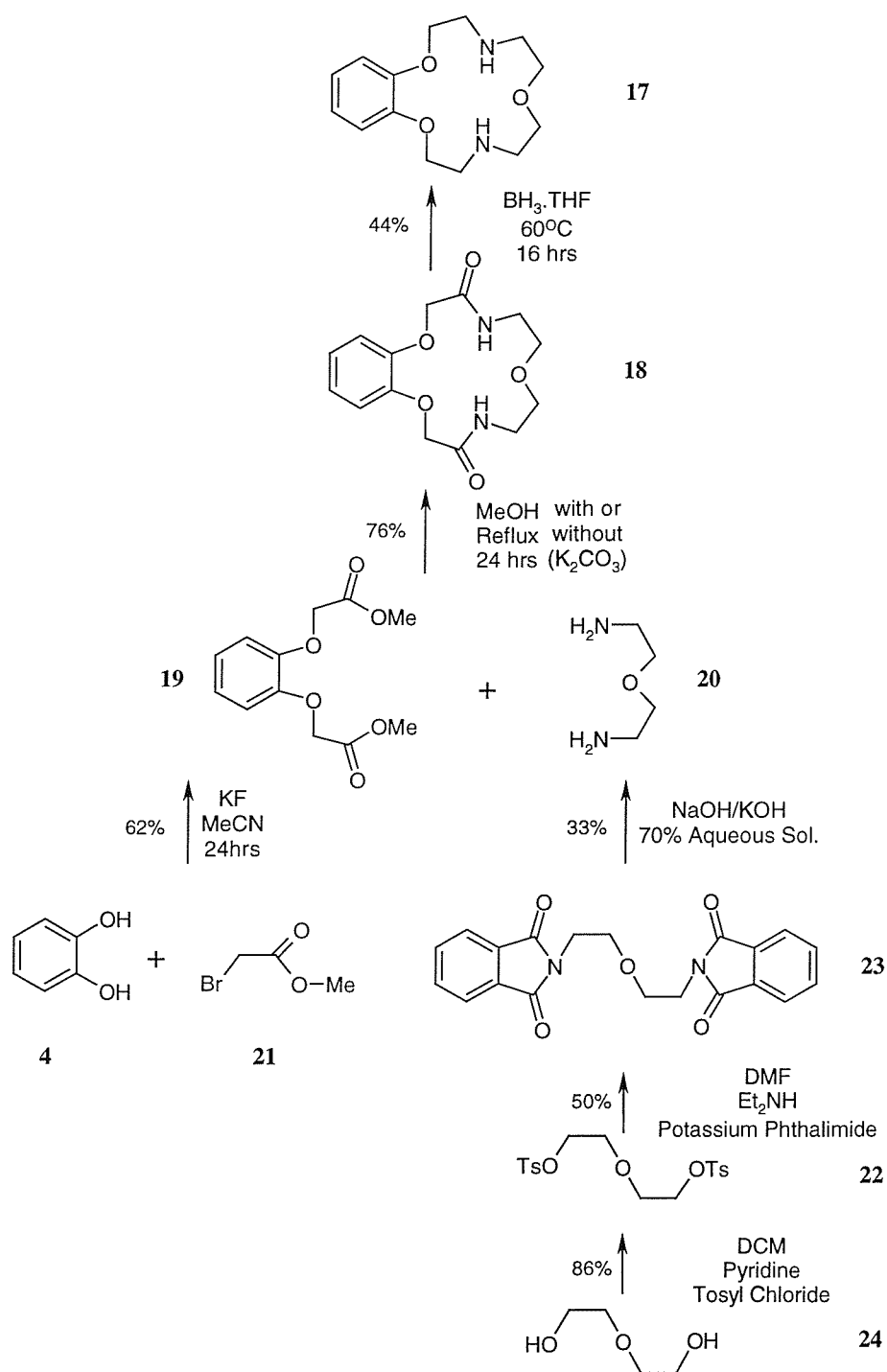
Scheme 10: Complete synthesis of 14,15-benzo-4,10-diaza-15-crown-5 (**17**)

2.2 Route to 5,6,8,9-Dibenzo-4,10-diaza-15-crown-5

It was recognised that while one benzene ring added some rigidity to the 15-membered ring, the effect would be even more pronounced with two rings. With this in mind and the desire to preserve the symmetry of the molecule (for ease of synthesis alone!) a study of a diaza-crown ether incorporating two benzene rings (in the 2,3 and 11,12 positions respectively) was proposed. The positions of the benzene rings required a slightly different synthetic approach to obtain the desired product [Scheme 11].
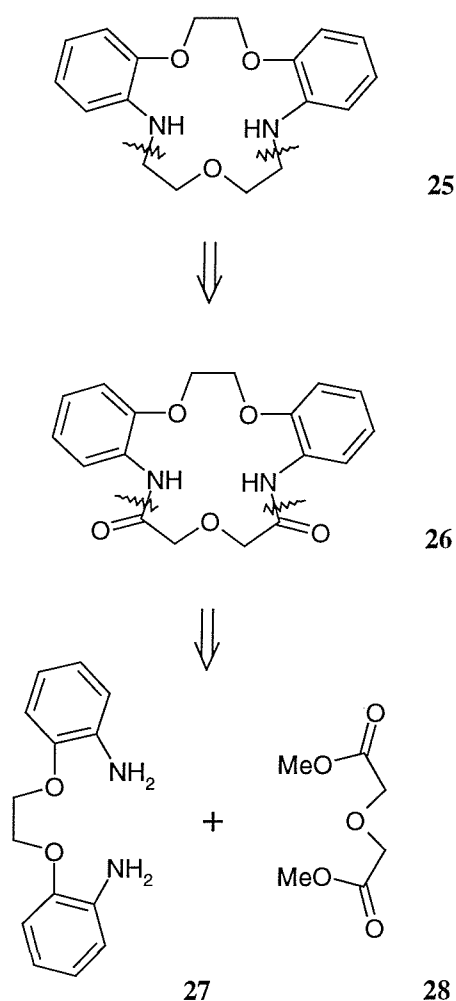
Scheme 11: Retrosynthetic analysis of dibenzo-15-crown-5

This analysis gives two precursors, which can each be synthesised from readily available starting materials.

2.2.1 Synthesis of Dinitro Ether 29

This method was adapted from a literature method[49] which had been concerned with the preparation of an unsymmetrical diamine (namely one with a methyl group *para* to the amine in one aromatic ring). The reaction involves the treatment of 2-nitrophenol with dibromoethane in the presence of potassium carbonate [Scheme 12, above] and although successful, the yield achieved in the present work was disappointingly low (49%) for such a simple reaction. As noted in section 2.1.2.2, difficulties with DMF removal could be a contributory factor here.
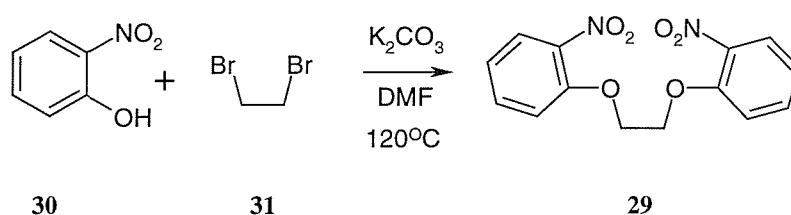
Scheme 12: Synthesis of dinitro compound 29

2.2.2 Reduction of the Dinitro Ether 29 to the Diamine 27

This reduction was performed using hydrazine and palladium over charcoal, the product being isolated in 69% yield, slightly less than that previously reported.[50] This may reflect the quality of the hydrazine used, or losses during removal of the catalyst by filtration through silica as Celite™ was not totally efficient in separating the palladium/charcoal from the desired filtrate.

2.2.3 Synthesis of Dimethyl Ester 28

The dimethyl ester 28 which is the other component required for the formation of the desired macrocycle is unlike its counterpart (19) in the synthesis of benzodiaza-15-crown-5 (17) as it can be directly prepared from the commercially available diglycolic acid [Scheme 13, below].

2.2.3.1 One Step Conversion A

The synthesis of the dimethyl ester 24 was performed by a literature[51] method giving a satisfactory yield of 28 (50%) allowing the synthesis to progress. Two attempts to improve upon this by adopting a different route met with little success.
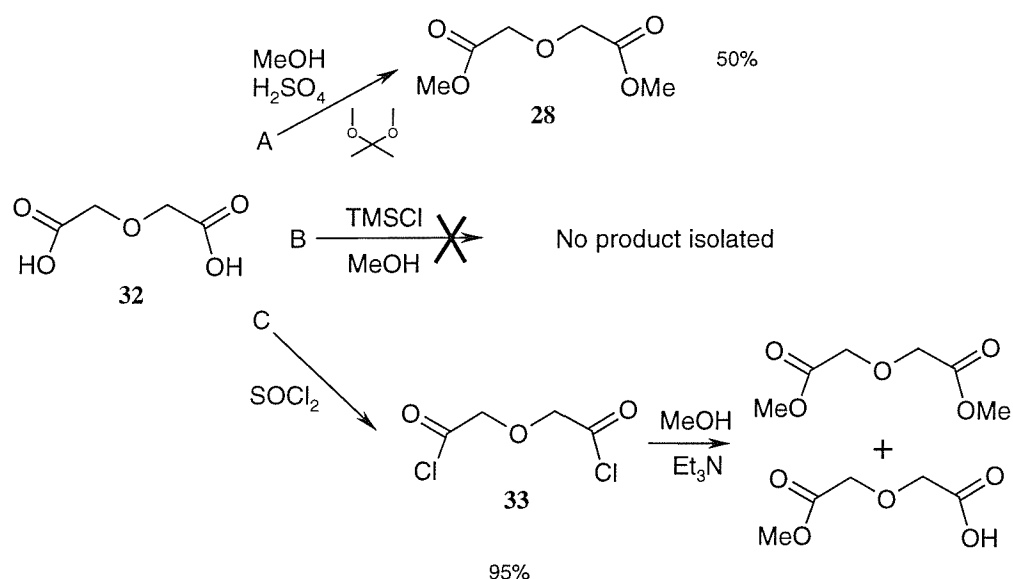
Scheme 13: Attempted routes to dimethyl ester **28**

2.2.3.2 One Step Conversion B

In an effort to find a more efficient route to the desired dimethyl ester **28**, diglycolic acid (**32**) was first treated with TMSCl and methanol. The reaction was tried twice, the second time with a four-fold increase in the reaction time. On both occasions, a white solid was isolated, however characterisation by NMR showed that this contained only starting material.

2.2.3.3 Two Step Conversion C

Once the direct route was ruled out, a two step route was investigated instead.[52] First the diacid **32** would be converted into the corresponding diacid chloride **29** and this would then be reacted with methanol to form the desired dimethyl ester. The acid chloride **33** was prepared by reaction with thionyl chloride. This produced a change in IR carbonyl stretching frequency from 1702 cm^{-1} for the diacid to 1800 cm^{-1} for the diacid chloride. However, in view of the sensitive and highly reactive nature of acid chlorides, the product was not purified beyond the removal of the excess thionyl chloride to give a 95% yield.

In the second step, diacid chloride **33** was reacted with methanol in the presence of excess triethylamine to mop up the HCl produced. The reaction was performed with dry reagents and under nitrogen, yet the solid product resisted recrystallisation attempts and is now an oil. It is possible that the recrystallisation solvent of ethanol has allowed for ester exchange. Characterisation has shown the presence of di- and monosubstituted methyl ester (^{13}C NMR shows three different carbonyl peaks, at δ 173, 171 and 170ppm).

2.2.4 Synthesis of Dibenzodiamide-15-crown-5 (26)
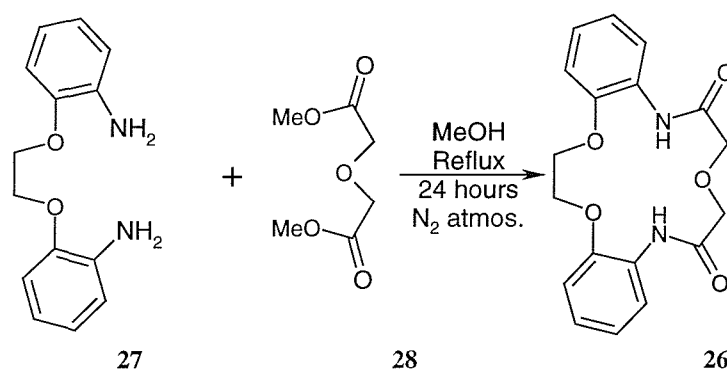
Scheme 14: Attempted cyclisation of dimethyl ester **28** and diamine **27**

Cyclisation was attempted in a manner similar to that used for the mono-benzo analogue (2.1.3) however this surprisingly proved unsuccessful with either an excess of starting diamine or of starting dimethyl ester. The probable reason is the reduced reactivity of aromatic amine **27** compared its aliphatic analogue amine **20**. Literature[53] suggested that it should be possible to induce cyclisation using high dilution techniques and by replacing the methyl ester by the more reactive acid chloride. This was successfully investigated [Scheme 15, below], producing the crown in 11% yield, problems with maintaining constant addition rates and reactant solubility contributing to the low yield.
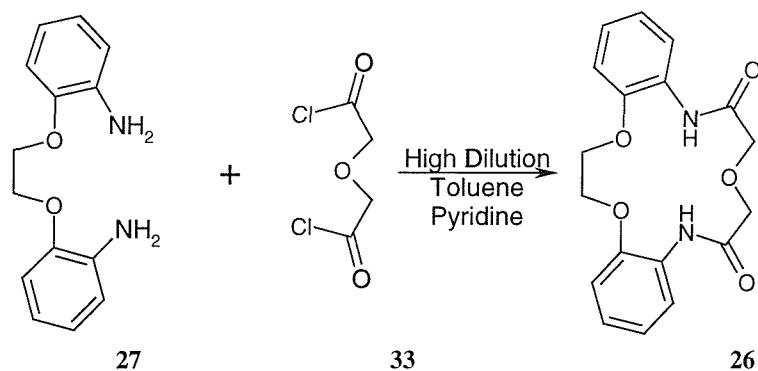
Scheme 15: High dilution cyclisation of dimethyl ester **27** and dicarbonyl chloride **31**

Unfortunately, time constraints and the need to explore functionalisation of the monobenzocrown in order to gain useful association constant data prevented an investigation of the reduction of the diamide crown to the diamine. The incomplete synthesis is summarised below, in Scheme 16.
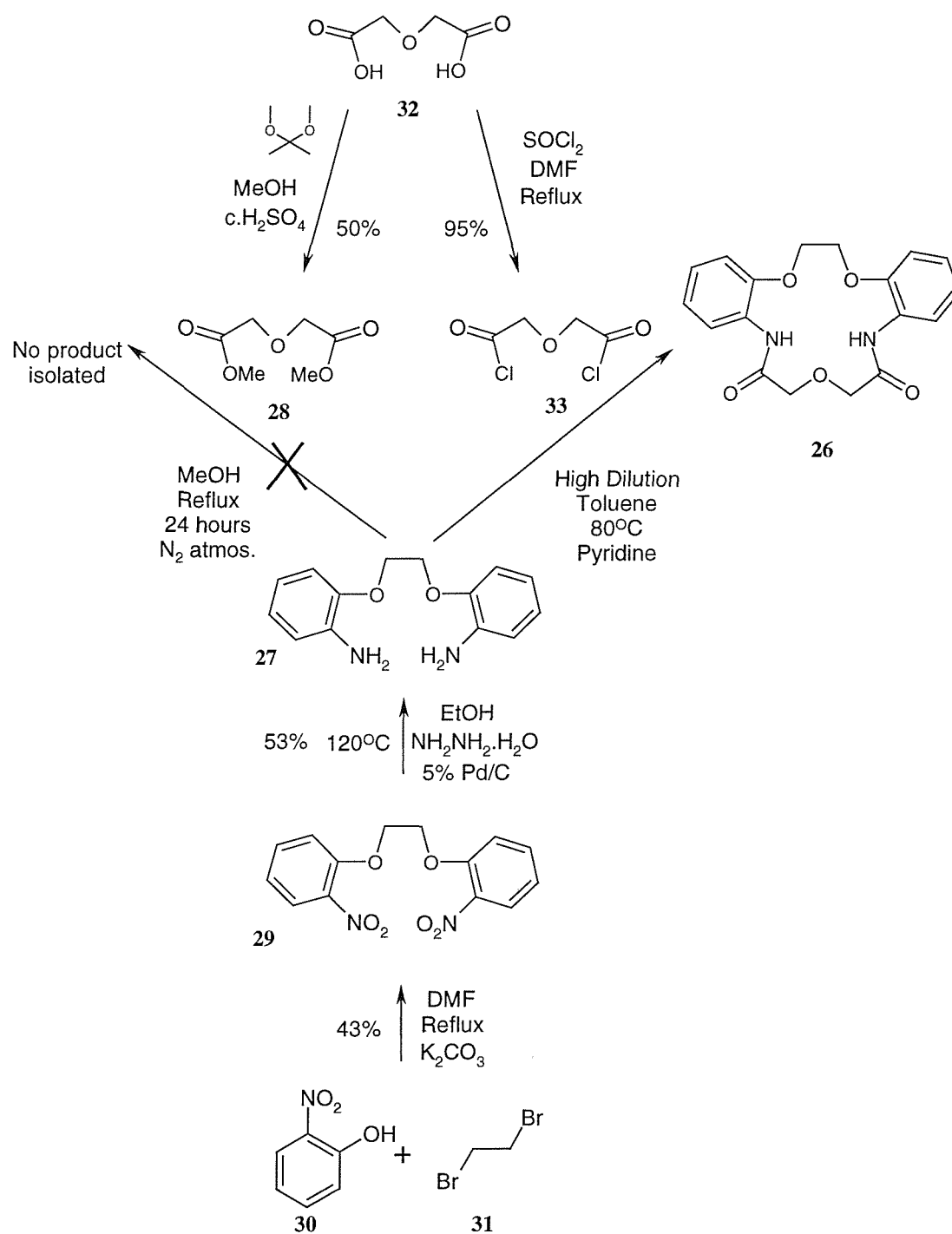
Scheme 16: Synthesis towards dibenzodiaza-15-crown-5

2.3 Incorporation of Azo-Dye Functionality

It was planned that simple azo-dyes would provide a logical starting point for possible chromophores and it was decided that attachment of these dyes should be investigated using analogues of the target crowns selected for study. The basic azo-dye unit involves the introduction of an azo (-N=N-) link between two aromatic systems. There are two logical alternatives for incorporation of the dye into the crown (see Scheme 17). In order to test the viability of these two approaches, analogues of each would be synthesised.
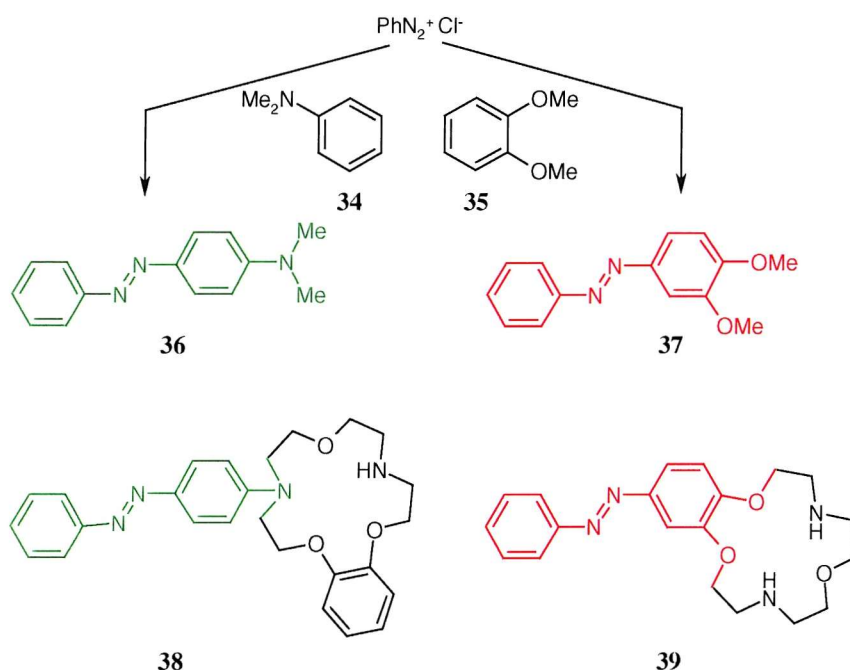
Scheme 17: Preparation of the azo-dye analogues (**36**) + (**37**) and their crown counterparts (**38**) + (**39**) with the analogue components coloured

Literature searches for preparations of the azo-dye crowns proved fruitless despite the fact that some azo-dye crowns are discussed in reviews.[40] In theory, both reactions seemed to be quite straightforward, the synthetic procedure being based on that of Methyl Orange (8).[42] The treatment of aniline with conc. HCl and sodium nitrite yields the diazonium ion which can simply be treated with the corresponding aromatic moiety (N,N-dimethylaniline (34) or 1,2-dimethoxybenzene (35)) in order to yield the desired dye. In practice, the results were not so simple. Both reactions gave unsatisfactory products (oils or a gummy solid) and whilst a positive mass spectrum of compound 36 was achieved, all other characterisation data proved inconclusive. Attempts at further purification of these materials were unsuccessful and, in view of the potentially more attractive nature of the preparation of a fluorescence sensor, it was decided not to continue this direction any further.

2.4 Incorporation of Fluorescent Functionality

As mentioned in section 1.4.2.2 much work has been carried out in the area of fluorescent crown sensors by de Silva and this was chosen as an attractive starting point for the development of sensors required in this project. The sensor 11b has been successfully synthesised[43k] by reaction of 9-chloromethylanthracene (40) and aza-15-crown-5 (41) in toluene.

40   **41**   **11b**
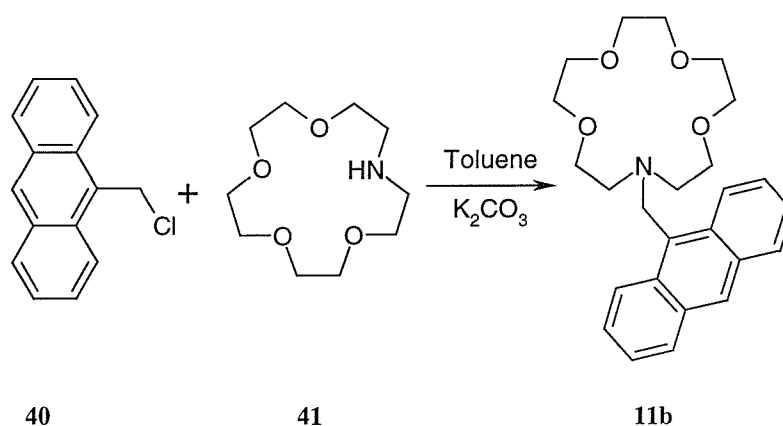
Scheme 18: Synthesis of de Silva's aza-15-crown-5 sensor

However, it was realised that, in the present work involving a diaza-crown system, problems would arise from addition at both nitrogen sites which would prevent further incorporation of the ester group required as a means of keeping the sensor inside the target cells. In an attempt to overcome this problem, it was proposed to react one equivalent of the carbonyl chloride of anthracene (**40**) or naphthalene (**42**) with one equivalent of diazacrown. Under these conditions, one of the amine groups in the crown should act as a base thereby impeding further reaction. This effect coupled with using an excess of the diazacrown might encourage monoacylation.

2.4.1 Acid Chloride Synthesis

Both anthracene and naphthalene carbonyl chlorides were readily synthesised by treatment of the corresponding carboxylic acid with thionyl chloride under nitrogen each being isolated in high yields.

2.4.2 Test Addition with Aza-18-Crown-6

A procedure for the preparation of the crown amides was developed using aza-18-crown-6 (**43**). Naphthalene 1-carbonyl chloride was added to aza-18-crown-6 and the resulting amide was successfully reduced with borane in THF, in 63% and 73% yield respectively. This new route to a previously synthesised crown[54] (**45**) produced a novel intermediate (**44**).
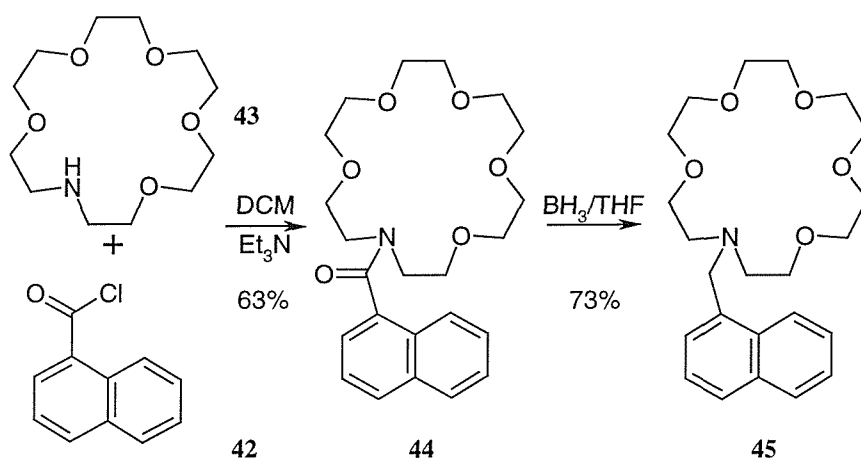
Scheme 19: Synthesis of a naphthalene-linked aza-18-crown-6 sensor (**45**)

The NMR spectra of each of these compounds proved much more complex than those of their crown precursors. The planar nature of the amide bond in **44** results in a loss of symmetry producing ten distinct methylene carbon environments. Even in **45** where there is no inherent restricted rotation, eight distinct carbon environments are still apparent. High temperature NMR experiments revealed that the molecular symmetry is restored above 110°C.

2.4.3 Attempted Monosubstitution of Benzodiaza-15-crown-5

As discussed above it was hoped that reaction of naphthalene 1-carbonyl chloride with excess of crown ether should favour monoacylation. Unfortunately, even these conditions produced only a disubstituted, but novel, product (**46**) in 66% yield. Again the planar amide bonds present in this structure resulted in a very complex proton and carbon NMR spectra. The aromatic region of the proton NMR clearly displayed characteristic naphthalene signals, but these were partly obscured. High temperature carbon NMR at 110°C allowed for the assignment of quaternary and tertiary peaks but the aliphatic peaks were hidden by coalescence and could not be resolved. Once again lack of time prevented further investigation of this reaction process or the possibility of selective protection.

2.5 Spectroscopic Binding Studies

The crowns that had been successfully synthesised and purified needed to be studied in order to establish their affinities for sodium or potassium. This is best defined by the aforementioned association constant (K_a, see section 1.3.1.2) which relates to the following equilibrium:

$$m\text{H} \; + \; n\text{G} \; \underset{K_d}{\overset{K_a}{\rightleftharpoons}} \; \text{H}_m\text{G}_n$$

Equation 1
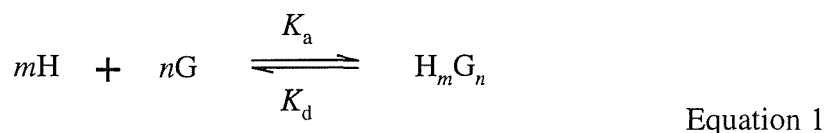
where   H is host

G is guest

m and n are the stoichiometry of each.

It is possible to evaluate this using most spectroscopic techniques and in the present study, both NMR and UV spectroscopic studies were used. Two different experiments can be applied to determine the stoichiometry and strength of association, respectively known as the continuous variations (Job) method[55] and titration.[56]

2.5.1 Job Method Theory

In this experiment, the change in the signal of the uncomplexed host is compared to that of the complexed host at a range of different concentrations. This is achieved by preparing a range of solutions with equal total molar quantity but differing molar ratios of the components. The response of each solution is measured and plotted against the molar fraction of guest ($= [\text{Guest}]/([\text{Host}] + [\text{Guest}])$). Each response is then corrected for concentration effects to produce a Job Plot.
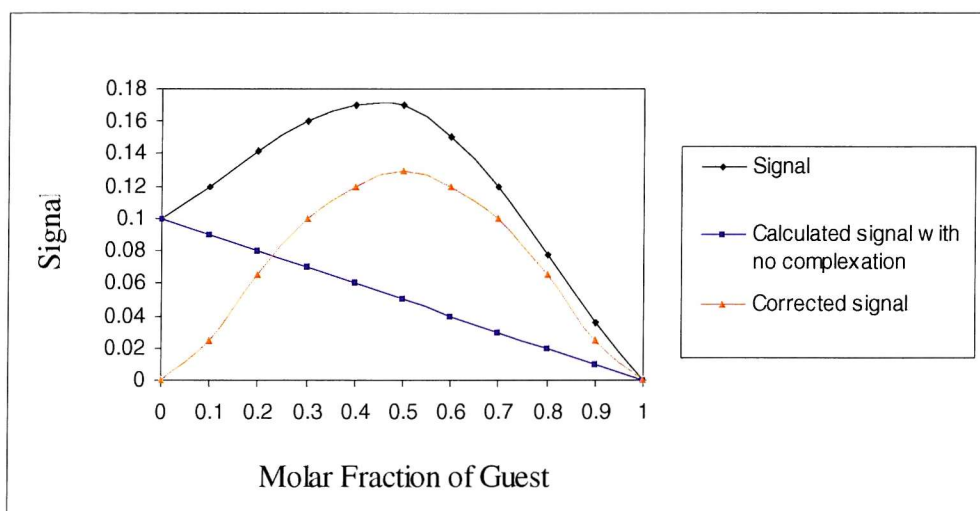
Figure 18: Simulated Job Plot displaying 1:1 stoichiometry

From the maximum of such a graph, it is possible to deduce the ratio of guest to host in the complex. In the example Figure 18, the maximum is at 0.5, corresponding to a 1:1 host-guest system. Unfortunately this plot only reveals the stoichiometry of binding and gives no indication of the strength of binding.

2.5.2 Titration Theory

In this experiment, the signal of the host at known concentration is measured as guest is added to the system. The resulting measurements can be plotted against the concentration of the guest to give a titration curve or binding isotherm. Using iterative mathematical techniques it is possible to solve these data and determine the association constant.
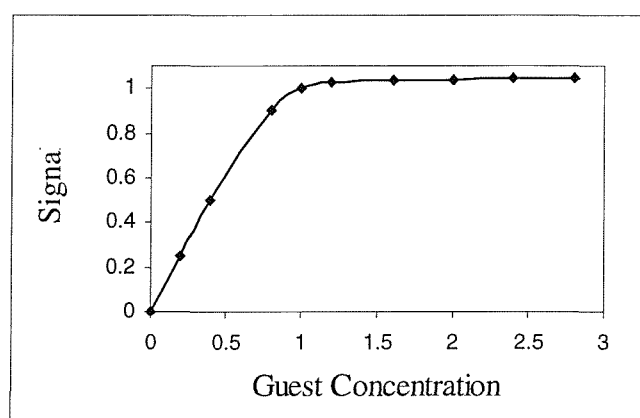
Figure 19: Simulated titration curve for 1:1 complex

Experimentally a problem occurs if two solutions are being added to each other, as each addition of the guest to the host causes a dilution of the host solution. This can be overcome by adding the titrant as a solution dissolved in the aliquot. For example, when guest A is titrated against host B a solution of A+B is added to the solution of B, where the concentration of B is the same in the aliquot and the receiving solution, thus maintaining a constant concentration of B. Alternatively, the change can be mathematically accounted for during the data fit or the guest can be added as a solid thereby avoiding dilution effects.

2.5.3 Carbon NMR Binding Studies

It was decided that the complex formation between several crown ethers and sodium salts should initially be studied using ^{13}C NMR titration experiments. The data obtained from these experiments would enable us to see the effect of structural changes on stoichiometry and strength of binding. The first experiments were carried out using the model system: benzo-15-crown-5 (47) and $NaBF_4$.

2.5.3.1 Benzo-15-Crown-5 Titration

The results of these studies are reported in Table 4 and summarised graphically in Figure 20. The results show how the chemical shifts decrease uniformly over a range of more than 2ppm for the ethylene carbons [d] upon complexation up to a one-to-one cation to crown ratio above which stoichiometry, little significant change is observed. Changes in the chemical shifts of the aromatic carbons [a, b and c] also occur but are less uniform, carbon *b* showing an increase in chemical shift whereas carbons *a* and *c* show a decrease. The chemical shifts cease to change significantly after 1:1 complexation is achieved, showing a plateau effect at ca 3:2 complexation. These data suggest that the crown preferentially forms a 1:1 complex and complexation perturbs the whole molecule not just the ethylene bridges.

Disappointingly, it was not possible to collect enough data to determine any K_a values as a mutually effective solvent could not be found for both host and guest.

$[Na^+]/$ [Crown]	a (ppm)	b (ppm)	c (ppm)	d (ppm)	e (ppm)	f (ppm)	g (ppm)	
0.0	114.0	120.9	149.2	70.8	69.2	68.7	70.3	
0.5	113.4	121.3	147.9	69.2	68.1	67.6	68.8	
1.0	113.2	121.7	147.1	68.3	67.4	66.9	67.9	
1.5	113.1	121.6	146.9	68.1	67.3	66.7	67.7	
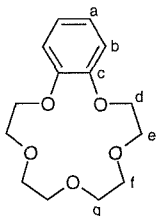
Table 4: ^{13}C NMR titration data for benzo-15-crown-5 with increasing sodium concentration

The systematic errors are limited to sample preparation and further reduced by re-using the same sample. The precision of these experiments is quite reasonable, the chemical shifts are reliable to ±0.1ppm and digitisation error is low due to the high number of data points per Hz. The overall accuracy is estimated at ±0.3ppm and is represented as such on the error bars in Figure 20.
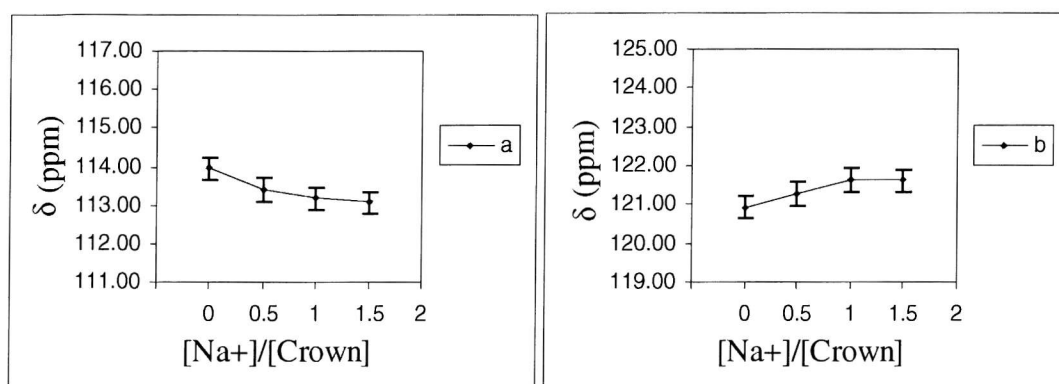
(a) Variation of δ for carbon a   (b) Variation of δ for carbon b
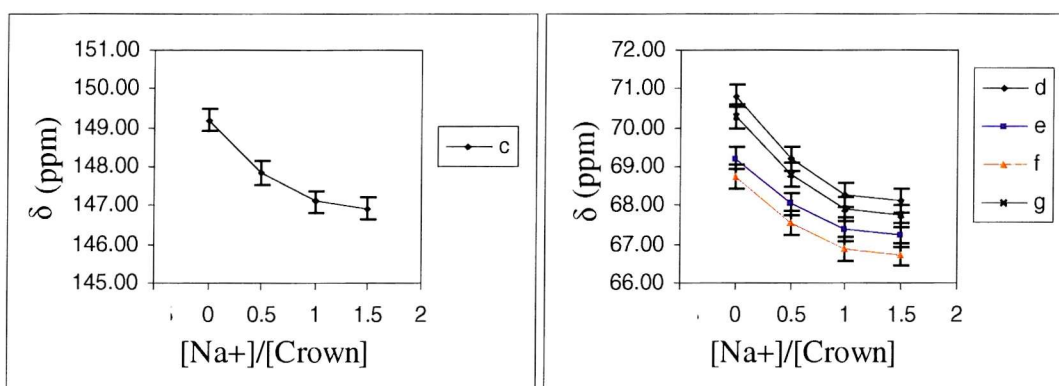
(c) Variation of δ for carbon c   (d) Variation of δ for carbons d, e, f & g

Figure 20: NMR titrations showing changes in ^{13}C chemical shifts for the carbon environments in benzo-15-crown-5 as a function of increasing molar ratios of sodium tetrafluoroborate

2.5.3.2 Further NMR Titration Experiments

Unfortunately, attempts at NMR titrations using the functionalised compounds were not as successful. The greater complexity of these molecules and a breakdown in their symmetry led to spectra which could not be accurately assigned. It was realised that using two-dimensional NMR experiments it might have been possible to completely assign each carbon environment, however it was decided that this was an overly lengthy route to obtain information that could be more easily gained using alternative techniques.

2.5.4 UV Binding Studies

Although the long term goal of the work is to produce sensors which can be monitored by fluorescence spectroscopy, the precision of this technique relative to UV absorbance is limited by a stronger dependence of the signal on instrumental parameters and irreproducible quenching effects due to light scattering and solvent impurities.[38] In addition, since only a simple chromophore is required, the presence of a fluorescent functionality is not a constraint for comparative studies with model systems. For these reasons, an attempt to determine the K_a values for the crowns was made with UV spectroscopy.

Each of the crowns that were tested contained aromatic regions incorporated within or attached to the crown ether ring and it was hoped that upon binding of a cation the energy levels of that chromophoric region would be perturbed sufficiently to allow measurements to be made. This was a reasonable assumption considering the conformational effects of complexation observed by the NMR titrations (see 2.5.3.1).

2.5.4.1 Job Method Experiments

Serial dilution experiments of the chosen crowns (**11b**, **17**, **44**, **45**, **46** and **47**) showed absorbance <1 at concentrations of 1×10^{-5} M for compounds with a fluorescent functionality and 1×10^{-4} M for those without. Each crown had a distinctive spectral signature with well defined maxima and fine structure. The spectra of each of the crowns can be seen below, in Figure 21.

Job method analysis of the data however was disappointing. Crowns **11b**, **17** and **46** showed either no response to complexation or no complexation in the presence of sodium or potassium. Crowns **44**, **45** and **47** gave a response but the job plots were poor and gave weak or inconclusive results. Generally analysis at the shorter wavelength (higher energy) showed little interaction, it was Job plots produced from analysis at longer wavelength absorption bands were the most sensitive to complexation effects if any.

It would seem that there is not enough of an interaction between the crown and guest cation to cause a significant, measurable change in the energy levels of the aromatic regions. The UV absorbance, whether reflected by a change in intensity or in wavelength, is therefore unchanged or undetectable.
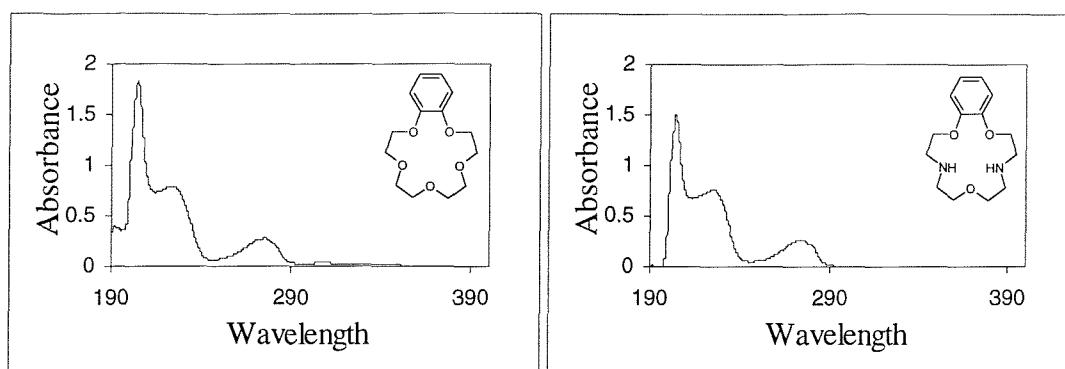
(a) UV spectum of **47** (1×10^{-4} M)   (b) UV spectum of **17** (1×10^{-4} M)
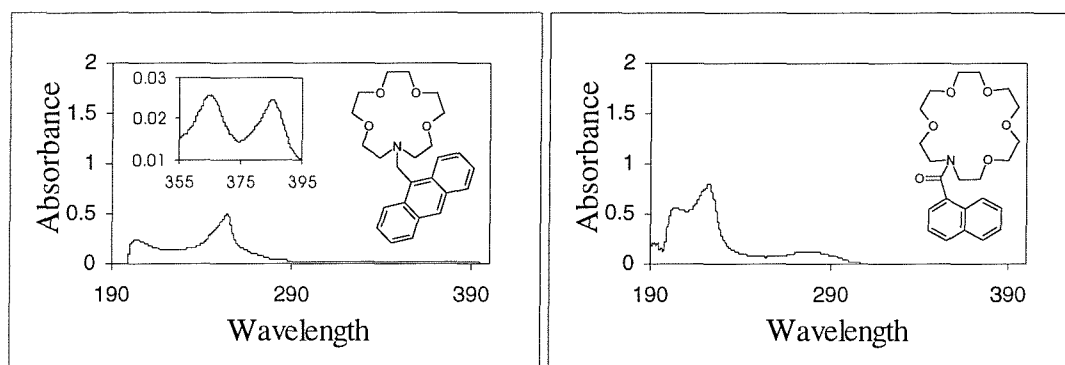
(c) UV spectum of **11b** (1×10^{-5} M)   (d) UV spectum of **44** (1×10^{-5} M)
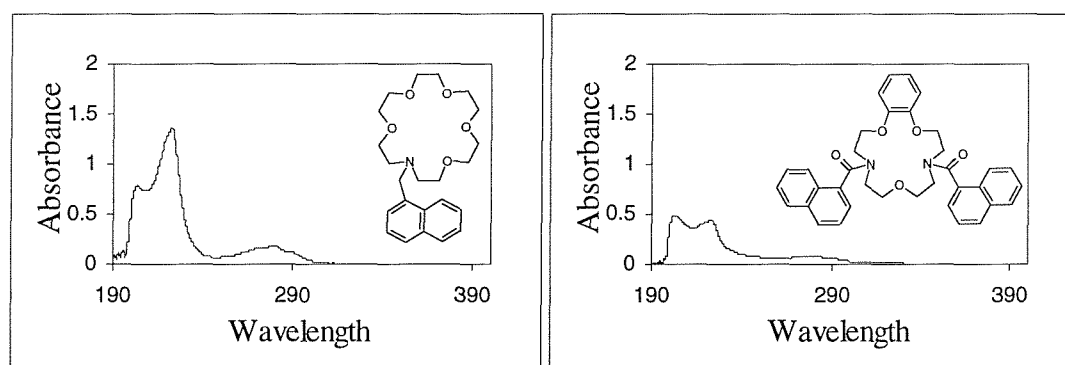
(e) UV spectum of **45** (1×10^{-5} M)   (d) UV spectum of **46** (1×10^{-5} M)

Figure 21: UV absorption spectra of studied crowns

2.5.4.2 Titration Experiments

In view of the relative lack of response shown by the crowns used in the present study during Job method experiments it was decided not to continue with any UV titration experiments.

2.6 Extraction Binding Studies

An alternate method to determine association constants involves extraction experiments. The procedure works by exploiting a crown's affinity for suitable cations, its insolubility in aqueous media and a UV responsive counter anion, in this case the picrate ion. By mixing two immiscible liquids each containing a solution of crown and picrate salt respectively, and then measuring the UV response of the picrate salt solution it is possible to determine the amount of guest extracted from the aqueous layer in to the organic layer. This technique has the distinct advantage of measuring the change in a species independent of the crown so a signal will always be obtainable. The methods and equations used in this experiment are based on the methods of Cram and co-workers.[57]

2.6.1 Determination of Association Constants

Solutions of crowns (**11b, 17, 18, 25, 44, 45, 46** and **47**) in $CDCl_3$ were used to extract aqueous solutions of sodium and potassium picrates. From the measurement of the ultraviolet absorbance of the organic or aqueous phase at 380 nm, the molar ratios of host to picrate (R) were calculated. Using the relationship in Equation 3 defined by the equilibrium summarised in Equation 4 it was possible to determine association constants for all the studied crowns

$$K_a = \frac{R}{(1-R)K_{di}\left\{[G_i]_{H_2O} - R[H_i]_{CDCl_3}\left(V_{CDCl_3}/V_{H_2O}\right)\right\}^2} \qquad \text{Equation 3}$$

where K_{di} is the distribution constant (see Equation 5)

$[G_i]_{H_2O}$ is the initial guest (picrate) concentration in the aqueous layer

$[H_i]_{CDCl_3}$ is the initial concentration of the host in chloroform

V_{CDCl_3} is the volume of chloroform

V_{H_2O} is the volume of water.

$$\text{H} \quad + \quad \text{M}^+\text{Pic}^- \quad \underset{CDCl_3}{\overset{K_a}{\rightleftharpoons}} \quad \text{M}^+\cdot\text{H}\cdot\text{Pic}^-$$
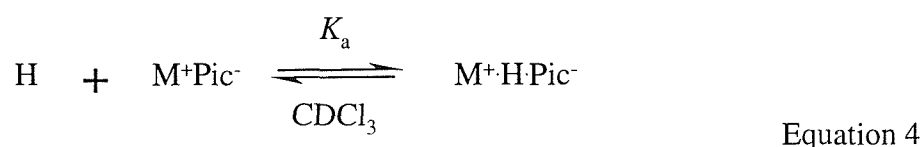
<div align="right">Equation 4</div>

$$K_{di} = \frac{[G^+M^-]_{CDCl_3}}{[G^+]_{H_2O}[M^-]_{H_2O}}$$

Equation 5

$$\Delta G^\circ = -RT \ln K_a$$

Equation 6

Section 4.7 contains a more detailed breakdown of the above equations, the results of which are summarised in Table 5. The data calculated from both the chloroform and water layers show good agreement (1-5%). However it has been shown[57] that the nature of the calculations means R values from the chloroform layer are more reliable when $R < 0.1$ wheras values from the water layer are more reliable if $R > 0.7$. For this reason all analysis is performed on values calculated on the chloroform layer, as no R values were >0.7 from the water layer and over 60% of the R values from the chloroform layer were <0.1. The only exception is crown **11b** for which the UV absorbance fine structure of the crown's spectrum overlaps with the absorbance band of the picrate salt, making the measurements unreliable.

Crown	Guest Cation	R	Log K_a	$-\Delta G^\circ$ (kcal/mol)
11b	Na^+	0.42	6.72	9.2
	K^+	0.03	4.74	6.4
17	Na^+	0.15	5.78	7.9
	K^+	0.07	5.14	7.0
18	Na^+	0.07	5.35	7.3
	K^+	0.06	5.05	6.9
25	Na^+	0.09	5.49	7.5
	K^+	0.08	5.21	7.1
46	Na^+	0.03	4.92	6.7
	K^+	0.01	4.34	5.9
47	Na^+	0.21	6.04	8.2
	K^+	0.22	5.90	8.0
44	Na^+	0.04	4.99	6.8
	K^+	0.12	5.47	7.4
45	Na^+	0.08	5.38	7.3
	K^+	0.16	5.68	7.7

Table 5: R, K_a and $-\Delta G^\circ$ values for all studied crowns against sodium and potassium cations

The systematic error in these experiments is quite high, as the number of measurements and calculations involved in the preparation of each sample before an absorbance can be recorded is high. This was reduced by using accurate molecular masses, a five point balance, type A volumetric flasks and a Gilson™ micropipette, whenever applicable. This reduction was shown by good reproducibility of the log K_a values when the experiment was repeated for compounds **17** and **47** and the difference was within 5% using data calculated from the water layer and within 2% for data obtained from the chloroform layer. The precision of the UV measurements is reasonable as the wavelength is measured at a resolution of 10 data points per nanometer reducing digitisation accordingly and the absorbance is measured to four decimal places but is probably only reliable to three decimal places. These factors suggest that calculated R values are quotable to 2 significant figures.

2.6.2 Analysis of the Spectral Response

Aside from determining the strength of the complexation it has been shown[58] that the magnitude of the bathochromic shift undergone by the main absorption band of the picrate salt is representative of the stoichiometry of the complex. 1:1 complexes of host to picrate salts are crown co-ordinated contact ion pairs wheres 2:1 complexes are crown separated ion pairs. The λ_{max} for an uncomplexed picrate salt is around 360nm; this value shifts to wavelengths higher than 380nm for 2:1 complexes and to wavelengths less than 380nm for 1:1 complexes. All the λ_{max} values recorded were in the range of 372-375nm, suggesting that all the complexes formed had 1:1 stoichiometry.

2.6.3 Analysis of Association Constants

The log K_a values displayed below show a pattern which is reasonably predictable. The 15-membered crowns (**11b**, **17**, **18**, **25**, **46** and **47**) show a preference for sodium over potassium while, as expected, the two 18-membered crowns included here (**44** and **45**) show a preference for potassium over sodium, demonstrating the importance of size matching as a predominate effect in complexation ability.
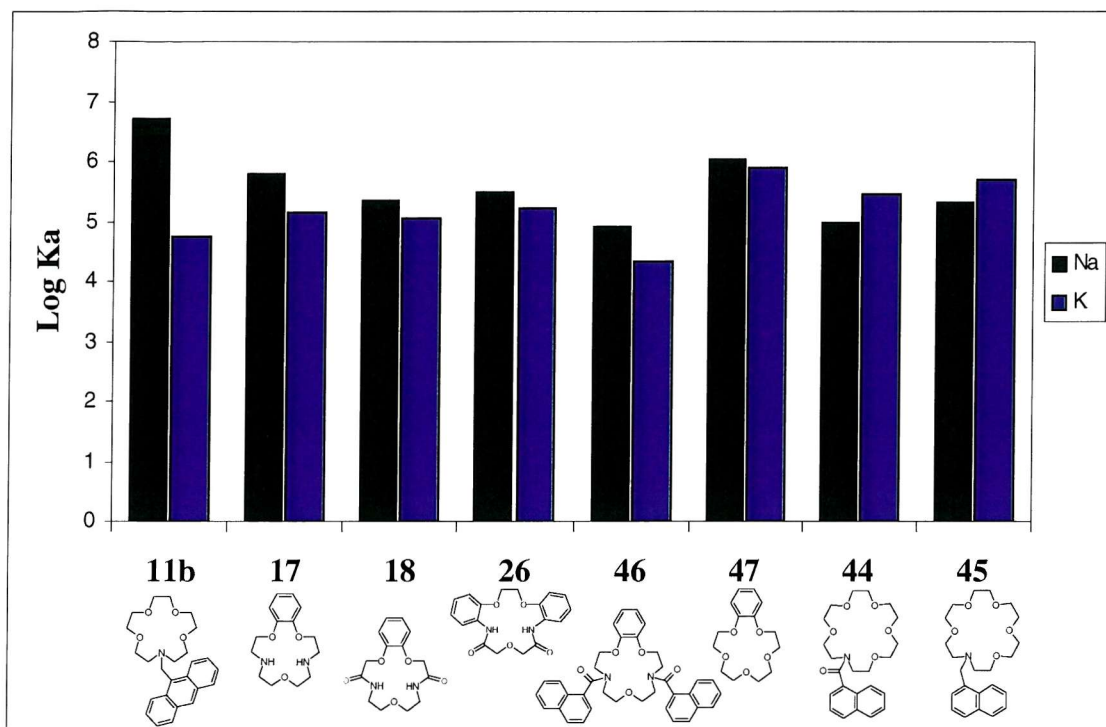
Figure 22: Comparison of log K_a values for sodium Vs potassium

The most noticeable feature is the considerable preference **11b** shows for sodium over potassium, as it contains the most flexible ring of the 5-membered crowns being studied, it is interesting to note the reduction of this preference with increased rigidity.

In addition the complexation strength with sodium is clearly influenced by structural characteristics. There is a decrease in K_a for sodium in the order **11b>47>17>18** which reflects the incorporation of the benzo unit into the macrocyclic ring, the presence of two amino groups in the macrocyclic ring and the presence of amide groups in the macrocyclic ring respectively. Presumably the increased rigidity of the crown and the increased "softness" of the donor atoms has a negative effect on the crowns ability to complex with sodium. Surprisingly this effect is not continued to crown **25** which contains two benzene rings in the macrocyclic ring yet displays slightly larger complexation strength to that of crown **18**, with only one.

The four functionalised crowns have higher log K_a values if the linker is a methylene group rather than a carbonyl. This is consistent with the findings for the other crowns as the planar nature of the amide bonds would impart structural rigidity to the crown. In addition the lone pair of an amide ring nitrogen would not be as available for binding as that of an amine as the electron density around the amide nitrogen would be much reduced due to the resonance structure of the amide. Although there are not really enough examples to prove this hypothesis it is further backed up by crown **46** having the weakest affinity for sodium and containing two amide linkers.

This amide linker effect coupled with the other structural modifications has seemingly achieved a significant reduction in K_a for sodium while maintaining a discrimination against potassium.

These results are pleasing as they clearly show that modifying the rigidity of the macrocycle and changing the donor atoms can influence the crown's binding properties in a reasonably predictive manner. In addition the nature of the change, a weakening in the complexation strength, is exactly what is desired in the present work. However, further analysis would need to be performed involving a larger range of crowns in different solvents to draw any wide-scale conclusions especially considering the fickle dependence of K_a values on the technique with which they are determined.[25]

2.7 Fluorescence Response

The ultimate aim of the synthesised sensors was to detect sodium levels by their fluorescence response. Serial dilution experiments of the four crowns that had been functionalised (**11b**, **44**, **45** and **46**) determined the concentrations at which emission spectra were within the spectral detection limits. Each of the crowns was excited at a wavelength determined from its UV absorption spectrum. The concentrations required were of the sub-micro- to nano-molar range (i.e. 1×10^{-7}M or 1×10^{-9}M), which in itself indicates the high fluorescent nature of these crowns, despite their simple format. As predicted any attempts to calculate binding constants by fluorescence were severely hampered by the large error in fluorescence measurements. This factor also contributed to considerable difficulties in obtaining quantitative rather than qualitative measurements.

The systematic errors are limited to sample preparation and associated calculations, unfortunately the nature of the technique also creates several sources of random error. The precision of the instrument was limited by a low data sampling interval (2 data points per nanometer) but the accuracy was increased by running the spectra slowly at a rate of 20nm per minute. The intensity was measured to six decimal places but is almost certainly only reliable to three decimal places. The determination of the area under the curve was an automated process performed by the fluorimeter's accompanying software, which leads to a reasonable precision of three decimal places for all quantum yields. The values should be treated carefully though as the associated error is expected to be quite high.

2.7.1 PET Behaviour

Preliminary experiments showed that a PET process dominated the fluorescence of all four crown ethers. Addition of excess acid (HCl) or base (NH_3) resulted in either a drastic enhancement or a quenching of the fluorescence respectively. Clearly at high pH any nitrogen lone pairs are totally "naked" and freely able to quench any fluorescence, conversely at low pH the lone pair is unavailable and fluorescence is maximised. However, although all reasonable efforts were made to minimise error and reproduce experimental conditions these results could not be reproduced with any consistency.

2.7.2 Response to Metal Ions

Attempts to determine the sensor's responses to sodium and potassium complexation were more successful. It was possible to record and reproduce the emission response of the crowns to a ten fold and one hundred fold excess of sodium or potassium. These spectra are not directly comparable due to the different concentrations at which they were run, but they do show the trends associated with complexation.
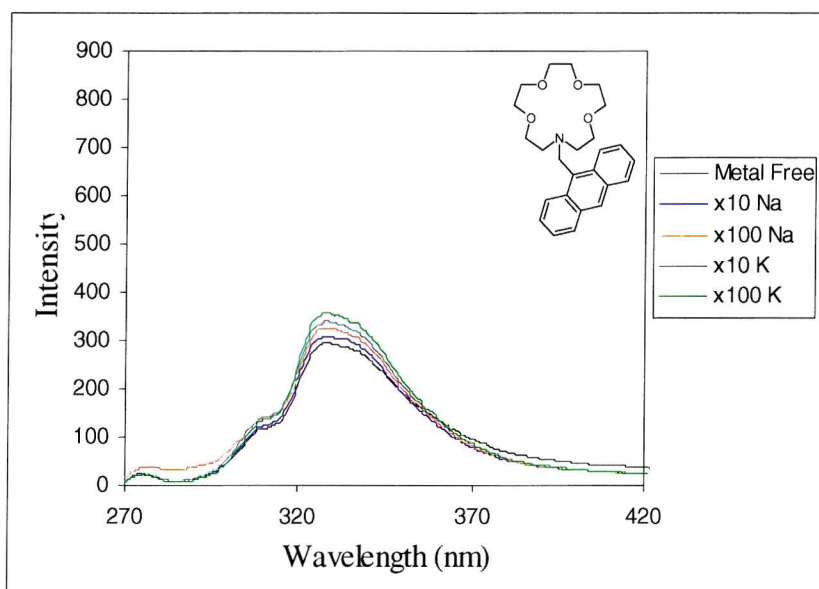
Figure 23: Fluorescence response for crown **11b** at 1×10^{-7}M

11b not only displays the smallest increase in intensity from a ten to one hundred fold excess but surprisingly, given the internal cavity size of its 15-crown-5 core unit, gives a larger response to potassium than to sodium.
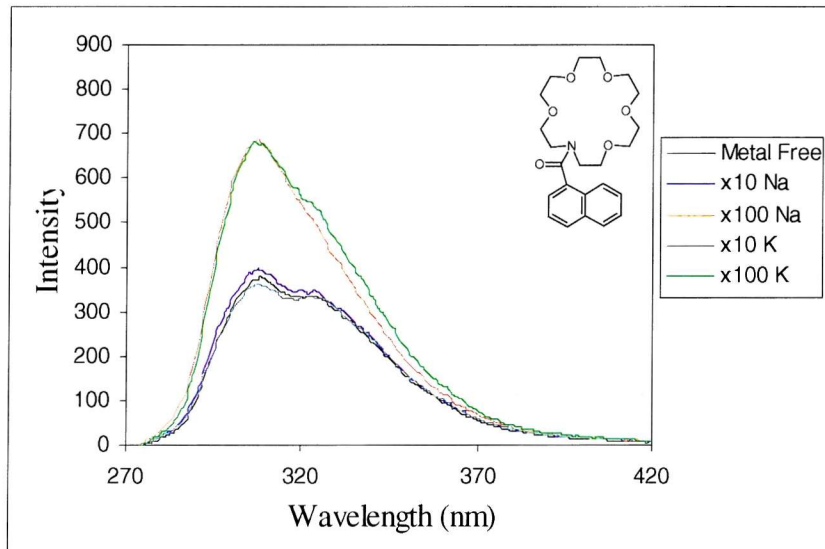
Figure 24: Fluorescence response for crown **44** at 1×10^{-9}M

Crown **44** gives a roughly equal response to each of the cations but the signal intensity increases markedly when the excess of cation is increased ten fold.
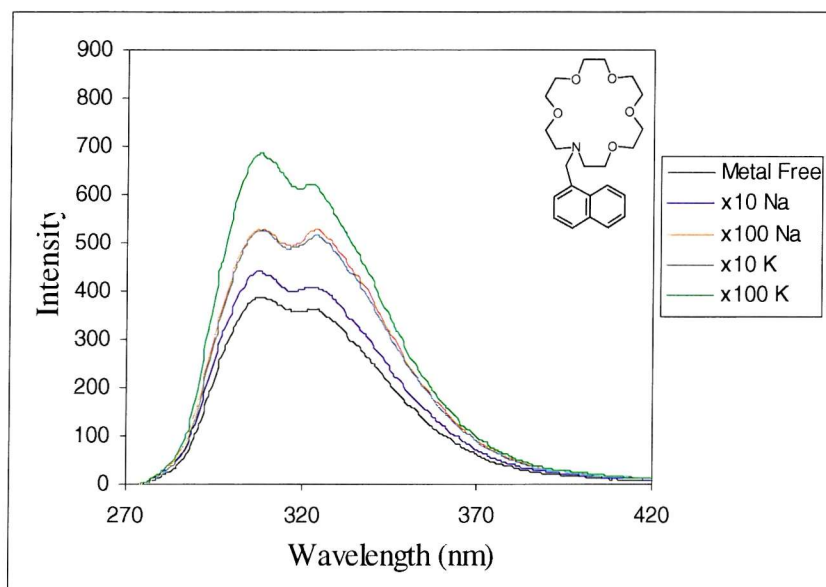
Figure 25: Fluorescence response for crown **45** at 1×10^{-9}M

45 shows a definitive response in favour of potassium, the one hundred fold sodium signal being only as strong as the ten fold potassium signal.
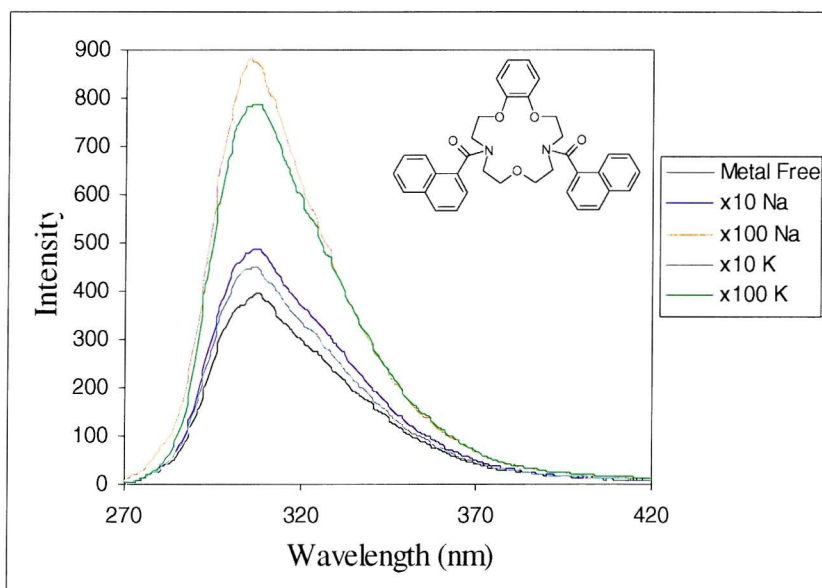
Figure 26: Fluorescence response for crown **46** at 1×10^{-7}M

Crown **46** shows a response that is not only more intense for sodium than potassium but one that increases significantly from a ten to one hundred fold increase in cation. On a general point it is notable that the none of the λ_{max} values undergo either a bathochromic or hypsochromic shift.

2.7.3 Quantum Yield Determinations

From these spectra it was possible to determine the fluorescence quantum yield (φ) of each of the studied crowns under investigation here. The quantum yield is defined by Equation 7, and a non-fluorescent molecule will have a quantum yield of zero or so close to zero that fluorescence is not measurable.

$$\varphi = \frac{\text{number of quanta emitted}}{\text{number of quanta absorbed}}$$

Equation 7

The measurement of absolute quantum yields presents significant experimental difficulties and results are actually less accurate than relative quantum yield measurements. For these reasons relative quantum yields are a far more favourable option. If the solutions are dilute enough (A<0.1) then the quantum yield (φ_u) can be determined by employing a fluorescence standard (the quantum yield of which is already known) and is defined by Equation 8.

The quantum yields are reported in Table 6. Values are low but not unexpectedly so. In previous determinations[43c] the quantum yield of **11b** was found to be 0.019 when complexed with a 10,000 fold excess of potassium and 0.057 when complexed with a 10,000 fold excess of sodium.

$$\varphi_u = \frac{\left(I_f\right)_u \varepsilon_s c_s}{\left(I_f\right)_s \varepsilon_u c_u} \varphi_s$$

Equation 8

where   u is the unknown

s is the fluorescence standard

φ is the quantum yield

$\left(I_f\right)$ is the fluorescent intensity; equal to the area under the curve

ε is the extinction coefficient

c is the concentration.

Crown	φ metal free	φ for K^+		φ for Na^+	
		10 fold excess	100 fold excess	10 fold excess	100 fold excess
11b	0.0100	0.012	0.012	0.010	0.011
44	0.0176	0.018	0.029	0.018	0.029
45	0.0339	0.047	0.058	0.039	0.048
46	0.0060	0.008	0.012	0.007	0.013

Table 6: Quantum yields for four fluorescent crown compounds against sodium or potassium at ten and one hundred fold excess

The quantum yields show the relative fluorescent strength of each of the crowns and it is interesting to note that the sensors with carbonyl linkers between crowns and their fluorescent functionality (**44** and **46**) show reduced fluorescence. This is an unexpected result, it was thought that the presence of an amide would automatically prevent lone pair quenching due to the redistribution of electron density. At the very least the extra rigidity imparted to the molecule was considered enough that it may increase the fluorescence. Unfortunately, literature searches for the photochemistry of amide bonds proved futile and clearly this is an area that needs to be investigated more fully.

The most encouraging point about these yields and their associated spectra is that the crowns can continue to give a response beyond 1:1 and that the change in fluorescence is measurable and quantifiable.

The results obtained so far should, however, be treated with caution, because of the large amount of uncertainties in the measurements. Although every attempt was made to keep the temperature constant, the level of impurities at a minimum and to reduce experimental error, the inherent complexity of the technique introduces considerable uncertainty.

3 CONCLUSIONS AND FUTURE WORK

The underlying objective of this work is to produce an optical sensor having the potential for sodium-ion sensing within a cellular matrix. The current project, which represents a first attempt to tackle this problem, has both highlighted the significant synthetic and analytical challenges presented and provided a useful insight into the way this problem may be approached.

Two novel functionalised crown ethers have been prepared and it has been shown, from a comparison of the behaviour of these with related structures, that their binding efficiencies are tuneable and show enough variation to present new avenues for further development.These ionophores are also able to show reasonable selectivity towards a desired cation, specifically sodium over potassium, but problems associated with the considerable solvent interaction effects have not been addressed in the present study. This area is of particular importance in any future work as an optimal sensor has to operate in the extra and intracellular matrix which is largely aqueous in nature.

The incorporation of simple fluorescence moieties into the crown ether skeleton has produced a fluoroionophore which shows discrimination between sodium and potassium. Although such fluoroionophores have the potential to show a greater response to complexation than any analogous chromoionophores, the spectroscopic technique involved present several significant experimental difficulties, which lead to increased error in response measurement thereby complicating the procedure.

Further work should be approached in three stages. Firstly a larger range of crowns should be prepared, with efforts towards optimising synthesis, in order to determine more accurately the exact effect of structural changes on the properties of the macrocyclic ring. Secondly any spectroscopic measurements should be made at a range of temperatures, pH's and most importantly in a range of solvents, to discover the dependence of the complexation properties on these crucial factors. Finally, attempts must now be made to incorporate ester functionalities into the fluoroionophore structure. Time constraints prevented this objective being investigated in the present work but in the future it is an essential factor in the production of a sensor that can be used effectively in the cellular environment.

4 EXPERIMENTAL

4.1 General Experimental

^{1}H and ^{13}C nuclear magnetic resonance (NMR) spectra were run on a Bruker AC300 spectrometer at 300MHz and 75MHz respectively or a Bruker AC400 spectrometer at 400MHz and 100MHz respectively. Chemical shifts (δ) are all quoted in parts per million (ppm) relative to residual solvent. Carbon NMR peaks are described as either quaternary (q), tertiary (t), secondary (s) or primary (p).

All electrospray positive (ES+) low-resolution mass spectra (LRMS) were run on a micromass balance, bench-top Quadrupole Open Lynx-OAMS. All fast atom bombardment (FAB) low-resolution mass spectra were run on a VG analytical 70-250-SE mass spectrometer.

All high-resolution mass spectra (HRMS) were run on a VG analytical 70-250-SE mass spectrometer. Spectra were run as fast atom bombardment in 3-nitrobenzyl alcohol (NBA) with polyethylene glycols (PEG's) and/or polyethylene glycolmethyl ethers (Me-PEG's) as mass calibrants or as electron ionisation (EI).

All infrared (IR) spectra were run on a Perkin–Elmer 1600 Fourier Transform spectrometer using sodium chloride discs or a solution cell. Only selected peaks are reported.

All fluorescence spectra were run on a Perkin-Elmer LS 50B luminescence spectrometer.

All UV spectra were run on a Shimadzu UV-1601 UV-visible spectrometer.

All melting points (MP) were performed on an Electrothermal melting point apparatus and are uncorrected.

Dichloromethane (DCM) was dried over calcium hydride and distilled (40°C).
Methanol was dried over calcium sulfate and distilled (65°C).
Triethylamine was dried over calcium hydride and distilled (89°C).
Tetrahydrofuran (THF) was dried over sodium wire with benzophenone and distilled (65-66°C).
Toluene was dried over calcium sulfate and distilled (110-111°C).

4.2 Synthesis of Benzodiaza-15-Crown-5

4.2.1 Synthesis of 2-(2-{[(4-Methylphenyl)sulfonyl]oxy}ethoxy)ethyl 4-methyl-1-benzenesulfonate (22)[59]
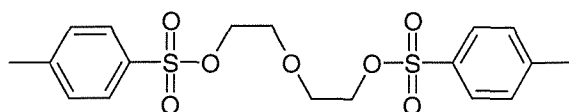
To diethylene glycol (4.57cm^3, 48mmol) was added DCM (50cm^3) and pyridine (9.74cm^3, 121mmol) at 0°C. 4-Methyl-1-benzenesulfonyl chloride (23g, 121mmol) was added portion-wise over 10 minutes before stirring for 16 hours at room temperature. DCM was removed under reduced pressure affording a white solid, to which ice water (80cm^3) was added. After trituration the resulting white suspension was separated by filtration and then washed successively with water (3x10cm^3), HCl (3x10cm^3) and finally water (3x10cm^3) before being crystallised from a mixture of petrol (40/60) and DCM to afford the product **22** (17.21g, 86%) as white crystals. MP: 83-85°C (lit.,[60] 86-87°C). ^{1}H NMR (CDCl$_3$): δ 7.67 (4H, d, J = 8.1 Hz), 7.33 (4H, d, J = 8.1 Hz), 4.10 (4H, t, J = 4.6 Hz), 3.58 (4H, t, J = 4.6 Hz), 2.45 (6H, s). ^{13}C NMR (CDCl$_3$): δ 145.1 (q), 132.9 (q), 130.1 (t), 128.1 (t), 69.2 (s), 68.8 (s), 21.8 (p). LRMS (ES+, m/z): 415 ([M+H]$^+$). IR (nujol mull, v_{max}, cm^{-1}): 1596m (**Ar**), 1493m (**Ar**), 1100m (**CH$_2$-O-CH$_2$**).

4.2.2 Synthesis of 2-{2-[2-(1,3-Dioxo-2,3-dihydro-1H-2-isoindolyl)ethoxy]ethyl}-1,3-isodolinedione (23)[61]
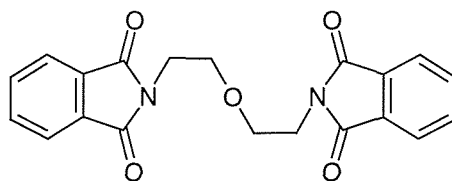
To potassium phthalimide (9.63g, 52mmol) was added 2-(2-{[(4-methylphenyl)sulfonyl]oxy}ethoxy)ethyl 4-methyl-1-benzenesulfonate **22** (9.5g, 23mmol), DMF (175cm^3) and diethylamine (3 drops). The solution was stirred with heating (140°C) for three hours. After heating the solution was left to cool overnight. The DMF was removed in three stages, first by reduced pressure (~20mmHg, 85°C) then by further reduced pressure (~9mm Hg, 70°C) and finally on the high vacuum line (~0.1mm Hg). The resulting pale orange solid was washed with hot water (100cm^3) and filtered dry under suction. The resulting white solid was recrystallised from glacial acetic acid with decolourising charcoal affording the product **23** (4.14g, 50%) which was dried on the high vacuum line (~0.1mm Hg). MP: 154-158°C (lit.,[62] 156°C). ^{1}H NMR (CDCl$_3$): δ7.71 (8H, m), 3.85 (4H, t, J = 5.5Hz), 3.73 (4H, t, J = 5.5Hz). ^{13}C NMR (CDCl$_3$): δ 168.2 (q), 133.9 (t), 132.2 (q), 123.3 (t), 67.6 (p), 37.3 (p). LRMS (ES+, m/z): 365 ([M+H]$^+$). IR (nujol mull, ν_{max}, cm^{-1}): 1716s (**Ar**), 1612w (**Ar**), 1103w (CH$_2$-O-CH$_2$).

4.2.3 Synthesis of 2-(2-Aminoethoxy)-1-ethanamine (20)[61]

$$H_2N \diagup\diagdown O \diagdown\diagup NH_2$$
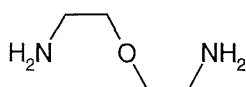
4.2.3.1 Using Hydrazine

2-{2-[2-(1,3-Dioxo-2,3-dihydro-1H-2-isoindolyl)ethoxy]ethyl}-1,3-isodolinedione **23** (4g, 11mmol) was suspended in refluxing methanol (50cm^3). Hydrazine hydrate (1.96cm^3, 63mmol) was then added affording a brown solution. After a white solid separated the solution was heated (65°C) for three hours and conc. HCl (5cm^3) was added. The methanol and hydrazine were removed by distillation (65°C) and the remaining white solid was filtered to leave a light brown liquor. This was basified with sodium hydroxide (1g). The supernatant brown layer was separated by filtration and the product was isolated on a continuous extraction column with ether run over a period of 12 hours. The ether was removed under reduced pressure and then on the high vacuum line (~0.1mm Hg) leaving an oily residue. *Spectroscopic characterisation of this has indicated no product formation.*

4.2.3.2 Using KOH and NaOH[63]

To a 70% aqueous solution of NaOH (8g, 0.2mol) and KOH (11.2g, 0.2mol) was added 2-{2-[2-(1,3-dioxo-2,3-dihydro-1H-2-isoindolyl)ethoxy]ethyl}-1,3-isodolinedione **23** (36.4g, 0.1mol). The aqueous phase was removed by distillation at 100-120°C. Water (75cm^3) was added and removed by distillation, before ether (100cm^3) was added and the mixture was refluxed for two hours. The ether was then removed by distillation before adding a final aliquot of water (150cm^3) which was removed by distillation. All four phases were evaporated under reduced pressure and the resulting oils were combined and purified by Kügel Rohr distillation, yielding the product **20** (3.42g, 33%) as a colourless liquid. ^{1}H NMR (CDCl$_3$): δ 3.38 (4H, t, J = 5.2Hz), 2.75 (4H, t, J = 5.2Hz). ^{13}C NMR (CDCl$_3$): δ 73.1 (s), 41.8 (s). IR (nujol mull, v_{max}, cm^{-1}): 3362s + 3292s (**NH$_2$**), 1119s (**CH$_2$-O-CH$_2$**).

4.2.4 Synthesis of Methyl 2-[2-(2-methoxy-2-oxoethoxy)phenyloxy)acetate (19)[45]
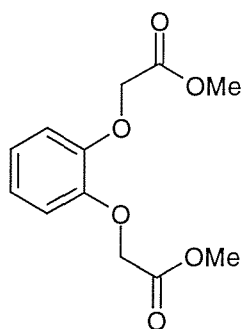
Anhydrous potassium fluoride (83.3g, 1440mmol), acetonitrile (167cm^3) and methyl bromoacetate (30.9g, 20.12cm^3, 202mmol) were degassed with nitrogen for ten minutes at reflux with mechanical stirring. After slight cooling, catechol (11.12g, 101mmol) was added. Mechanical stirring was continued and the whole was bought to reflux under a nitrogen atmosphere. These conditions were maintained for 24 hours. The reaction was then allowed to cool to room temperature with stirring. The mixture was filtered under suction and the solid residue was washed with ethyl acetate (4x50cm^3). The filtrates were combined and the solvents were removed under reduced pressure. The resulting oil was dissolved in DCM (85cm^3) and washed with 10% sodium hydroxide solution (3x100cm^3). The aqueous phase was back-extracted with DCM (80cm^3) and the combined organic phases were dried (Na_2SO_4). The solvent was removed under reduced pressure, leaving a green solid. The solid was recrystallised from ether with decolourising charcoal to afford the product **19** (15.93g, 62%) as a light green solid, which was dried on the high vacuum line (~0.1mm Hg). MP: 53-57°C (lit.,[64] 56-57°C). ^{1}H NMR (CDCl$_3$): δ 6.85 (4H, m), 4.67 (4H, s), 3.72 (6H, s). ^{13}C NMR (CDCl$_3$): δ 169.6 (q), 148.1 (q), 122.8 (t), 115.5 (t), 66.7 (s), 52.3 (p). LRMS (ES+, *m/z*): 272 ([M+NH$_4$]$^+$). IR (nujol mull, $v_{max,}$ cm^{-1}): 1754s (**C=O**), 1592s (**Ar**).

4.2.5 Synthesis of 3,4,5,6,9,10,11,12,-Octahydro-2H,8H-1,7,13,4,10-benzotrioxadiazacyclopentadecine-3,11-dione (18)[44]
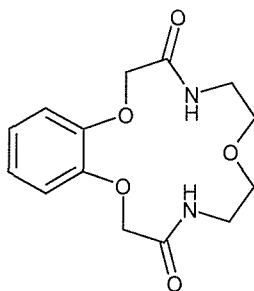
4.2.5.1 Using Diamine **20** as a dih ydrochloride salt

To methyl 2-[-2-(-methoxy-oxoethoxy)phenoxy]acetate **19** (1.52g, 6mmol) was added 2-(2-aminoethoxy)-1-ethanamine dihydrochloride **20** (0.88g, 5mmol), methanol (60cm^3) and potassium carbonate (0.68g, 5mmol). The solution was stirred with heating (65°C) for 50 hours. Upon cooling a solid precipitated out yielding **18** (1.123g, 76%) as a white crystalline solid. MP: 223-225°C (lit.,[65] 221-222°C). ^{1}H NMR ((CD$_3$)$_2$SO): δ 7.72 (2H, t, J = 4.8Hz), 7.09 –6.90 (4H, m), 4.42 (4H, s) 3.56 (4H, t, J = 5.0Hz), 3.4 (4H, t, J = 5.0Hz). ^{13}C NMR ((CD$_3$)$_2$SO): δ 167.0 (q), 146.4 (q), 121.7 (t), 113.3 (t), 68.1 (s), 67.4 (s), 38.2 (s). LRMS (ES+, m/z): 295 ([M+H]$^+$). IR (nujol mull, ν$_{max,}$ cm^{-1}): 3434s (-CONH-), 1667m (-CONH-), 1593m (**Ar**), 1506m (**Ar**).

4.2.5.2 Using Diamine **20** with N o Hydrochloride

To methyl 2-[-2-(-methoxy-oxoethoxy)phenoxy]acetate **19** (6g, 23.7mmol) was added 2-(2-aminoethoxy)-1-ethanamine **20** (2.05g, 19.7mmol), methanol (150cm^3). The solution was stirred with heating (65°C) for 27 hours. Upon cooling a white crystalline solid **18** (4.11g, 71%) formed. MP: 222-224°C (lit.,[65] 221-222°C). ^{1}H NMR ((CD$_3$)$_2$SO): δ 7.72 (2H, t, J = 4.8Hz), 7.09 –6.90 (4H, m), 4.42 (4H, s) 3.56 (4H, t, J = 5.0Hz), 3.4 (4H, t, J = 5.0Hz). ^{13}C NMR ((CD$_3$)$_2$SO): δ 167.0 (q), 146.4 (q), 121.7 (t), 113.3 (t), 68.1 (s), 67.4 (s), 38.2 (s). LRMS (ES+, m/z): 295 ([M+H]$^+$). IR (nujol mull, ν$_{max,}$ cm^{-1}): 3434s (-CONH-), 1682m (-CONH-), 1594m (**Ar**), 1507m (**Ar**).

4.2.6 Synthesis of 3,4,5,6,9,10,11,12-Octahydro-2H,8H-1,7,13,4,10-benzotrioxadiazacyclopentadecine (17)[44]
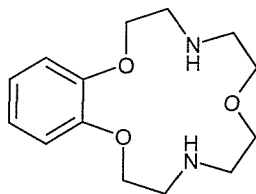
To 3,4,5,6,9,10,11,12-octahydro-2H,8H-1,7,13,4,10-benzotrioxadiazacyclo-pentadecine-3,11-dione **18** (1g, 3.4mmol) was added 1M borane in THF (21cm^3, 21mmol) under nitrogen. The solution was brought to reflux, stirred for 24 hours and then allowed to cool. Methanol (10cm^3) and 3M HCl (10cm^3) were then added before removing the solvent under reduced pressure. Methanol (10cm^3) was added and removed under reduced pressure a further three times. To the white residue DCM (25cm^3) and 2M HCl (20cm^3) were added. The organic phase was separated and the aqueous phase was basified to pH 12 using solid NaOH (~1g). The aqueous phase was extracted with DCM (5x30cm^3) and the combined organic phases were dried over potassium carbonate. After filtration and removal of the DCM under reduced pressure, a white solid **17** (0.396g, 44%) was obtained which was recrystallised from 60-80 pet. ether and decolourising charcoal. MP: 92-94°C (lit.,[65] 97-100°C). ^{1}H NMR ((CD$_3$)$_2$SO): δ 7.01 – 6.85 (4H, m), 4.02 (4H, t, J = 4.8Hz), 3.51 (4H, t, J = 4.6Hz), 2.88 (4H, t, J = 4.8Hz), 2.7 (4H, t, J = 4.6Hz). ^{13}C NMR ((CD$_3$)$_2$SO): δ 148.3 (q), 121.0 (t), 113.0 (t), 69.0 (s), 67.9 (s), 49.1 (s), 48.2 (s). LRMS (FAB, m/z): 267 ([M+H]$^+$). IR (nujol mull, $v_{max,}$ cm^{-1}): 3205s (>N-H), 1593m (Ar), 1506m (Ar). UV (MeOH, λ_{max}, cm^{-1}): 255.4 (ε/dm^{3}mol^{-1}cm^{-1} 7567), 274.8 (2673), 280.4sh (2164).

4.3 Attempted Synthesis Dibenzodiaza-15-Crown-5

4.3.1 Synthesis of 1-Nitro-2-[2(2-nitrophenoxy)ethoxy]benzene (29)[49]
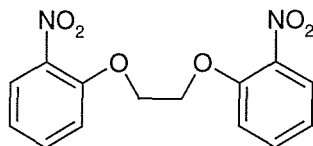
To 2-nitrophenol (13.9g, 100mmol) were added 1,2-dibromoethane (4.31cm^3, 50mmol), potassium carbonate (13.8g, 0.1mol) and DMF (100cm^3). The resulting orange solution was stirred with heating (120°C) until reaction was complete (5 hours) by TLC. After cooling, the solution was diluted with water (750cm^3) and the resulting yellow precipitate was filtered off leaving a bright red filtrate. The precipitate was washed repeatedly with aqueous potassium carbonate (10x20cm^3) and water (4x25cm^3). The resulting off-white precipitate was dried under vacuum for 16 hours. The solid was recrystallised from glacial acetic acid and the wet material was dried on a high vacuum line (~0.1mm Hg) affording the product **29** (6.57g, 43%) as an off-white powder. MP: 167-171°C (lit.,[66] 169-170°C). ^{1}H NMR (CDCl$_3$): δ 7.84 (2H, dd, J = 1.5, 8.1Hz), 7.59 (2H, ddd, J= 1.5, 7.4, 8.7Hz), 7.25 (2H, dd, J = 0.9, 8.5Hz), 7.11 (2H, ddd, J = 1.1, 7.2, 8.3Hz), 1.55 (4H, s,). ^{13}C NMR (CDCl$_3$): δ 150.5 (q), 139.4 (q), 134.0 (t), 124.5 (t), 120.6 (t), 115.2 (t), 67.7 (s). LRMS (ES+, m/z): 305 ([M+H]$^+$). IR (nujol mull, $v_{max,}$ cm^{-1}): 1604s (**Ar**), 1581s (**Ar**). TLC (silica, DCM, visualised under UV): R$_f$ (2-nitrophenol) = 0.69, R$_f$ (Product **29**) = 0.49.

4.3.2 Synthesis of 2-[2-(2-Aminophenoxy)ethoxy]aniline (27)[50]
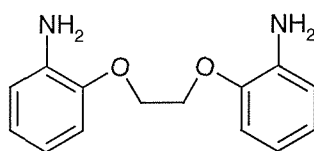
A stirred mixture of 1-nitro-2-[2(2-nitrophenoxy)ethoxy]benzene **29** (6.0g, 20mmol), ethanol (250cm^3), hydrazine hydrate (6.1cm^3, 6.26g, 125mmol) and palladium on activated charcoal (5%, 0.3g) was heated to reflux for 30 minutes and then filtered whilst hot through silica. Crystallisation was spontaneous and after cooling the product **27** (2.55g, 53%) was collected and dried on the high vacuum line (6 hours, ca. 0.1mm Hg). MP: 131-133°C (lit.,[50] 132-133°C). ^{1}H NMR (CDCl$_3$): δ 6.85 (4H, m), 6.75 (4H, m), 3.6 (2H, s), 2.21 (4H, s). ^{13}C NMR (CDCl$_3$): δ 146.4 (q), 137.0 (q), 122.1 (t), 118.6 (t), 115.5 (t), 112.7 (t), 67.6 (s). LRMS (ES+, m/z): 245 ([M+H]$^+$). IR (nujol mull, ν_{max}, cm^{-1}): 3429s + 3358s (-C-**NH$_2$**), 1610m (**Ar**), 1504m (**Ar**), 1460m (**Ar**).

4.3.3 Synthesis of Methyl 2-(2-methoxy-2-oxoethoxy)acetate (28)
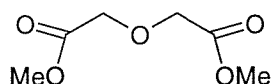
4.3.3.1 First Attempt[51]

To a solution of diglycolic acid **32** (6.03g, 45mmol) in methanol (15cm^3) was added 2,2-dimethoxypropane (12.28cm^3, 100mmol) and conc. sulfuric acid (1cm^3) with stirring at room temperature for three hours. The methanol was removed under reduced pressure and the oily residue was dissolved in water (60ml) before extraction with ether (3x60cm^3). The organic phases were combined and dried over sodium sulfate. The ether was removed under reduced pressure and the resulting liquid was distilled by Kügel Rohr apparatus to yield **28** (3.6g, 50%) as a white solid. MP: 36-38°C (lit.,[51] 37.5-39°C). ^{1}H NMR (CDCl$_3$): δ 4.25 (4H, s), 3.75 (6H, s). ^{13}C NMR (CDCl$_3$): δ 170.2 (q), 68.2 (s), 52.1 (p). LRMS (ES+, m/z): 185 ([M+Na]$^+$). IR (nujol mull, ν_{max}, cm^{-1}): 1754s (**C=O**).

4.3.3.2 Second Attempt[67]

To diglycolic acid (5g, 37mmol) was added methanol (100cm^3) and chlorotrimethylsilane (9.39cm^3, 74mmol) with stirring and a drying tube. The reaction was left for three hours thirty minutes before removing the solvent under reduced pressure. The resulting oil was acidified with 2M HCl (10cm^3) and then washed with DCM (3x50cm^3). The combined organic phases were dried (MgSO$_4$), filtered and the solvent was removed under reduced pressure, leaving a white solid. *Characterisation by ^{1}H NMR showed only starting material.*

4.3.3.3 Third Attempt[68]

To a solution of 2-(2-chloro-2-oxoethoxy)ethanoyl chloride **33** (6g, 29mmol) dissolved in DCM (50cm^3) was added a solution of methanol (23.2cm^3, 725mmol) and triethylamine (41cm^3, 290mmol) in DCM (50cm^3) under nitrogen atmosphere, dropwise over one hour. The reaction was stirred for a further 30 minutes before extracting with 2M HCl (3x100cm^3) and then back extracting the aqueous extracts with DCM (100cm^3). The combined organic extracts were dried (MgSO$_4$), filtered and the solvent removed under reduced pressure, leaving an off white solid. An attempt at recrystallisation was made with ethanol but no crystals were formed. When the ethanol was removed under vacuum an oil remained. *NMR characterisation suggests di- and mono- substituted ester.*

^{1}H HMR (CDCl$_3$): δ 4.26(s), 4.25(s), 4.23(s), 3.77(s), 3.75(s). ^{13}C NMR (CDCl$_3$): δ 172.9 (q), 170.8 (q), 170.3 (q), 68.6 (s), 68.5 (s), 68.2(s), 52.4 (p), 52.2 (p).

4.3.4 Synthesis of 2-(2-Chloro-2-oxoethoxy)ethanoyl Chloride (33)[69]
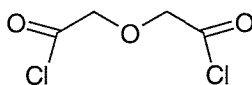
To diglycolic acid **32** (5g, 37mmol) was added thionyl chloride (10.73cm^3, 148mmol) and 1 drop DMF. This was heated to reflux with stirring until gas evolution ceased. After cooling the excess thionyl chloride was distilled off (atmospheric pressure, 79°C), leaving the product **33** (6g, 95%) as a dark red oil. ^{1}H NMR (CDCl$_3$): δ 4.59 (4H, s). IR (liquid film, $v_{max,}$ cm^{-1}): 1800s (**C=O**). *The unstable nature of this product prevented further characterisation.*

4.3.5 Synthesis of 6,7,10,11,17,18 Hexahydro-5H, 9H-dibenzo[e,n] [1,4,10,7,13]trioxadiaxacyclopentadecine-5,9-dione (26)
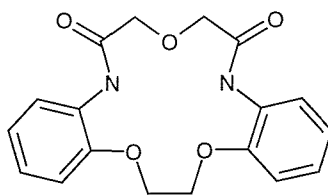
4.3.5.1 Using an Excess of Dimethyl Ester[44]

To bis(2-aminophenoxy)ethane **27** (2g, 8.2mmol) was added methyl 2-(2-methoxy-2-oxoethoxy)acetate **28** (1.59g, 9.8mmol) and methanol (60cm^3). The solution was stirred, under nitrogen at reflux for 24 hrs. The methanol was removed under reduced pressure leaving a creamy solid that was recrystallised from methanol. *NMR characterisation shows only the two starting materials, methyl 2-(2-methoxy-2-oxoethoxy)acetate and bis(2-aminophenoxy)ethane.*

4.3.5.2 Using an Excess of Diamine[44]

To bis(2-aminophenoxy)ethane **27** (1.82g, 7.4mmol) was added methyl 2-(2-methoxy-2-oxoethoxy)acetate **28** (1g, 6.2mmol) and methanol (60cm^3). The solution was stirred, under nitrogen at reflux for 24 hrs. After cooling a solid precipitated out, this was collected at the pump, yielding a white crystalline solid. *NMR characterisation shows only the two starting materials, methyl 2-(2-methoxy-2-oxoethoxy)acetate and bis(2-aminophenoxy)ethane.*

4.3.5.3 Using High Dilution[53]

Dry toluene (250cm³) was heated to gentle reflux with stirring. To this was added the 2-(2-chloro-2-oxoethoxy)ethanoyl chloride **33** (0.505g, 2.95mmol) in toluene (90cm³) and bis(2-aminophenoxy)ethane **27** (0.72g, 2.95mmol) in toluene (230cm³), dropwise over 5 hours. Once addition was complete, the reaction mixture was stirred for a further three hours before cooling to room temperature. The solvent was removed under reduced pressure, leaving a creamy brown solid, which was collected and washed with 1M HCl (100cm³). The resulting solid was collected by filtration and dissolved in DCM (250cm³), dried over magnesium sulphate, filtered and the solvent removed under reduced pressure to produce an orange coloured solid. This was recrystallised from acetic acid and decolourising charcoal, to afford the product as a cream coloured solid **26** (0.08g, 11%) which was dried under high vacuum. MP: 217-219°C (lit.,[53] 212 °C). ^{1}H NMR (CDCl₃): δ 9.5 (2H, s), 8.55 (2H, dd, J=2.0, 7.5Hz), 7.05 (6H, m), 4.42 (4H, s), 4.24 (4H, s). ^{13}C NMR (CDCl₃): δ 165.5 (q), 146.7 (q), 128.3 (q), 124.4 (t), 123.0 (t), 120.1 (t), 113.7 (t), 70.6 (s), 68.4 (s). LRMS (FAB, m/z): 343 ([M+H]$^+$). IR (solution in DCM, ν$_{max}$ cm^{-1}): 1421s (**Ar**), 1540 (**Ar**), 1692s (**C=O**).

The above procedure was performed by Robert Wood.[70]

4.3.6 Synthesis of *N,N*-Dimethyl-*N*-{4-[2-phenyl-1-diazene]phenyl} amine (36)[42]
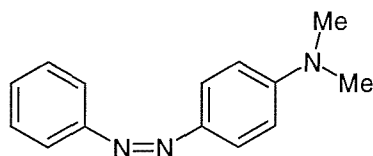
Aniline (5g, 4.9cm³, 54mmol) was dissolved in conc. HCl (15ml) and water (25cm³) before cooling to 0-5°C. A cold solution of sodium nitrite (5g, 72mmol) dissolved in water (25cm³) was added slowly with stirring. The reaction was left stirring for 25 minutes. To this was added a solution of *N,N*-dimethylaniline (**34**) (6.54g, 6.84cm³, 54mmol) in glacial acetic acid (3.1cm³). The reaction was left stirring at room temperature for a further 10 minutes. The resulting suspension was filtered under suction leaving a bright red solid (7.27g, 60%). LRMS (ES+): 226 ([M+H]$^+$). *All other characterisation was inconclusive.*

4.3.7 Synthesis of 1-(3,4-Dimethoxyphenyl)-2-phenyl-1-diazene (37)[42]
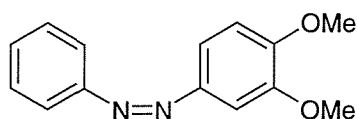
Aniline (5g, 4.9cm^3, 54mmol) was dissolved in conc. HCl (15ml) and water (25cm^3) before cooling to 0-5°C. A cold solution of sodium nitrite (5g, 72mmol) dissolved in water (25cm^3) was added slowly with stirring. The reaction was left stirring for 25 minutes. To this was added a solution of veratrole (35) (7.46g, 8.08cm^3, 54mmol) in glacial acetic acid (3.1cm^3). The reaction was left stirring at room temperature for a further 10 minutes. The resulting suspension was left to stand for 15 hours before extracting with DCM (3x150cm^3). The combined organic phases were dried (MgSO$_4$) and the solvent was removed under reduced pressure, leaving a red oil. *Spectroscopic characterisation has proved inconclusive.*

4.4 Fluorescence Functionalisation

4.4.1 Synthesis of 9-Anthrancecarbonyl Chloride (40)
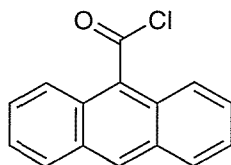
To anthracene-9-carboxylic acid (2.22g, 10mmol), was added to thionyl chloride (10cm^3, 16.31g, 14mmol). The solution was heated at reflux, with stirring, excluding light under a nitrogen atmosphere for one hour. The excess thionyl chloride was removed under reduced pressure. To the remaining dark brown solid was added toluene (12cm^3) which was removed under reduced pressure. This was repeated twice leaving the product 40 as a dark yellow solid (2.31g, 96%). MP: 95-98°C (lit.,[71] 96-97°C). ^{1}H NMR (CDCl$_3$): δ 8.52 (1H, s), 8.18 (2H, dd, J = 8.8, 0.8Hz), 8.05 (1H, d, J = 8.5Hz), 7.66 (2H, ddd, J = 8.8, 6.8, 1.5Hz), 7.38 (2H, ddd, J = 8.5, 6.8, 0.8Hz). ^{13}C NMR (CDCl$_3$): δ 170.0 (q), 132.1 (q), 131.1 (q), 131.1 (q), 129.2 (t), 128.4 (t), 126.6 (q), 126.3 (t), 124.3 (t). IR (nujol mull, v_{max}, cm^{-1}): 1778s (C=O). *The unstable nature of this product prevented further characterisation.*

4.4.2 Synthesis of 1-Naphthalenecarbonyl Chloride (42)
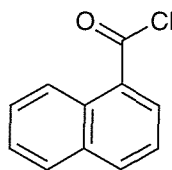
To 1-naphthoic acid (5g, 30mmol), was added to thionyl chloride (21.7cm^3, 35.4g, 0.3mol). The solution was heated at reflux, with stirring, excluding light under a nitrogen atmosphere for one hour. The excess thionyl chloride was removed under reduced pressure leaving the product **42** as a dark liquid (5.65g, 94%). ^{1}H NMR (CDCl$_3$): δ 8.79 (1H, d, J = 8.5Hz), 8.6 (1H, d, J = 7.4Hz), 8.16 (1H, d, J = 8.1Hz) 7.95 (1H, d, J = 8.1Hz), 7.71 (1H, t, J = 8.0Hz), 7.62 (1H, t, J = 6.7Hz), 7.58 (1H, t, J = 8.1Hz). ^{13}C NMR (CDCl$_3$): δ 167.6 (q), 136.5 (t), 135.6 (t), 133.9 (q), 130.8 (q), 129.7 (t), 129.6 (q), 129.0 (t), 127.2 (t), 125.2 (t), 124.7 (t). IR (nujol mull, $\nu_{max,}$ cm^{-1}): 1750s (**C=O**), 1592w (**Ar**), 1571m (**Ar**), 1509s (**Ar**), 1461m (**Ar**). *The unstable nature of this product prevented further characterisation.*

4.4.3 Synthesis of 1-Naphthyl(1,4,7,10,13-pentaoxa-16-azacycloocta-decanyl)methanone (44)[54]
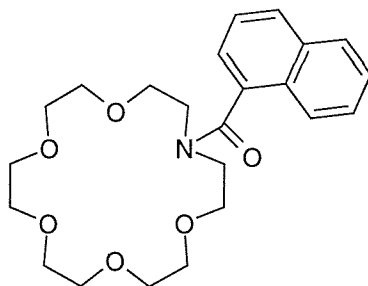
To a solution of aza-18-crown-6 (0.5g, 1.9mmol), triethylamine (0.26cm^3, 0.19g, 1.9mmol) and DCM (10cm^3) was slowly added a solution of 1-naphthalenecarbonyl chloride (0.13g, 0.6mmol) and DCM (12cm^3) over 15 minutes with stirring, under a nitrogen atmosphere. After complete addition the solution was stirred for a further 16 hours. The solvent was removed under reduced pressure to give a dark brown oil. The oil was taken up in DCM (15cm^3) and washed with 2M HCl (3x15cm^3). The organic phase was separated, dried over sodium sulfate, filtered and the solvent removed under reduced pressure. The resulting oil was placed on the high vacuum line for 5 hours yielding the product **44** (0.21g, 74%). ^{1}H NMR (CDCl$_3$): δ 7.81-7.72 (3H, m), 7.46-7.32 (4H, m), 3.51 (24H, m). ^{13}C NMR (CDCl$_3$): δ 171.7 (q), 135.2 (q), 133.9 (q), 130.0 (q), 129.3 (t), 128.7 (t), 127.3 (t), 126.7 (t), 125.5 (t), 125.4 (t), 124.1 (t), 71.2 (s), 71.1 (s), 71.0 (s) 70.9 (s), 70.9 (s), 71.6 (s), 70.0 (s), 70.0 (s), 50.0 (s), 46.3 (s). LRMS (ES+, m/z): 440 ([M+Na]$^+$). HRMS (FAB, m/z): 418.22218 ([M+H]$^+$), C$_{23}$H$_{31}$NO$_6$ requires M$^+$ = 417.22506. IR (nujol mull, ν$_{max}$, cm^{-1}): 3499b (-CONH-), 1631s (**CONH-**), 1507w (**Ar**), 1115w (**CH$_2$-O-CH$_2$**). UV (MeOH, λ$_{max}$, cm^{-1}): 222.4 (ε/dm^{3}mol^{-1}cm^{-1} 79740), 272.2sh (11340), 280.8 (13000), 291.8sh (8500).

4.4.4 Synthesis of 16-(1-Naphthylmethyl)-1,4,7,10,13-pentaoxa-16-azacyclooctadecane (45)
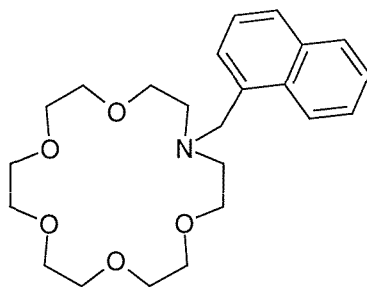
To 1-naphthyl(1,4,7,10,13-pentaoxa-16-azacycloocta-decanyl)methanone

(0.17g,0.4mmol) was added borane in THF (1M, 2.7cm^3, 2.7mmol) under nitrogen.

The solution was heated to reflux with stirring. After 16 hours all solvent had

evaporated and a further aliquot of borane (1M, 2.7cm^3, 2.7mmol) was added. After

24 hours the solution was cooled. Methanol (10cm^3) was added, followed by HCl

(2M, 15cm^3) before removing the solvent under reduced pressure. Methanol (10cm^3)

was added and removed under reduced pressure a further three times. To the white

residue DCM (25cm^3) and 2M HCl (30cm^3) was added. The organic phase was

separated and the aqueous phase was basified to pH 12 with lithium hydroxide (2M

sat., 40cm^3). The aqueous phase was extracted with DCM (5x30cm^3) before removing

the DCM under reduced pressure to give a dark oil **45** (0.12g, 73%). ^{1}H NMR

(CDCl$_3$): δ 8.35 (1H) 7.87-7.73 (2H, m), 7.55-7.37 (3H, m), 4.11 (2H, s) 3.78-3.54

(20H, m), 2.87 (4H, t, J = 5.7Hz). ^{13}C NMR (CDCl$_3$): δ 135.5 (q), 133.9 (q), 132.6

(q), 128.5 (t), 127.9 (t), 127.4 (t), 125.8 (t), 125.6 (t), 125.4 (t), 124.9 (t), 71.0 (s), 70.9

(s), 70.9 (s), 70.5 (s), 70.1 (s), 58.8 (s), 54.4 (s), 49.2 (s). LRMS (ES+, m/z): 404

([M+H]$^+$). IR (nujol mull, $\nu_{max,}$ cm^{-1}): 1631m (**Ar**), 1121w (CH$_2$-**O**-CH$_2$). UV (MeOH,

λ_{max}, cm^{-1}): 223.2 (ε/dm^{3}mol^{-1}cm^{-1} 44170), 272.2sh (7530), 280.6 (7970), 292.6sh

(5310).

4.4.5 Synthesis of 13-(9Anthrylmethyl)-1,4,7,10-tetraoxa-13-azacyclo-pentadecane (11b)[43k]
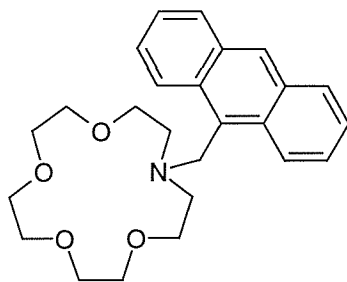
9-(Chloromethyl)anthracene (0.14g, 0.62mmol) was dissolved in the minimum volume of hot toluene (15ml). To this was added aza-15-crown-5 (0.147g, 0.67mmol) and potassium carbonate (0.092g, 0.67mmol). This was stirred and heated at reflux and for 27 hours. The solution was filtered while hot. After cooling the filtrate was extracted with 4M HCl (3x15cm^3). The aqueous phase was neutralised with solid potassium carbonate (ca. 2g) and extracted with chloroform (4x30cm^3). The organic phase was then dried over magnesium sulfate and evaporated to give a yellow oil. On standing solidification occurred and the product 11b was recrystallised from ethanol (0.14g, 55%). MP: 69-71°C (lit.,[43k] 71°C) ^{1}H NMR (CDCl$_3$): δ 8.4 (2H, d, J = 8.8Hz), 8.3 (1H, s), 7.85 (2H, d. J= 7.7Hz), 7.48-7.33 (4H, m), 4.5 (2H, s), 3.67-3.44 (20H, m), 2.93 (4H, t, J = 6.1Hz). ^{13}C NMR (CDCl$_3$): δ 131.6 (q), 131.5 (q), 130.6 (q), 129.1 (t), 127.6 (t), 125.7 (t), 125.4 (t), 125.0 (t), 124.1 (t), 71.1 (s), 70.7 (s), 70.2 (s), 54.3 (s), 52.7 (s). LRMS (ES+, m/z): 410 ([M+H]$^+$). IR (nujol mull, ν_{max}, cm^{-1}): 1677m (Ar), 1589m (Ar), 1168w (CH$_2$-O-CH$_2$). UV (MeOH, λ_{max}, cm^{-1}): 254.2 (ε/dm^{3}mol^{-1}cm^{-1} 49730), 365.2 (2590), 385.2 (2450).

4.4.6 Synthesis of 1-Naphthyl[10-(1-naphthylcarbonyl)-3,4,5,6,9,10,11,12,-octahydro-2H,8H-1,7,13,4,10-benzotrioxa diazacyclopentadecin-4-yl]methanone (46)
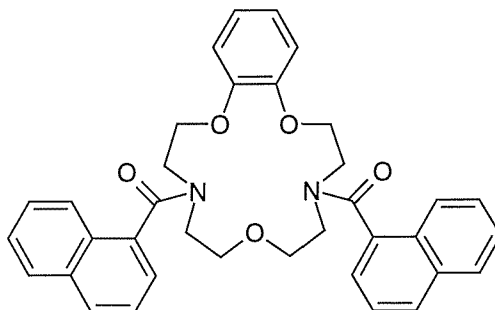
To a solution of 3,4,5,6,9,10,11,12-octahydro-2H,8H-1,7,13,4,10-benzotrioxadiazacyclopentadecine (0.5g, 1.9mmol) and DCM (10cm^3) was added a solution of 1-naphthalene carbonyl chloride (0.13g, 0.53mmol) and DCM (12cm^3). The solution was stirred for 16 hours. The solvent was removed under reduced pressure to give a dark brown oil. The oil was taken up in DCM (25cm^3) and washed with ammonium hydroxide (4x20cm^3). The organic layer was reduced to give a dark brown oil which partially solidified on standing. This was purified by column chromatography (5% MeOH in DCM) to yield the product **46** as a pale brown solid (0.26g, 66%). MP: 94-96°C. ^{1}H NMR (CDCl$_3$): δ 7.94-7.52 (6H, m), 7.52-7.10 (8H, m), 7.01-6.52. (4H, m), 4.48-4.24 (2H, m), 4.24-3.88 (4H, m), 3.88-3.10 (10H, m). ^{13}C NMR ((CD$_3$)$_2$SO, 383°K): δ.171.7 (q), 149.5 (q), 135.3 (q), 134.2 (q), 130.4(q), 129.6 (t), 129.0 (t), 127.5 (t), 127.0 (t), 125.5 (t), 124.3 (t), 122.4 (t), 114.7 (t), aliphatic peaks obscured due to coalescence. LRMS (ES+, m/z): 575([M+H]$^+$). HRMS (EI, m/z): 574.24451 (M$^+$), C$_{36}$H$_{34}$N$_2$O$_5$ requires M$^+$ = 574.24677. IR (nujol mull, v$_{max}$, cm^{-1}): 3497b (-CONH-), 1639s (CONH-), 1512w (Ar), 1112w (CH$_2$-O-CH$_2$). UV (MeOH, λ$_{max}$, cm^{-1}): 222.2 (ε/dm^{3}mol^{-1}cm^{-1} 136110), 272.2sh (16490), 280.8 (17980), 291.4sh (11220).

4.5 NMR Titrations

4.5.1 Benzo-15-Crown-5

Each solution was prepared sequentially from the previous solution by careful addition of the required amount of sodium tetrafluoroborate as a solid.

Solution 1; 100% crown: Benzo-15-crown-5 (44.67mg, 0.17mmol) in d^6-acetone (1cm^3).

Solution 2; 1 crown : 0.5 Na$^+$: Benzo-15-crown-5 (0.04467g, 0.17mmol) and sodium tetrafluoroborate (9.17mg, 0.085mmol) in d^6-acetone (1cm^3).

Solution 3; 1 crown : 1 Na$^+$: Benzo-15-crown-5 (0.04467g, 0.17mmol) and sodium tetrafluoroborate (9.17mg, 0.17mmol) in d^6-acetone (1cm^3).

Solution 4; 1 crown : 1.5 Na$^+$: Benzo-15-crown-5 (0.04467g, 0.17mmol) and sodium tetrafluoroborate (9.17mg, 0.255mmol) in d^6-acetone (1cm^3).

All spectra were run at 75MHz as specified in section 4.1 and are calibrated to the residual acetone peak at 30.2ppm

4.6 UV Job Plots

4.6.1 Method

Solutions of the hosts to be studied (**11b, 17, 44, 45, 46** and **47**) were prepared in methanol at concentrations required for a spectra in which the largest absorbance band obeyed the Beer-Lambert law (1×10^{-4} M or 1×10^{-5} M). Solutions of sodium and potassium perchlorate were prepared in methanol at equivalent concentrations.

For each Job plot series ten measurements were made, at molar ratios of host to guest ranging from 10:0 to 0:10. The solutions were prepared *in situ* in the cuvette, by adding the required volume of host and guest solution (one molar equivalent is equal to 0.1cm^3) to produce a total volume of 1cm^3.

The absorbance of each solution assuming no complexation, was calculated by multiplying the absorbance of the pure host solution by a factor equivalent to the volume of host actually present in the cuvette, i.e. *0.9, 0.8, 0.7* etc.

4.6.2 Raw Job Plot Data

Host:Guest	Absorbance at 254.2 nm	Calculated no complexation abs.	Difference
10:0	0.487	0.487	0.000
9:1	0.438	0.454	0.016
8:2	0.389	0.389	0.000
7:3	0.341	0.346	0.005
6:4	0.292	0.311	0.019
5:5	0.243	0.257	0.014
4:6	0.195	0.212	0.017
3:7	0.146	0.156	0.010
2:8	0.097	0.114	0.016
1:9	0.049	0.067	0.018
0:10	0.000	0.000	0.000

Table 7: Job plot data for crown **11b** against $NaClO_4$ at 1×10^{-5} M

Host:Guest	Absorbance at 254.0 nm	Calculated no complexation abs.	Difference
10:0	0.496	0.496	0.000
9:1	0.446	0.466	0.020
8:2	0.397	0.410	0.013
7:3	0.347	0.346	-0.001
6:4	0.298	0.304	0.006
5:5	0.248	0.252	0.004
4:6	0.198	0.208	0.009
3:7	0.149	0.153	0.004
2:8	0.099	0.110	0.011
1:9	0.050	0.061	0.011
0:10	0.000	0.000	0.000

Table 8: Job plot data for crown **11b** against $KClO_4$ at 1×10^{-5} M

Host:Guest	Absorbance at 274.8 nm	Calculated no complexation abs.	Difference
10:0	0.289	0.289	0.000
9:1	0.260	0.274	0.014
8:2	0.231	0.243	0.012
7:3	0.202	0.212	0.010
6:4	0.173	0.189	0.016
5:5	0.144	0.149	0.004
4:6	0.115	0.130	0.015
3:7	0.087	0.099	0.012
2:8	0.058	0.082	0.024
1:9	0.029	0.048	0.019
0:10	0.000	0.000	0.000

Table 9: Job plot data for crown **17** against $NaClO_4$ at 1×10^{-4} M

Host:Guest	Absorbance at 274.8 nm	Calculated no complexation abs.	Difference
10:0	0.267	0.267	0.000
9:1	0.241	0.252	0.011
8:2	0.214	0.241	0.027
7:3	0.187	0.212	0.025
6:4	0.160	0.190	0.030
5:5	0.134	0.144	0.010
4:6	0.107	0.122	0.015
3:7	0.080	0.092	0.012
2:8	0.053	0.070	0.016
1:9	0.027	0.043	0.016
0:10	0.000	0.000	0.000

Table 10: Job plot data for crown **17** against $KClO_4$ at 1×10^{-4} M

Host:Guest	Absorbance at 280.8 nm	Calculated no complexation abs.	Difference
10:0	0.130	0.130	0.000
9:1	0.117	0.137	0.020
8:2	0.104	0.112	0.007
7:3	0.091	0.102	0.011
6:4	0.078	0.117	0.039
5:5	0.065	0.108	0.043
4:6	0.052	0.090	0.038
3:7	0.039	0.076	0.037
2:8	0.026	0.062	0.036
1:9	0.013	0.048	0.035
0:10	0.000	0.000	0.000

Table 11: Job plot data for crown **44** against $NaClO_4$ at 1×10^{-5} M

Host:Guest	Absorbance at nm	Calculated no complexation abs.	Difference
10:0	0.706	0.706	0.000
9:1	0.636	0.647	0.012
8:2	0.565	0.583	0.018
7:3	0.494	0.534	0.039
6:4	0.424	0.445	0.021
5:5	0.353	0.378	0.025
4:6	0.282	0.307	0.024
3:7	0.212	0.252	0.040
2:8	0.141	0.177	0.036
1:9	0.071	0.114	0.044
0:10	0.000	0.000	0.000

Table 12: Job plot data for crown **44** against $KClO_4$ at 1×10^{-5} M

Host:Guest	Absorbance at 280.2 nm	Calculated no complexation abs.	Difference
10:0	0.080	0.080	0.000
9:1	0.072	0.092	0.020
8:2	0.064	0.091	0.027
7:3	0.056	0.098	0.042
6:4	0.048	0.112	0.064
5:5	0.040	0.094	0.054
4:6	0.032	0.071	0.039
3:7	0.024	0.048	0.024
2:8	0.016	0.051	0.035
1:9	0.008	0.054	0.046
0:10	0.000	0.000	0.000

Table 13: Job plot data for crown **45** against $NaClO_4$ at 1×10^{-5}M

Host:Guest	Absorbance at 277.4nm	Calculated no complexation abs.	Difference
10:0	0.070	0.070	0.000
9:1	0.063	0.085	0.022
8:2	0.056	0.094	0.039
7:3	0.049	0.099	0.051
6:4	0.042	0.078	0.036
5:5	0.035	0.067	0.033
4:6	0.028	0.060	0.032
3:7	0.021	0.057	0.036
2:8	0.014	0.052	0.038
1:9	0.007	0.047	0.040
0:10	0.000	0.000	0.000

Table 14: Job plot data for crown **45** against $KClO_4$ at 1×10^{-5}M

Host:Guest	Absorbance at 276.2 nm	Calculated no complexation abs.	Difference
10:0	0.271	0.271	0.000
9:1	0.244	0.243	-0.001
8:2	0.217	0.220	0.003
7:3	0.190	0.194	0.004
6:4	0.162	0.169	0.006
5:5	0.135	0.137	0.001
4:6	0.108	0.136	0.027
3:7	0.081	0.109	0.028
2:8	0.054	0.069	0.015
1:9	0.027	0.043	0.016
0:10	0.000	0.000	0.000

Table 15: Job plot data for crown **46** against $NaClO_4$ at 1×10^{-4}M

Host:Guest	Absorbance at 276.2 nm	Calculated no complexation abs.	Difference
10:0	0.298	0.298	0.000
9:1	0.268	0.280	0.012
8:2	0.238	0.215	-0.023
7:3	0.208	0.190	-0.019
6:4	0.179	0.166	-0.012
5:5	0.149	0.119	-0.030
4:6	0.119	0.110	-0.009
3:7	0.089	0.083	-0.006
2:8	0.060	0.055	-0.004
1:9	0.030	0.048	0.018
0:10	0.000	0.000	0.000

Table 16: Job plot data for crown **46** against $KClO_4$ at 1×10^{-4}M

Host:Guest	Absorbance at 280.8 nm	Calculated no complexation abs.	Difference
10:0	0.180	0.180	0.000
9:1	0.162	0.213	0.051
8:2	0.144	0.203	0.059
7:3	0.126	0.171	0.045
6:4	0.108	0.161	0.054
5:5	0.090	0.153	0.063
4:6	0.072	0.144	0.072
3:7	0.054	0.127	0.073
2:8	0.036	0.105	0.069
1:9	0.018	0.097	0.079
0:10	0.000	0.000	0.000

Table 17: Job plot data for crown **47** against $NaClO_4$ at 1×10^{-5}M

Host:Guest	Absorbance at 280.6 nm	Calculated no complexation abs.	Difference
10:0	0.221	0.221	0.000
9:1	0.199	0.239	0.040
8:2	0.177	0.250	0.073
7:3	0.155	0.230	0.075
6:4	0.133	0.206	0.073
5:5	0.111	0.197	0.087
4:6	0.089	0.180	0.091
3:7	0.066	0.163	0.096
2:8	0.044	0.111	0.066
1:9	0.022	0.113	0.091
0:10	0.000	0.000	0.000

Table 18: Job plot data for crown **47** against $KClO_4$ at $1 \times 10^{-5}M$

4.7 Extraction Experiments

4.7.1 Method[57]

The values of the extinction coefficients (ε) and distribution constants (K_{di}, see Equation 5) of the picrate salts between water and $CDCl_3$ were taken from literature.[72]

Picrate Salt	Conc. (M)	ε ($M^{-1}cm^{-1}$)	K_{di} (M^{-1})
Na^+	0.01529	16900	0.00174
K^+	0.01533	16900	0.00255

Table 19: Concentration, ε and K_d values for sodium and potassium picrate salts

Solutions of each host (**11b, 17, 18, 25, 44, 45, 46** and **47**) were prepared in 0.015M concentrations (or 0.0075M for hosts **17** and **25**) in $CDCl_3$. To a $0.5cm^3$ aliquot of each host solution ($1cm^3$ for **18** and **25**) was added a $0.5cm^3$ of 0.015M aqueous sodium or potassium picrate solution. The solutions were shaken for 2 minutes before allowing the layers to separate for 10 minutes. Aliquots ranging from $0.01cm^3$ to $0.1cm^3$ (depending on colour intensity) were taken from the organic phases and were diluted to $5cm^3$ with CH_3CN. From each of the aqueous phases $0.01cm^3$ aliquots were taken and diluted to $5cm^3$ with CH_3CN. The UV absorbance of each sample was measured and using the Beer-Lambert law [Equation 9] R values for each crown were calculated [Equation 10 for measurements made on the chloroform layer or Equation 11 for measurements made on the aqueous layer].

$$A = \varepsilon\, c\, l \qquad\qquad\qquad \text{Equation 9}$$

$$R = \left(\frac{[G]_{CDCl_3}}{[H_i]_{CDCl_3}}\right)_{equil} = \frac{AD_{CDCl_3}}{\varepsilon\, l [H_i]_{CDCl_3}\left(V_{CDCl_3}/V_{H_2O}\right)} \qquad \text{Equation 10}$$

$$R_{H_2O} = \left(\frac{[G]_{CDCl_3}}{[H_i]_{CDCl_3}}\right)_{equil} = \frac{\left\{[G_i]_{H_2O} - AD_{H_2O}/(\varepsilon\, l)\right\}\left(V_{H_2O}/V_{CDCl_3}\right)}{[H_i]_{CDCl_3}} \qquad \text{Equation 11}$$

where A is the absorbance

c is the concentration

ε is the extinction coefficient of the picrate salt

l is the path length (1cm)

R is the molar ratio of picrate to host in the CDCl$_3$ layer at equilibrium

$[G]_{CDCl_3}$ is the concentration of picrate extracted into the CDCl$_3$ layer

$[H_i]_{CDCl_3}$ is the initial concentration of the host in the CDCl$_3$ layer

D is the dilution factor of the removed aliquot

V_{CDCl_3} is the volume of chloroform

V_{H_2O} is the volume of water.

R_{H_2O} is the molar ratio of picrate to host in the CDCl$_3$ layer at equilibrium calculated

from the aqueous layer

4.7.2 Raw Extraction Data

Table 20 and Table 21 below list the aliquot volume, absorbance and R values used in calculating K_a and -G^o values from the chloroform and water layers.

Host	Guest	Vol. of aliquot (µl)	Abs.	R
46	Na⁺	10	0.111	0.21
	K⁺	10	0.116	0.22
17	Na⁺	10	0.039	0.075
	K⁺	10	0.035	0.068
11b	Na⁺	20	0.209	0.21
	K⁺	20	0.047	0.046
18	Na⁺	100	0.037	0.015
	K⁺	100	0.029	0.011
25	Na⁺	100	0.048	0.019
	K⁺	100	0.039	0.015
44	Na⁺	20	0.036	0.035
	K⁺	20	0.026	0.026
47	Na⁺	20	0.032	0.031
	K⁺	20	0.013	0.013
45	Na⁺	10	0.039	0.067
	K⁺	10	0.033	0.057

Table 20: Data calculated from chloroform layer

Host	Guest	Vol. of aliquot (µl)	Abs.	R
46	Na⁺	10	0.360	0.30
	K⁺	10	0.398	0.23
17	Na⁺	10	0.315	0.39
	K⁺	10	0.480	0.074
11b	Na⁺	10	0.209	0.61
	K⁺	10	0.503	0.030
18	Na⁺	10	0.510	0.053
	K⁺	10	0.502	0.13
25	Na⁺	10	0.500	0.13
	K⁺	10	0.509	0.072
44	Na⁺	10	0.312	0.40
	K⁺	10	0.493	0.049
47	Na⁺	10	0.494	0.044
	K⁺	10	0.505	0.025
45	Na⁺	10	0.473	0.075
	K⁺	10	0.474	0.076

Table 21: Data calculated from water layer

Host	Calculations based upon:	Guest	Vol. of aliquot (μl)	Abs.	R
17	$CDCl_3$	Na^+	10	0.054	0.10
		K^+	10	0.039	0.075
	H_2O	Na^+	20	0.45	0.13
		K^+	20	0.485	0.064
47	$CDCl_3$	Na^+	10	0.118	0.23
		K^+	10	0.111	0.21
	H_2O	Na^+	10	0.341	0.34
		K^+	10	0.399	0.23

Table 22: Data for repeat run of **17** and **47**

4.8 Fluorescence Measurements

Each sample was prepared *in situ* in the cuvette by addition of $0.1cm^3$ of the guest at ten times the required concentration in methanol, $0.1cm^3$ or $0.01cm^3$ of the host under study at ten times the required concentration in methanol and then making the sample up to a total volume of $1cm^3$ with methanol. All spectra were recorded at 21-24°C.

4.8.1 Quantum Yield Determination Data

Crown	Excitation Wavelength (nm)	ε (M^{-1})	c (M)	Cation	$\left(I_f\right)_u$	φ_u
11b	254	47300	1×10^{-7}	None	10816.63	0.0105
				10x K^+	12428.83	0.0120
				100x K^+	12722.70	0.0123
				10x Na^+	11310.65	0.0109
				100x Na^+	12379.76	0.0120
44	222	79740	1×10^{-9}	None	17558.51	0.0027
				10x K^+	17496.40	0.0027
				100x K^+	29311.58	0.0045
				10x Na^+	18418.21	0.0029
				100x Na^+	28431.90	0.0044
45	222	44170	1×10^{-9}	None	18727.55	0.0052
				10x K^+	26124.62	0.0073
				100x K^+	32069.64	0.0090
				10x Na^+	21375.30	0.0060
				100x Na^+	26741.38	0.0075
46	222	136110	1×10^{-7}	None	16356.61	0.0009
				10x K^+	20238.05	0.0012
				100x K^+	31684.85	0.0018
				10x Na^+	18765.12	0.0011
				100x Na^+	33890.98	0.0019

Table 23: Quantum yield data for the four studied crowns

Anthracene in methanol was used as the fluorescence standard for all quantum yield determinations.

Excitation Wavelength (nm)	ε [73] (M^{-1})	φ_s [74]	c (M)	$\left(I_f\right)_s$
254	1698	0.29	1x10-7	10755.46
222	10964	0.29	1x10-9	39811.35
222	10964	0.29	1x10-7	63376.66

Table 24: Quantum yield data for anthracene

SECTION 2 HYDROGELS

"The man who makes no mistakes does usually not make anything."

Edward John Phelps

5 INTRODUCTION

5.1 Cartilage Replacement Project

During the year, I was approached by a group of fourth year undergraduate engineers from the University of Southampton working on a project involving the design, synthesis and evaluation of replacement cartilage for human joints such as the knee. This project had arisen from collaboration between Professor Gregson from the Department of Engineering, a group of orthopaedic doctors and Mr David Barrett a consultant knee surgeon from Southampton General Hospital. Their brief was to design, develop and manufacture a prototype artificial cartilage replacement. This replacement would have similar properties to those of cartilage, would accommodate minimally invasive surgery and could be secured firmly in place, eventually allowing long-term bonding by the in-growth of bone into the material. This work was coincidentally occurring in parallel with the above work, the aim being to entirely replace damaged cartilage, rather than to understand cartilage injuries, and so develop better treatments for damaged cartilage.

The focus of the engineers' project was to investigate the possibility of using a material called a hydrogel (consisting of PVA and water), for the replacement of human cartilage. The hydrogel, once synthesised to the correct mechanical properties, would be cut and pinned into place during a surgical procedure which would aim to minimise damage to the surrounding knee.

In order to facilitate the incorporation of the new gel into the joint and onto the bone surface it would ideally have a bio-organic agent incorporated into its make-up. The medical team involved in the project recommended that hydroxyapatite would be a desirable choice.

The group had performed background research on the subject and approached me in a purely synthetic capacity. After discussion and consultation with a representative of the group the final brief required the synthesis of a range of PVA hydrogels in sizes determined by the moulds provided, each with a hydroxyapatite concentration gradient through the gel. The completed gels also had to be delivered by a certain date, as available testing time was limited.

5.2 Hydrogel Background

A hydrogel is defined as "a gel which contains water but is not soluble in water"[75] and in this case the required gels consist solely of PVA and water. The synthesis has two distinct parts, the first of which involves the preparation of a PVA solution of the desired concentration. The second step is a freeze/thaw cycle that anneals the solution into the desired gel structure. Both are straightforward but rather painstaking processes.

5.2.1 Hydrogel Preparation

Previous hydrogel syntheses [75,76] have used PVA having a low molecular weight and a high degree of saponification, i.e. polymer in which >99% of the ester groups have been hydrolysed [Scheme 20]. This circuitous route to PVA is necessary because of the unstable nature of vinyl alcohol relative to its tautomeric aldehydic form, ethanal.
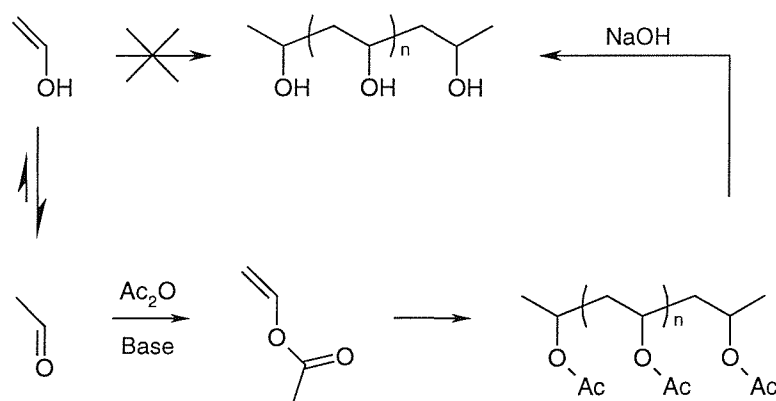
Scheme 20: Synthetic route to PVA

Stage one of the hydrogel preparation simply involves dissolution of the required amount of PVA in the correct volume of water, the ratio of PVA to water being measured weight for weight. The most important factor in the first stage of hydrogel synthesis is the removal of dissolved gases from the PVA solution as their presence will obviously create minute air bubbles and therefore create possible areas for mechanical failure. In order to achieve this, distilled water is used and the solution, once prepared, is left under vacuum.

The second stage requires the solution to be cast in a mould and then stored at -20°C for ten hours before warming the mould to 5°C for twenty hours. This cycle is repeated until the desired level of mechanical strength is achieved.

5.2.2 Hydrogel Chemistry

The gel is formed during the annealing stage through the crystallisation of PVA molecules. It appears that significant or extended freezing is detrimental to this crystallisation process.[75] For this reason the gel is switched between the two temperatures at regular periods, in order to minimise any degradation of the gel. It would also seem the introduction of DMSO to the PVA water solution reduces the tendency for freezing and therefore enhances crystallisation process. The DMSO can be removed after gel formation by washing with excess water.

5.2.3 Hydroxyapatite

Hydroxyapatite is a bio-organic agent compound of calcium, phosphorous, oxygen and hydrogen and its most common molecular formula is: $Ca_{10}(PO_4)_6(OH)_2$.[77] Hydroxyapatite should provide a long term bonding process that will replace the short-term surgical pins used to first hold the gel in place. In theory the bone will absorb the hydroxyapatite present in the gel and then grow into the porous cavities left behind. This will allow the gel to be bonded directly to the bone without need for an adhesive, allowing the new joint to act more like the original bone and cartilage. In addition to this the hydroxyapatite and gel should form a polymer matrix composite which would impart greater stiffness to the gel as a whole.

5.3 Aims of the Research

- Synthesis of a range of suitable hydrogels by 15/03/99

6 RESULTS AND DISCUSSION

6.1 Hydrogel Synthesis

The synthesis of hydrogels with a range of PVA concentrations presented a very different challenge from the other work carried out during this project. While in theory the PVA simply has to be dissolved in the desired amount of water, there were three main factors which made the synthesis rather demanding; (i) the insolubility of PVA; (ii) the need for the exclusion of gases from the final solution; and (iii) the need for the introduction of a concentration gradient of hydroxyapatite. These problems led to substantial time being spent on dry runs and testing ideas and possible methods. For this reason, the final procedure represents the culmination of a significant amount of development work.

6.1.1 PVA Solubility

Although PVA hydrogels have been reported with upwards of 40% PVA content[76] extreme difficulty was found in producing solutions containing much more than 16% PVA. A maximum temperature of 75°C was used while dissolving the PVA as it was suggested that the solution should not be boiled in order to avoid degradation of the product. This led to great difficulties in dissolving any substantial quantities of PVA without vigorous stirring, since this would introduce problems with aeration of the solution (see 6.1.2) and resulted in disappointing concentrations of PVA. After the synthesis had been optimised it was later found that heating of the solution up to 95°C and then leaving the solution to stand for a period of time resulted in far greater solubility and no problems of decomposition were evident. This procedure should be incorporated in any future synthesis, hopefully leading to the creation of gels with higher PVA contents.

6.1.2 Exclusion of Dissolved Gases

In order to minimise the concentration of dissolved gases in the final solution the original synthesis used distilled water and once the PVA solution had been made up it would be placed under vacuum (~20mm Hg). However, as a result of the solubility problems encountered (see 6.1.1), vigorous stirring had to be employed which led to a great deal of aeration. In order to overcome this, an ultrasonic bath was utilised while the solution was held under vacuum. This caused nucleation of the dissolved gases into bubbles so that they would be removed more effectively while under vacuum. This proved to be very effective, the aerated gels produced being considerably more opaque than their non-aerated counterparts.

6.1.3 Hydroxyapatite Concentration Gradient

The introduction of a hydroxyapatite gradient, crucial to the success of the gel, was the most difficult part of the assignment. At first, coating the surface of the gel with a dusting of hydroxyapatite was attempted. However, it proved nearly impossible to apply a uniform layer to the surface. It was also very important to provide a concentration gradient of hydroxyapatite throughout the gel in order to allow the bone to bond to the gel as strongly as possible. Next consideration was given to suspending hydroxyapatite in the solution, pouring it into the mould and allowing the particles to settle near the base of the gel. It was realised this was not possible because of the high viscosity of the gel and the freezing of the sample in the annealing process.

Consultation with Dr. Paul Wyeth, led to two possible solutions: (i) centrifuging a solution in order to create a concentration gradient; or (ii) creation of the gel in layers, each layer having progressively lower hydroxyapatite content. Both had their disadvantages. The centrifuge option was flawed in a similar fashion to the initial gravity-settling plan. A layering process involving different hydroxyapatite concentrations would probably just lead to partial diffusion before annealing/setting could occur.

After some thought it was realised that, rather than applying the layers one on top of each other at the very outset, the first layer could be set in the mould and subjected to one freeze/thaw cycle before applying a second layer and so on. This would eventually produce a gel of the required thickness with the desired gradient in place. The only possible problem with this approach was the possibility that the separate layers would create substantial lines of weakness inside the gel. This fear was partly allayed when a test run of this process showed a finished gel to be visibly homogeneous.

6.1.4 Freeze/Thaw Annealing

It was decided that six freeze/thaw cycles would give the final gel the desired level of mechanical strength. However since each of the gels would be composed of three different layers, each built up over time, the first layer would undergo a total of eight treatment cycles the next layer seven and the final layer six. This resulted in all layers undergoing at least six cycles of annealing. This significantly increased the total annealing time to 240 hours from 180 hours. Once completed the gels were stored in the fridge in the presence of a little distilled water in order to prevent them from drying out.

6.2 Hydrogel Characterisation

It had been planned to characterise the gels using solid state carbon NMR. However, since the gels were taken for immediate mechanical testing and characterisation, it has not been possible to complete these experiments.

6.2.1 Hydrogel Testing

The hydrogel project was submitted and marked under the title 'The Letterbox Knee' (referring to the use of non-evasive of surgery to introduce replacement cartilage) and achieved an average mark of 79%. The testing which was performed was very comprehensive and is summarised below:

6.2.1.1 Tensile testing

These tests were undertaken to characterise each of the three different hydrogel samples. They were designed to determine the stress-strain behaviour of each of the hydrogels and hence determined the Young's modulus, the ultimate tensile strength, the yield stress and the final fracture stress of the hydrogels.

The three best results were taken for each hydrogel type and the average stress-strain curves are plotted below.
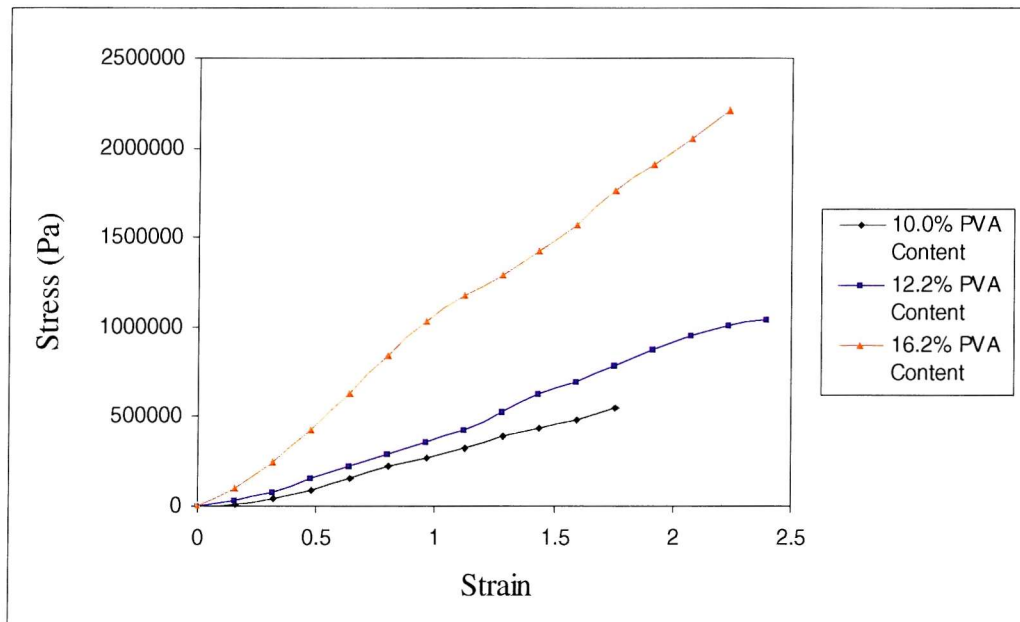
Figure 27: The average stress-strain behaviour of the three hydrogels

From these graphs the average properties of each of the hydrogels was determined. These are given below.

Properties	Hydrogel PVA Content		
	16.4%	*12.2%*	*10.0%*
Maximum extension (mm)	120.00	122.50	90.00
Maximum Load (N)	54.00	33.00	17.00
Maximum Stress (MPa)	2.40	1.10	0.55
Maximum Strain	2.40	2.45	1.80
Young's Modulus (MPa)	1.00	0.47	0.33

Table 25: Summary of average hydrogel properties

As can be seen from the graphs, the stress-strain behaviour of the hydrogels is mostly linear, from which it was deduced that the hydrogels only exhibit elastic deformation – there is no plastic deformation. Consequently, the hydrogels do not appear to have a yield stress, since they do not yield.

6.2.1.2 Wear testing

This was a comparative test, whereby the hydrogels were compared with other polymers and with other prosthetic devices in terms of their coefficients of friction and their mass wear rates.
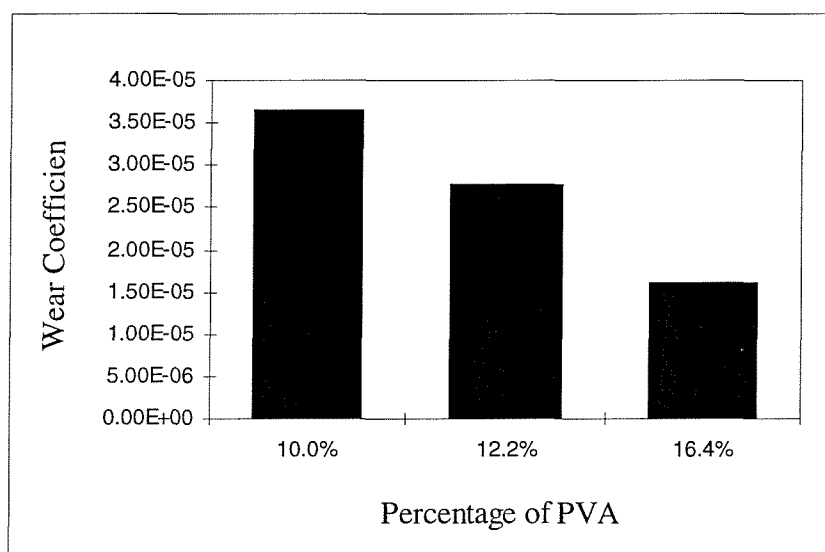
Figure 28: Mass wear rate of hydrogels

Although there were some problems with the reproducibility of test conditions, the values determined give an impression of how the different hydrogels compare with one another by comparison of the order of magnitude of the frictional coefficients, the wear rates of the hydrogels and the loads that they can sustain.

Both the mass wear rates and frictional coefficients compared very favourably with conventional prosthetics; in fact, the frictional coefficient of the 16.4% hydrogel was well within the range of natural cartilage.

6.2.1.3 Creep testing

This was again a comparative test and compared the compressive creep of the three different hydrogels with one another and with cartilage.

The 10% creep of the 16.4% PVA hydrogel compares well with that of cartilage, as does its creep rate, which is lower than that for cartilage. These results were encouraging and showed that the greater the PVA concentration, the greater the creep resistance and that the creep rate of cartilage can be matched or even exceeded by increasing the PVA content.
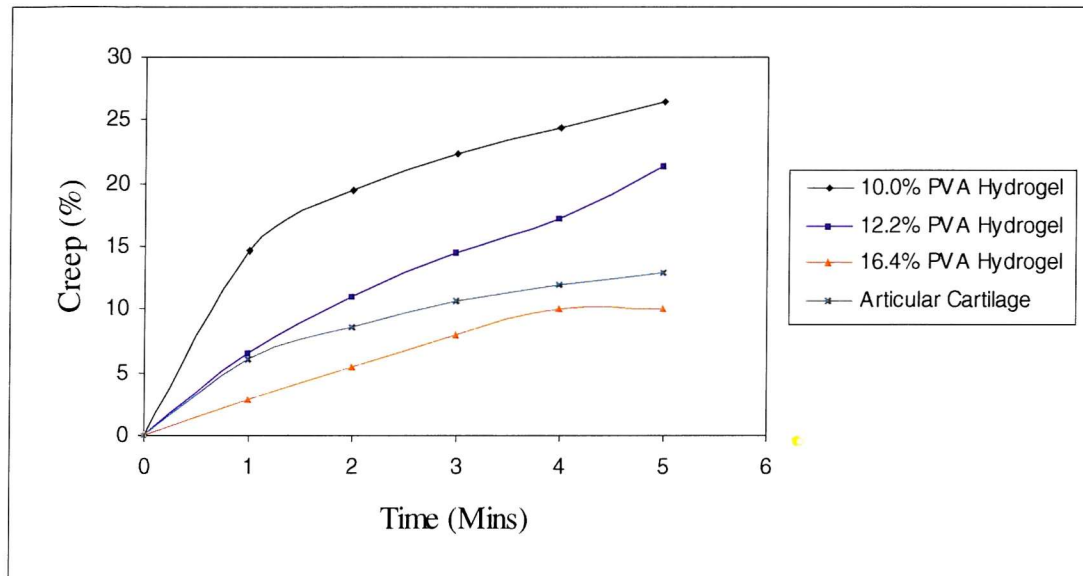
Figure 29: Graphs showing the percentage creep of the hydrogels under continuous compressive stress compared with articular cartilage under the same stress

6.2.1.4 Impact Testing

This was a pass or fail test and approximates the impact forces on the cartilage in the knee, albeit in a very crude manner.

All the hydrogels coped with successive impacts from 2 to 8cm. The hydrogel with 10.0% PVA failed at an impact of 9cm compared to 10cm for the 12.4% and 16.4% PVA hydrogels which is as expected. However all showed complete failure under loads that would be considered mild in the harsh environment of the knee.

6.2.1.5 Optical analysis

This procedure was used to analyse the layered structure of the hydrogels in order to see if the interface between the various layers was noticeable. It also provides insight into to view the hydroxyapatite concentration and distribution within the hydrogels. Analysis was performed with an optical microscope and showed three distinct layers.
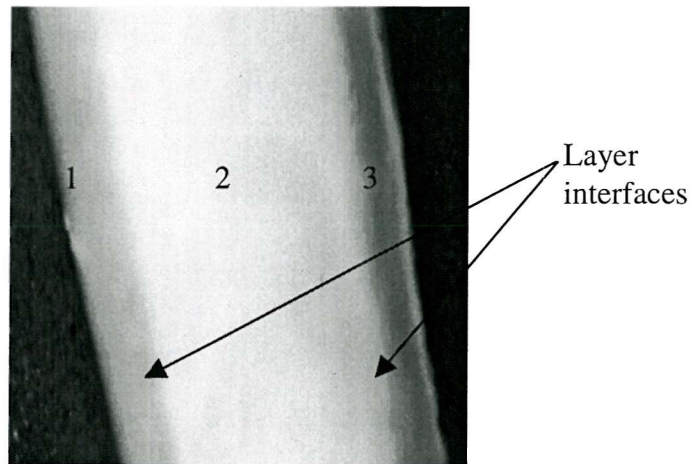
Figure 30: Three layers of a hydrogel, displaying the hydroxyapatite gradient

It is also worth noting that optical analysis showed that the layering technique, which was used to introduce the hydroxyapatite gradient, created visible layers [Figure 30] but mechanical testing showed no major lines of weakness at these layer interfaces.

7 CONCLUSIONS AND FUTURE WORK

A total of 12 hydrogels were made, four in each of three PVA concentrations, 10.0%, 12.2% and 16.4%. These were supplied on time and in the moulds provided. In addition they incorporated a hydroxyapatite gradient, which had been a particular challenge. It was found, as expected, that the hydrogel with the highest PVA content had the most desirable properties, i.e. approaching that of human cartilage. Yet these materials were still, as is so often the case, well behind nature in their capabilities. In general the gels did not have a high enough PVA concentration to mimic human cartilage effectively and the manufacturing process led to an inconsistency in the thickness of the gels produced.

In future, there is much potential in this area both from the chemical and engineering angles. Synthetically, more research should be carried out into the possible methods and techniques for hydrogel preparation. Once research has been completed, efforts could be made to create gels with much higher PVA concentrations. These new gels could undergo further mechanical testing with an aim to incorporating them into deceased animals' joints to see how they might mimic joint behaviour.

8 EXPERIMENTAL

8.1 General Experimental

Polyvinylalcohol (PVA) was 99+% hydrolysed with an average molecular weight of 89,000 to 98,000 used as received from Aldrich.

The ultrasonic bath employed was a Bransonic B1200E-1 device operating at 47kHz.

8.2 Synthesis of X% PVA Hydrogel with Hydroxyapatite Gradient

- *where X = percentage of PVA required, to a maximum of 16.4%*

To water ($100cm^3 - Xcm^3$) was added PVA (Xg) slowly with stirring at ~75°C. The solution was de-gassed in an ultrasonic bath while under vacuum (~20 mm Hg) for 16 hours. Hydroxyapatite (0.2g) was added to a sample of the solution (20g). The solution was then poured into the mould to a depth of one millimetre, covered with parafilm and kept at -20°C for ten hours. The mould and gel were then kept at 5°C for twenty hours. Hydroxyapatite (0.1g) was added to a sample of solution (20g). The solution was poured on top of the previous gel layer to a depth of one millimetre, covered with parafilm and stored at -20°C for ten hours. The gel was then held at 5°C for twenty hours. More PVA solution was poured on top of the previous gel layers to a depth of one millimetre, covered with parafilm and kept at -20°C for ten hours. The gel was then stored at 5°C for twenty hours. This was repeated a further five times. The completed gels were stored under water at 5°C.

SECTION 3 APPENDICES & REFERENCES

"These rough notes and our dead bodies must tell the tale."

Robert Falcon Scott

9 APPENDICES

Appendix A: List of Compounds

IUPAC; trivial

1) 4-(6-{13-[2-(2,4-dicarboxyphenyl)-5-methoxybenzo[*b*]furan-6-yl]-1,4,10-trioxa-7,13-diazacyclopentadecynyl}-5-methoxybenzo[*b*]furan-2-yl)isophthalic acid; SBFI

2) 2-{2-[2-(2-hydroxyphenoxy)ethoxy]ethoxy}phenol

3) 6,7,9,10,17,18,20,21-octahydrodibenzo[*b,k*][1,4,7,10,13,16]hexaoxacyclo octadecin; dibenzo-18-crown-6

4) Pyrocatechol; catechol

5) Di(2-chloroethyl) ether

6) 1,4,7,10,13,16-hexaoxacyclooctadecane; 18-crown-6

7) 1,4,8,11-tetraazacyclotetradecane; cyclam

8) Sodium 4-{ -2-[4-(dimethylamino)phenyl]-1-diazaenyl}-1-benzenesulfonate; methyl orange

9) 2-(6hydroxy-3-oxo-3H-9-xanthenyl)benzoic acid, fluorescein

10) 2-[(4-hydroxyphenyl)(4-oxo-2,5-cyclohexadienyliden)methyl]benzoic acid; phenolphthalein

11) De Silva's first generation sensors

    a) 16-(1,4-dihydro-9-anthracenylmethyl)-1,4,7,10,13-pentaoxa-16-azacyclo octadecane; *N*-(9-anthrylmethyl)monoaza-18-crown-6

    b) 13-(1,4-dihydro-9-anthracenylmethyl)-1,4,7,10,-tetraoxa-13-azacyclo pentadecane; *N*-(9-anthrylmethyl)monoaza-15-crown-5

12) 2-[(1,4-dihydro-9-anthracenylmethyl)(2-hydroxyethyl)amino]-1-ethanol; *N*-(9-anthrylmethyl)diethanolamine

13) De Silva's second generation sensors

    a) 10-(3,4-dimethoxybenzyl)-1,4,9,10-tetrahydro-9-anthracenecarboitrile

    b) 10-(2,3,5,6,8,9,11,12-octahydro-1,4,7,10,13-benzopentaoxacyclopentadecin-15-ylmethyl)-1,4,9,10-tetrahydro-9-anthracenecarbonitrile

    c) 10-(2,3,5,6,8,9,11,12,14,15-decahydro-1,4,7,10,13,16-benzohexaoxacyclo octadecin-18-ylmethyl)-1,4,9,10-tetrahydro-9-anthracenecarbonitrile

14) 10-{[(2,3,5,6,8,9,11,12- octahydro-1,4,7,10,13-benzopentaoxacyclopentadecin-15-ylmethyl)(propyl)amino]methyl}-1,4,9,10-tetrahydro-9-anthracenecarbonitrile

15) Di[(acetyloxy)methyl]4-(6-{13-[2-(2,4-di{[(acetyloxy)methoxy]carbonyl}phenyl)-5-methoxybenzo[*b*]furan-6-yl]-1,4,10-trioxa-7,13-diazacyclopentadecynyl}-5-methoxybenzo[*b*]furan-2-yl)isophthalate; SBFI-AM

16) 1,4,10-trioxa-7,13-diazacyclopentadecane; diaza-15-crown-5

17) 3,4,5,6,9,10,11,12-octahydro-2*H*,8*H*-1,7,13,4,10-benzotrioxadiazacyclo pentadecine; benzodiaza-15-crown-5

18) 3,4,5,6,9,10,11,12-octahydro-2*H*,8*H*-1,7,13,4,10-benzotrioxadiazacyclo pentadecine-3,11-dione; benzodiamide-15-crown-5

19) Methyl 2-[2-(2-methoxy-2-oxoethoxy)phenyloxy)acetate

20) 2-(2-aminoethoxy)-1-ethanamine

21) methyl 2-bromoacetate

22) 2-(2-{[(4-methylphenyl)sulfonyl]oxy}ethoxy)ethyl 4-methyl-1-benzenesulfonate

23) 2-{2-[2-(1,3-dioxo-2,3-dihydro-1*H*-2-isoindolyl)ethoxy]ethyl}-1,3-isodolinedione

24) 2-(2-hydroxyethoxy)-1-ethanol; diethylene glycol

25) 6,7,10,11,17,18-hexahydro-5*H*,9*H*-dibenzo[e,n][1,4,10,7,13]trioxadiaxacyclo pentadecine; dibenzodiaza-15-crown-5

26) 6,7,10,11,17,18-hexahydro-5*H*,9*H*-dibenzo[e,n][1,4,10,7,13]trioxadiaxacyclo pentadecine-5,9-dione; dibenzodiamide-15-crown-5

27) 2-[2-(2-Aminophenoxy)ethoxy]aniline

28) Methyl 2-(2-methoxy-2-oxoethoxy)acetate

29) 1-nitro-2-[2(2-nitrophenoxy)ethoxy]benzene

30) 2-nitrophenol

31) 1,2-dibromoethane

32) 2-(carboxymethoxy)acetic acid; diglycolic acid

33) 2-(2-chloro-2-oxoethoxy)ethanoyl chloride

34) *N*,*N*-dimethyl-*N*-phenylamine; *N*,*N*-dimethylaniline

35) 1,2-dimethoxybenzene; veratrole

36) *N*,*N*-dimethyl-*N*-{4-[2-phenyl-1-diazenyl]phenyl}amine

37) 1-(3,4-dimethoxyphenyl)-2-phenyl-1-diazene

38) 1-[4-(3,4,5,6,9,10,11,12-octahydro-2*H*,8*H*-1,7,13,4,10-benzotrioxadiazacyclopentadecin-4-yl)phenyl]-2-phenyl-1-diazene

39) 1-(3,4,5,6,9,10,11,12-octahydro-2*H*,8*H*-1,7,13,4,10-benzotrioxadiazacyclopentadecin-15-yl)-2-phenyl-1-diazene

40) 9-(chloromethyl)anthracene

41) 1,4,7,10-tetraoxa-13-azacyclopentadecane; aza-15-crown-5

42) 1-(chloromethyl)naphthalene

43) 1,4,7,10,13-pentaoxa-16-azacyclooctadecane; aza-18-crown-6 .

44) 1-naphthyl(1,4,7,10,13-pentaoxa-16-azacycloocta-decanyl)methanone

45) 16-(1-naphthylmethyl)-1,4,7,10,13-pentaoxa-16-azacyclooctadecane

46) 1-Naphthyl[10-(1-naphthylcarbonyl)-3,4,5,6,9,10,11,12,-octahydro-2H,8H-

    1,7,13,4,10-benzotrioxa diazacyclopentadecin-4-yl]methanone

47) 2,3,5,6,8,9,11,12-octahydro-1,4,7,10,13-benzopentaoxacyclopentadecin;

    benzo-15-crown-5

10 REFERENCES

1 Stockwell, R.A., *Clin. Anat.*, 1991, **4**, 161·

2 Wilkins, R.J., Browning, J.A., Urban, J.P.G., *Biorheology*, (in press)

3 Maroudas, A., Joints and Synovial Fluid, Academic Press New York, 1980, **2**, 239

4 Urban, J.P.G., Hall, A.C., Articular cartilage and Osteoarthritis, Raven Press New York, 1992, 393

5 Hall, A.C., Horwitz, E.R., Wilkins, R.J., *Exp. Physiol.*, 1996, **81**, 535

6 Wilkins, R.J., Browning, J.A., Ellory, J.C., *J. Memb. Biol.*, (review, accepted)

7 Mobasheri, A., Hall, A.C., Urban, J.P., France, S.J., Smith, A.L., *Int. J. Biochem. Cell. Biol.*, 1997, **29**, 649

8 Haugland, R.P., Handbook of Fluorescent Probes and Research Chemicals, 6th Edition, Molecular Probes, 1996

9 Minta, A., Tsien, R.Y., *J. Biol. Chem.*, 1989, **264**, 1949

10 Hunter, C.A., *J. Am. Chem. Soc.*, 1992, **114**, 5303

11 Lehn, J.M., *Angew. Chem., Int. Ed. Engl.*, 1988, **27**, 89

12 Constable, E.C., *Chem. Ind.*, 1994, **2**, 56

13 Weston, S.C., Ph.D. Thesis, University of Southampton, 1993

14 Fabbrizzi, L., Poggi, A., *Chem. Soc., Rev.*, 1995, **24**, 197

15 Pinalli, R., Nachtigall, F.F., Ugozzoli, F., Dalcanale, E., *Angew. Chem., Int. Ed. Engl.*, 1992, **38**, 2377

16 Lehn, J.M., *Struct. Bonding*, 1973, **16**, 1

17 (a) Tecila, P., Dixon, R.P., Slobodkin, G., Alavi, D.S., Waldeck, D.H., Hamilton, A.D., *J. Am. Chem. Soc.*, 1990, **112**, 9408, (b) Whitesides, G.M., Mathias, J.P., Seto, C.T., *Science*, 1991, **254**, 1312, (c) Linsey, J.S., *New J. Chem.*, 1991, **15**, 153, (d) Pfeil, A., Lehn, J.M., *J. Chem. Soc., Chem. Commun.*, 1992, 838

18 Fredericks, J.R., Hamilton, A.D., Comprehensive Supramolecular Chemistry, Permagon, 1996, **9**, 565

19 Lehn, J.M., Rigault, A., *Angew. Chem., Int. Ed. Engl.*, 1988, **27**, 1095

20 Pedersen, C.J., *Org. Synth.*, 1972, **52**, 66

21 Pedersen, C.J., *J. Inclusion Phenom.*, 1988, **6**, 337

22 Weber, E., Toner, J.L., Goldberg, I., Vögtle, F., Laidler, D.A., Stoddart, J.F., Bartsch, R.A., Liotta, C.L., Crown Ethers and Analogs, John Wiley & Sons, 1989

23 Jolly, W.L., Preparative Inorganic Reactions, John Wiley & Sons, 1971, **6**

24 Antsyshkina, A.S., Porai-Koshits, M.A., Makhaev, V.D., Borisov, A.P., Kedrova,
   Mal'tseva, N.N., *Koord. Khim.*, 1992, **18**, 474

25 (a) Izatt, R.M., Bradshaw, J.S., Nielsen, S.A., Lamb, J.D., Christensen, J.J., *Chem.
   Rev.*, 1985, **85**, 271, (b) Izatt, R.M., Christensen, J.J., Eatough, D.J., *Chem. Rev.*,
   1974, **74**, 351, (c) Izatt, R.M., Pawlak, K., Bradshaw, J.S., *Chem. Rev.*, 1991, **91**,
   1721

26 Jurisson, S., Schlemper, E.O., Troutner, D.E., Canning, L.R., Nowotnik, D.P.,
   Neirinckx, R.D., *Inorg. Chem.*, 1986, **25**, 543

27 Jurrison, S., Berning, D., Jia, W., Ma, D., *Chem. Rev.*, 1993, **93** 1137

28 Dietrich, B., Lehn, J.M., Savauge, J.P., *Tetrahedron Lett.*, 1969, **34**, 2885

29 Dietrich, B., Lehn, J.M., Savauge, J.P., *Tetrahedron Lett.*, 1969, **34**, 2889

30 Cram, D.J., *Science*, 1974, **183**, 803

31 Smith, D.R., *Chem. Ind.*, 1994, **1**, 14

32 Ha, J.C., Dougherty, D.A., *Chem. Rev.*, 1997, **97**, 1303

33 Grossel, M.C., Cheetham, A.K., Hope, D.A.O., Weston, S.C., *J. Org. Chem*, 1993,
   58, 6654 and references therein

34 Gokel, W.G., Comprehensive Supramolecular Chemistry, Permagon, 1996, **1**, 61

35 Cabbiness, Margerum, *J. Am. Chem. Soc.*, 1969, **91**, 6540

36 Hancock, R.D., Crown Compounds: Toward Future Applications, New York, 1992,
   Chapter 10

37 Trueblood, K.N., Knobler, C.B., Maverick, E., Helgson, R.C., Bruce Brown, S.,
   Cram, D.J., *J. Am. Chem. Soc.*, 1981, **103**, 5594

38 Schneider, H.J., Yatsimirsky, A., Principles and Methods in Supramolecular
   Chemistry, John Wiley & Sons, 2000

39 Gokel, G., Crown Ethers & Cryptands, The Royal Society of Chemistry, 1991, 22

40 (a) Dix, J.P., Vögtle, F., *Chem. Ber.*, 1980, **113**, 457, (b) Dix, J.P., Vögtle, F., *Chem.
   Ber.*, 1981, **114**, 638, (c) Löhr, H., Vögtle, F., *Acc. Chem. Res.*, 1985, **18**, 65

41 Williams, D.H., Flemming, I., Spectroscopic Methods in Organic Chemistry, 5th
   Edition, McGraw Hill, 1995

42 Vogel, A.I., Practical Organic Chemistry, 5th Edition, Longman, 1957, 951

43 (a) De Silva, A.P., Rupasinghe, R.A.D.D., *J. Chem. Soc., Chem. Commun.*, 1985, **111**, 8672 , (b) Ayadim, M., Habib-Jiwan, J.L., de Silva, A.P., Soumillion, J.P., *Tetrahedron Lett.*, 1996, **37**, 7039, (c) De Silva, A.P., de Silva, S.A., *J. Chem. Soc., Chem. Commun.*, 1986, 1709, (d) De Silva, A.P., Sandanayake, K.R.A.S., *J. Chem. Soc., Chem. Commun.*, 1989, 1183, (e) De Silva, A.P., Gunaratne, H.Q.N., *J. Chem. Soc., Chem. Commun.*, 1990, 186, (f) De Silva, A.P., Gunaratne, H.Q.N., McCoy, C.P., *Nature*, 1993, **364**, 42, (g) De Silva, A.P., Gunaratne, H.Q.N., Sandanayake, K.R.A.S., *Tetrahedron Lett.*, 1990, **36**, 5193, (h) De Silva, A.P., Gunaratne, H.Q.N., Gunnlaugsson, T., McCoy, C.P., Maxwell, P.R.S., Rademacher, J.T., Rice, T.E., *Pure & Appl. Chem.*, 1996, **68**, 1443, (i) De Silva, A.P., Gunaratne, H.Q.N., McCoy, C.P., *J. Chem. Soc., Chem. Commun.*, 1996, 2399, (j) De Silva, A.P., Gunaratne, H.Q.N., Rice, T.E., *Angew. Chem. Int. Ed. Engl.*, 1996, **35**, 2116, (k) Bissell, R.A., Calle, E., de Silva, A.P., de Silva, S.A., Gunaratne, H.Q.N., Habib-Jiwan, J.L., Peiris, S.L.A., Rupasinghe, R.A.D.D., Samarasinghe, T.K.S.D., Sandanayake, K.R.A.S., Soumillion, J.P, *J. Chem. Soc. Perkin Trans.2*, 1992, **9**, 1559

44 Parker. D., Macrocycle Synthesis: A Practical Approach, Oxford University Press, 1996, 26

45 Amabilino, D.B., Ph.D. Thesis, University of Southampton, 1991, 236

46 Gibson, M.S., Bradshaw, R.W., *Angew Chem. Int. Ed.*, 1968, 7, 919

47 Ozser, M.E., M.Res. Thesis, University of Southampton, 1998, 58

48 Parker, A.J., *Chem. Rev.*, 1969, **69**, 1

49 Grynkiewicz, G., Poenie, M., Tsien, R.Y., *J. Biol. Chem.*, 1985, **260**, 3440

50 Parker, R., Part Two Thesis, University of Oxford, 1995, 42

51 Henry, D.W., Silverstein, R.M., *J. Org. Chem.*, 1996, **31**, 2391

52 Rasshofer,W., *Chem. Ber.*, 1979, **112**, 2095

53 Formanovski, A.A., Murakhovskaya, A.S., *Chem. Heterocycl. Compd.*, 1985, 225

54 Kubo, K., Ishige, R., Kubo, J., Sakurai, T., *Talanta*, 1999, **48**, 181

55 Job, P., *Ann. Chim.*, (Paris), 1928, **9**, 113

56 Macomber, R.S., *J. Chem. Educ.* 1992, **69**, 375

57 Koenig, K.E., Lein, G.M., Stuckler, P., Kaneda, T., Cram, D.J., *J. Am. Chem. Soc.*, 1979, **101**, 3553

58 (a) Wong, K.H., Bourgoin, M., Smid, J., *J. Chem. Soc., Chem. Commun.*, 1974, 715, (b) Bourgoin, M., Wong, K.H., Hui, J.Y., Smid, J., *J. Am. Chem. Soc.*, 1975, **97**, 3462

59 Harwood, L.M., Moody, C.J., Experimental Organic Chemistry, Blackwell Scientific Publications, 1989

60 Conforth, J.W., Morgan, E.D., Potts, K.T., Rees, R.J.W., *Tetrahedron*, 1973, **29**, 1659

61 Nelson, S.M., *J. Chem. Soc., Dalton Trans.*, 1983, 2525

62 Dietrich, B., Lehn, J.M., Sauvage. J.P., Blanzat, J., *Tetrahedron*, 1973, **29**, 1629

63 Anikin, V.F., Ganin, E.V., Rozynov, B.V., Zakharova, R.M., Kamalov, G.l., *Chem. Heterocycl. Compd.* , 1982, **18**, 193

64 Archer, A.W., Claret, P.A., Hayman, D.F., *J. Chem. Soc. (B)*, 1971, 1231

65 Jurczak, J., Stankiewicz, T., Salanski, P., Kasprzyk, S., Lipkowski, P., *Tetrahedron*, 1993, **49**, 1478

66 Cannon, R.D., Chiswell, B., Venanzi, L.M., *J. Chem. Soc. (A)*, 1967, 1277

67 Parker, R.A., Unpublished Results

68 Hamilton, D., Ph.D. Thesis, University of Southampton, 1993, 108

69 Bardwell, S.W.R., 3rd Year Project, University of Southampton, 1998, 25

70 Wood, R.J., 3rd Year Project, University of Southampton, 2000, 51

71 Benniston, A.C., Harriman, A., Lynch, V.M., *Tetrahedron Lett.*, 1994, **35**, 1473

72 Moore, S.S., Tarnowski, T.L., Newcomb, M., Cram, D.J., *J. Am. Chem. Soc.*, 1977, **99**, 6399

73 Weast, R.C. (Ed.), Handbook of Chemistry and Physics, 55th Edition, 1974

74 Birks, J.B., Photophysics of Aromatic Molecules, John Wiley & Sons, 1970

75 Hyon, S., Cha, W., Ikada, Y., *Polymer Bulletin*, 1989, **22**, 119

76 Moriyama, S., Unpublished results

77 Suzuki, T., Ishigaki, K., Miyake, M., *J. Chem. Soc., Faraday Trans. 1*, 1984, **80**, 3157